ตัวรับรู้ดีเอ็นเอฐานกระดาษโดยใช้พิโรลิดินิลพีเอ็นเอสำหรับการตรวจวัดฮิวแมนแพปพิลโลมาไวรัส มัยโคแบคทีเรียมทูเบอร์คูโลซิสและเมอร์สโคโรนาไวรัส

นางสาวปฤญจพร ทีงาม

วิทยานิพนธ์นี้เป็นส่วนหนึ่งของการศึกษาตามหลักสูตรปริญญาวิทยาศาสตรดุษฎีบัณฑิต
สาขาวิชาปิโตรเคมี
คณะวิทยาศาสตร์ จุฬาลงกรณ์มหาวิทยาลัย
ปีการศึกษา 2559

PAPER-BASED DNA SENSORS USING PYRROLIDINYL PNA FOR HUMAN PAPILLOMAVIRUS, MYCOBACTERIUM TUBERCULOSIS AND MERS CORONAVIRUS DETECTION

Miss Prinjaporn Teengam

A Dissertation Submitted in Partial Fulfillment of the Requirements
for the Degree of Doctor of Philosophy Program in Petrochemistry
Faculty of Science
Chulalongkorn University
Academic Year 2016

Thesis Title	PAPER-BASED DNA SENSORS USING PYRROLIDINYL PNA FOR HUMAN PAPILLOMAVIRUS, MYCOBACTERIUM TUBERCULOSIS AND MERS CORONAVIRUS DETECTION
By	Miss Prinjaporn Teengam
Field of Study	Petrochemistry
Thesis Advisor	Professor Orawon Chailapakul, Ph.D.
Thesis Co-Advisor	Professor Tirayut Vilaivan, Ph.D.
	Adisorn Tuantranont, Ph.D.

Accepted by the Faculty of Science, Chulalongkorn University in Partial Fulfillment of the Requirements for the Doctoral Degree

.....Dean of the Faculty of Science
(Associate Professor Polkit Sangvanich, Ph.D.)

THESIS COMMITTEE

.....Chairman
(Assistant Professor Warinthorn Chavasiri, Ph.D.)

.....Thesis Advisor
(Professor Orawon Chailapakul, Ph.D.)

.....Thesis Co-Advisor
(Professor Tirayut Vilaivan, Ph.D.)

.....Thesis Co-Advisor
(Adisorn Tuantranont, Ph.D.)

.....Examiner
(Associate Professor Sirilux Poompradub, Ph.D.)

.....Examiner
(Associate Professor Nattaya Ngamrojanavanich, Ph.D.)

.....External Examiner
(Associate Professor Weena Siangproh, Ph.D.)

ปฤญจพร ทีงาม : ตัวรับรู้ดีเอ็นเอฐานกระดาษโดยใช้พิโรลิดินิลพีเอ็นเอสำหรับการตรวจวัดฮิวแมนแพปพิลโลมาไวรัส มัยโคแบคทีเรียมทูเบอร์คูโลซิสและเมอร์สโคโรนาไวรัส (PAPER-BASED DNA SENSORS USING PYRROLIDINYL PNA FOR HUMAN PAPILLOMAVIRUS, MYCOBACTERIUM TUBERCULOSIS AND MERS CORONAVIRUS DETECTION) อ.ที่ปรึกษาวิทยานิพนธ์หลัก: ศ. ดร.อรวรรณ ชัยลภากุล, อ.ที่ปรึกษาวิทยานิพนธ์ร่วม: ศ. ดร.ธีรยุทธ วิไลวัลย์, ดร.อดิสร เตือนตรานนท์, 102 หน้า.

วิทยานิพนธ์ฉบับนี้มีจุดมุ่งหมายเพื่อพัฒนาตัวรับรู้ทางชีวภาพชนิดใหม่ โดยใช้พิโรลิดินิลเพปไทด์นิวคลีอิกแอซิด เป็นสารชีวภาพสำหรับการตรวจวิเคราะห์ดีเอ็นเอ ซึ่งบ่งชี้โรคชนิดต่างๆ หัวข้อในงานวิจัยนี้สามารถแบ่งออกเป็น 2 ส่วน ในส่วนแรก คือ การพัฒนาตัวรับรู้ดีเอ็นเอ โดยใช้อุปกรณ์ตรวจวิเคราะห์ฐานกระดาษร่วมกับการตรวจวัดทางเคมีไฟฟ้า เทคนิคสแควร์เวฟโวลแทมเมตรีและเทคนิคอิมพีแดนซ์สเปคโทรสโกปี ถูกใช้ในการหาปริมาณไวรัสฮิวแมนแพปพิลโลมาและมัยโคแบคทีเรียมทูเบอร์คูโลซิส ตามลำดับ ระบบทั้งสองนี้มีความไวในการตรวจวิเคราะห์โดยมีค่าขีดจำกัดการตรวจวัดที่ต่ำระดับ 2.3 นาโนโมลาร์ สำหรับไวรัสฮิวแมนแพปพิลโลมา และ 1.24 นาโนโมลาร์ สำหรับมัยโคแบคทีเรียมทูเบอร์คูโลซิส ส่วนที่สอง เป็นการพัฒนาตัวรับรู้ดีเอ็นเอ โดยใช้อุปกรณ์ตรวจวิเคราะห์ฐานกระดาษร่วมกับการตรวจวัดเชิงสี โดยตัวรับรู้ทางชีวภาพที่นำเสนอนี้ ถูกออกแบบสำหรับการตรวจวัดเมอร์สโคโรนาไวรัส มัยโคแบคทีเรียมทูเบอร์คูโลซิส และไวรัสฮิวแมนแพปพิลโลมาในคราวเดียวกัน อนุภาคนาโนของเงินถูกใช้เป็นสารที่ทำให้เกิดการเปลี่ยนแปลงสี โดยสีที่เปลี่ยนไปนี้จะขึ้นอยู่กับปริมาณของดีเอ็นเอ ซึ่งมีขีดจำกัดการตรวจวัดอยู่ที่ 1.53, 1.27 และ 1.03 นาโนโมลาร์ สำหรับเมอร์สโคโรนาไวรัส มัยโคแบคทีเรียมทูเบอร์คูโลซิส และไวรัสฮิวแมนแพปพิลโลมา ตามลำดับ ความจำเพาะเจาะจงของตัวรับรู้ทางชีวภาพทั้งสามชนิดที่ได้พัฒนาขึ้น ถูกแสดงโดยคุณสมบัติที่โดดเด่นของพิโรลิดินิลเพปไทด์นิวคลีอิกแอซิด นอกจากนี้ตัวรับรู้ชีวภาพที่ได้พัฒนาขึ้น ยังประสบความสำเร็จในการประยุกต์ใช้สำหรับการตรวจวิเคราะห์ดีเอ็นเอเป้าหมายในตัวอย่างทางชีวภาพอีกด้วย จากผลการทดลองแสดงให้เห็นว่า ตัวรับรู้ดีเอ็นเอฐานกระดาษที่ได้นำเสนอนี้ มีศักยภาพในการเป็นอุปกรณ์ทางเลือก ที่มีราคาถูก ใช้งานง่าย มีความไวและความจำเพาะเจาะจงในการตรวจวัดดีเอ็นเอ เมื่อเทียบกับวิธีดั้งเดิม

สาขาวิชา ปิโตรเคมี ลายมือชื่อนิสิต .....

ปีการศึกษา 2559 ลายมือชื่อ อ.ที่ปรึกษาหลัก .....

ลายมือชื่อ อ.ที่ปรึกษาร่วม .....

ลายมือชื่อ อ.ที่ปรึกษาร่วม .....

5572825123 : MAJOR PETROCHEMISTRY

KEYWORDS: BIOSENSOR / PAPER-BASED ANALYTICAL DEVICE / PYRROLIDINYL PEPTIDE NUCLEIC ACID / ELECTROCHEMICAL DETECTION / COLORIMETRIC DETECTION

PRINJAPORN TEENGAM: PAPER-BASED DNA SENSORS USING PYRROLIDINYL PNA FOR HUMAN PAPILLOMAVIRUS, MYCOBACTERIUM TUBERCULOSIS AND MERS CORONAVIRUS DETECTION. ADVISOR: PROF. ORAWON CHAILAPAKUL, Ph.D., CO-ADVISOR: PROF. TIRAYUT VILAIVAN, Ph.D., ADISORN TUANTRANONT, Ph.D., 102 pp.

This dissertation aimed to develop a novel biosensor using pyrrolidinyl peptide nucleic acid (acpcPNA) as a bioreceptor for the determination of DNA, which indicate the different types of disease. The topic in this research can be divided into 2 parts. The first part is the development of DNA sensors using paper-based analytical device coupled with electrochemical detection. Square-wave voltammetry (SWV) and electrochemical impedance spectroscopy (EIS) were used for the quantification of human papillomavirus (HPV) and *Mycobacterium tuberculosis* (MTB), repectively. These systems offer sensitive determination with a low detection limit of 2.3 nM (HPV) and 1.24 (MTB). The second part is the development of DNA sensors using paper-based analytical device coupled with colorimetric detection. The proposed biosensor was designed for the simultaneous determination of Middle East Respiratory Syndrome coronavirus (MERS-CoV), MTB and HPV. Silver nanoparticles (AgNPs) was used as a colorimetric reagent to obtain the color change, which is dependent on the DNA concentration. The limit of detection was found to be 1.53, 1.27 and 1.03 nM for MERS-CoV, MTB and HPV, respectively. The selectivity for three developed biosensor was demonstrated by the outstanding properties of acpcPNA. Moreover, the developed biosensors were successfully applied to detect DNA target in biological sample. These results indicate that the proposed paper-based DNA sensors have potential to be an alternative device for low-cost, simple, sensitive and selective for DNA detection relative to traditional methods.

Field of Study: Petrochemistry
Academic Year: 2016

Student's Signature .....
Advisor's Signature .....
Co-Advisor's Signature .....
Co-Advisor's Signature .....

ACKNOWLEDGEMENTS

Firstly, I would like to express my deepest appreciation to my thesis advisor, Professor Dr. Orawon Chailapakul, for her helpful advice, kind encouragement and excellent support throughout my Ph.D. study. Her guidance helped me to overcome problems and accomplish the related research.

My sincere appreciation also goes to my co-advisor, Prof. Dr. Tirayut Vilaivan and Dr. Adisorn Tuantranont for kind support, encouragement, guidance and giving a new knowledge. Without their participation and input, this dissertation could not have been successfully conducted.

Special thanks also extend to Professor Dr. Charles S. Henry from Colorado State University. For my 6 mounts in his group, I am extremely grateful for his kind supports and affectionate encouragement. I am also thankful for Professor Dr. Toshihiko Imato, who provided me an opportunity to join his group as an internship. Thanks to all member in his group for friendship and valuable experiences.

I would also like to thank to associate Professor Dr. Weena Siangproh for the continuous support from time to time. She constantly provided contribution and excellent advice with enthusiasm and kindness.

Additionally, I would like to thank my thesis examination committee, Assistance Professor Dr. Warinthorn Chavasiri, Associate Professor Dr. Sirilux Poompradub and Associate Professor Dr. Nattaya Ngamrojanavanich, who gave helpful comments and suggestions in this dissertation.

I also would like to acknowledge the financial support during my Ph.D. from Thailand Graduate Institute of Science and Technology (TG-44-09-55-014D), the 90th Anniversary of Chulalongkorn University Fund (GCUGR1125582020D) and the Ratchadapisek Sompoch Endowment Fund (2016), Chulalongkorn University (CU-59-008-HR).

I am thankful for the members of electrochemical group at Chulalongkorn University for their help, kindness, warm friendship and all experiences we have had in the last five years.

Finally and most importantly, I would like to express my sincerest gratitude and deepest appreciation to my beloved family and especially my affectionate parents. This dissertation would not have been possible without their helpfulness, financial support, and encouragement throughout my education and my life.

CONTENTS

Page

Page

Page

Page

Page

LIST OF TABLES

LIST OF FIGURES

LIST OF ABBREVIATIONS

DNA	Deoxyribonucleic Acid
RNA	Ribonucleic Acid
PNA	Peptide Nucleic Acid
acpcPNA	Pyrrolidinyl Peptide Nucleic Acid
PADs	Paper-based Analytical Devices
AEG	N-(2-amino-ethyl) glycyl
μm	Micrometer
CV	Cyclic Voltammetry
SWV	Square-Wave Votammetry
E_p	Peak potential
$E_{p,a}$	Anodic peak potential
$E_{p,c}$	Cathodic peak potential
i_p	Peak current
$i_{p,a}$	Anodic peak current
$i_{p,c}$	Cathodic peak current
n	Number of electron
A	Electrode area
D	Diffusion coefficient
ν	Scan rate
EIS	Electrochemical Impedance Spectroscopy
Ac	Acetyl
AQ	Anthraquinone
G	Graphene
PANI	Polyaniline
HPV	Human papillomavirus
POC	Point-of-care
ePADs	Electrochemical Paper-based Analytical Devices
HMDE	Hanging Mercury Drop Electrode

NMP	N-methyl-2-pyrrolidone
WE	Working Electrode
CE	Counter Electrode
RE	Reference Electrode
CSA	Camphor-10-sulfonic acid
TEM	Transmission Electron Microscopy
Glu	Glutamic acid
Lys	Lysine
MS	Mass Spectrometer
TFA	Trifluoroacetic Acid
µL	Microliter
nM	Nanomolar
PBS	Phosphate Buffer Saline
PCR	Polymerase Chain Reaction
Hz	Herze
mV	Millivolt
min	Minute
SPCE	Screen-Printed Carbon Electrode
R_{ct}	Charge-transfer resistance
Ω	Ohm
K_{et}	Heterogeneous electron-transfer rate constant
F	Faraday's constant
LOD	Limit of detection
LOQ	Limit of quantitation
MWCNT	Multi-walled Carbon Nanotubes
PtE	Platinum Electrode
Ch	Chitosan
AuE	Gold Electrode
AuNRs	Gold nanorods
PT	Polythionine
GCE	Glassy Carbon Electrode

RSD	Relative Standard Deviation
AgNPs	Silver nanoparticles
MERS-CoV	Middle East respiratory syndrome coronavirus
MTB	*Mycobacterium tuberculosis*
SNPs	Single-nucleotide polymorphisms
TB	Tuberculosis
RT-PCR	Reverse Transcription Polymerase Chain Reaction
AuNPs	Gold nanoparticles
mL	Milliliter
HPLC	High Performance Liquid Chromatography
PDMS	Polydimethylsiloxane
DNA_{com}	Complementary DNA
DNA_{nc}	Non-complementary DNA
CCC	Critical Coagulation Concentration
NaCl	Sodium Chloride
DNA_{m1}	Single-base mismatch
DNA_{m2}	Two-base mismatch
SD	Standard Deviation
BSA	Bovine Serum Albumin
3DPAD	Three-dimensional Paper-based Analytical Device

CHAPTER I
INTRODUCTION

1.1 Introduction

Nowadays, biosensor has become popular in numerous fields including environmental [1-3], food analysis [4-6] and in the area of human health monitoring and diagnostics [7-9]. Biosensor is a small devices consisting of two main parts, including biological element and physical transducer. The selective biological element acts as bioreceptor for recognizing a specific analyte [10-12] while a physical transducer converts the change of biological reaction into a measurable signals, which are proportional to the concentration of analytes [13-15]. In general, analytical techniques used for bio-analysis require a complicated steps, much labor, time and expensive instruments whereas biosensors eliminate the need of the sample preparation and hence offer great promise for several on-site analytical applications of rapid and low cost measurements which could be in remote areas where sophisticated instrument facilities are not available [16].

Nucleic acids, such as DNA or RNA, are the sensing element which has been extensively used as a probe for a wide range of biosensors and bio-analytical assays [17]. The general concept of DNA-based biosensor relies on the highly specific hybridization of the probe with its complementary strands of DNA/RNA. The probe is one of the key parameters that control the selectivity of the detection. While most DNA biosensors commonly used short oligonucleotides as a probe, there are limitations such as low specificity due to the electrostatic repulsion between probe and DNA target. To overcome these issues, other alternative probes have been used with great success in recent years.

Peptide nucleic acid (PNA) [18, 19], a synthetic polymer designed to mimic the structure and function of DNA, has attracted increasing interest in term of DNA biosensors with high sensitivity and specificity. PNA consists of a peptide-like backbone replacing the sugar-phosphate in natural DNA or RNA. PNA has been widely

applied as biomolecular probe in biochemical sensing applications due to its excellent characteristics, such as sequence-specific binding to DNA or RNA, resistance to nuclease and protease enzyme, and strong binding to the target DNA.

Recently, Vilaivan's group proposed a new conformationally pyrrolidinyl PNA system (acpcPNA) which possesses an α,β-peptide backbone deriving from D-proline/2-aminocyclopentanecarboxylic acid [20-22]. A stronger binding affinity and higher specificity toward complementary DNA compare to DNA and Nielsen's PNA make acpcPNA a potentially useful probe for DNA biosensor [23-26].

In order to improve the DNA biosensor for diagnostic devices especially for developing countries, the crucial factors to be considered are cost, operational simplicity as well as speed and efficiency, especially for early stage screening of biomarkers specific for the disease of interest. Towards this goal, paper-based analytical devices (PADs) have attracted much interest as an alternative sensor designed for point-of-use application [27, 28]. Currently, there are two detection modes being coupled with PADs, including electrochemical and colorimetric detections. Electrochemical detection has attracted much attention and rapidly increased since it provides a good combination of simplicity, low power requirements, low limits of detection, and ease of quantitation. Colorimetric assays are also appropriate detection mode for PADs mainly because the signal readout can be made without requiring specialized instruments. It provided semi-quantitative results that can be detected by visually observing changes in color [29, 30]. Moreover, quantitative analysis of colorimetric assays can be accomplished by using optical technologies such as digital cameras [31, 32] and scanners [33, 34] in combination with an image processing software to extract the color hue and/or intensity and convert these values to the amount of the analytes.

In this dissertation, paper-based DNA biosensor was developed for determination of disease biomarkers using the outstanding properties of acpcPNA as a probe. The proposed system was divided into 2 sections based on the detection mode: electrochemical and colorimetric detections. Three developed systems are described as follows;

1. Electrochemical paper-based peptide nucleic acid biosensor for detecting human papillomavirus.
2. Electrochemical impedance-based DNA sensor using pyrrolidinyl peptide nucleic acid for MTB detection.
3. Multiplex paper-based colorimetric DNA sensor using pyrrolidinyl peptide nucleic acid-induced AgNPs aggregation for detecting MERS-CoV, MTB and HPV oligonucleotides.

To achieve the best analytical performance, various experimental conditions were optimized. These developed systems were successfully used for quantitative detection of the interested analytes with high sensitivity and selectivity. The performance of the devices were also compared with other reported methods.

1.2 Research objectives

The three main goals of this work are as follow:

1. To develop paper-based DNA biosensor with electrochemical and colorimetric detection for the determination of disease biomarker using acpcPNA as a sensing probe.
2. To investigate unique strategy to improve the sensitivity for each system.
3. To apply these proposed systems for the determination of the target analyte in relevant biological samples.

1.3 Scope of the research

To achieve the research objective in this work, paper-based DNA biosensors with electrochemical and colorimetric detection were developed. acpcPNA was used as a sensing probe which is the key element to determine the detection selectivity. Using optimal condition, analytical performance of each system including linear working range, detection limit, reproducibility and stability were examined. To evaluate the applicability of these systems, the proposed DNA biosensors were applied to measure the specific analytes (HPV, MTB and MERS-CoV DNA) in biological samples. All results were discussed in this dissertation.

CHAPTER II

THEORY

2.1 Biosensor

The term “biosensor” refers to “an analytical device that converts biological reactions into measurable signals which are proportional to analyte concentration” [35]. This sensing device comprised of two major components including a specific biological element and physical component. Biological element such as enzymes, antibody, nucleic acid and cell are used to recognize and interact with their specific analyte. Physical components are usually referred to as transducers which convert the interactions into signals. Figure 2.1 shows schematically components of a typical biosensor.

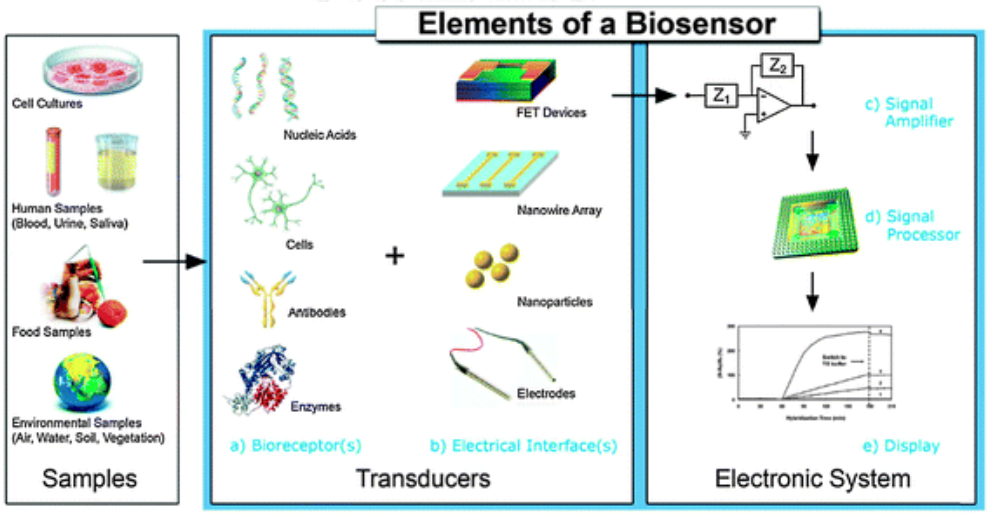

Figure 2.1 A schematic representation of biosensor components [36].

2.1.1 Principle

The general principle of a biosensor consists of two parts in combination: a bio-recognition component and transducer. A biological entity that can interact specifically with other biological element, often called a bioreceptor, such as enzyme, nucleic acid and antibody is used to recognize

with a specific analyte. The transducer part then converts the biochemical interaction of the analyte with the bioreceptor into measurable electronic or other signals, which ideally should be proportional to the analyte concentration.

2.1.2 Types of biosensors

Biosensors can be classified into two types based on bio-recognition element and transduction modes. Bio-recognition elements can be further separated into many types such as immunosensors (enzymes, antibodies), DNA-based sensor (nucleic acid) and whole cell biosensors (micro-organisms). The basis of different transducers biosensors relies on the physiochemical change resulting from bio-recognition element. Hence, the type of transducers biosensors can be classified as electrochemical (amperometric, potentiometric and conductometric), optical (absorbance, fluorescence and chemiluminense), thermal and mass-based signal transduction. The types of biosensors are summarized as shown in Figure 2.2.

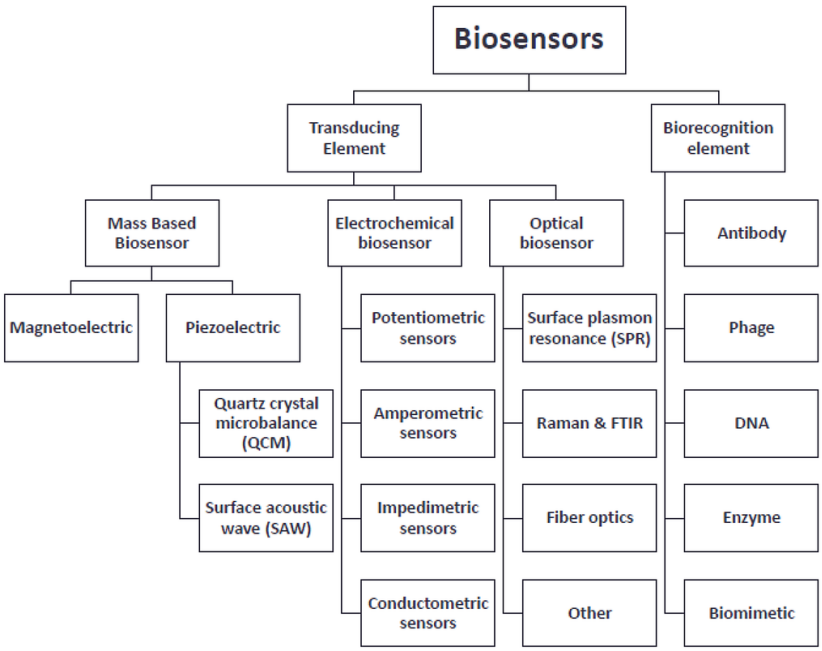

Figure 2.2 Types of biosensors [37].

2.1.2.1 Electrochemical biosensor

Electrochemical transducers are mainly served as the transduction elements. The basic principle of electrochemical biosensor is based on the chemical reaction generating ion or electrons which cause the change in electrical properties of solution and can be used as measuring parameter. A typical electrochemical biosensor consists of three electrode system. A sensing working electrode and reference electrode separated by an electrolyte. A counter electrode is used to complete the circuit for current flow. Electrochemical biosensor can be divided depended on the measuring electrical parameters such as

(i) Potentiometric: the measuring variations in open circuit potential.
(ii) Amperometric: the measuring of currents due to the electroactive species reduction or oxidation.
(iii) Impedimetric: the impedance measuring of the system upon immobilization of biolayers onto the electrode surface.

2.1.2.2 Optical biosensor

The typical concept of optical biosensor is relied on the interaction of optical field with a biorecognition element. There are two general modes of optical biosensor, including label-free and label-based [38]. The label-free is performed by monitoring signal generated directly by the interaction between analyte and transducer. On the other hand, label-based mode relies on the use of a label provided the optical signal which can be detected by a colorimetric, fluorescent or luminescent assay.

2.2 Bioreceptor

Bioreceptor is designed to interact with the specific analyte to produce a signal that will be converted into a measurable signal by the transducer. High selectivity for the specific analyte among a matrix of other chemical or biological components is a

key requirement of the bioreceptor. While the type of biomolecule used can vary widely, biosensors can be divided based on common types bioreceptor interactions including: anitbody/antigen, enzymes/ligands, nucleic acids/DNA, cellular structures/cells, or biomimetic materials.

Peptide nucleic acid (PNA) is one important class of bioreceptor for sensing of nucleic acid analytes. PNA is designed to mimic the DNA ability of hybridizing to complementary DNA, RNA or PNA on the basis of Watson-Crick base pairing [39, 40]. The neutral and achiral PNA backbone comprised of N-(2-amino-ethyl) glycyl (AEG) units linked by peptide bonds instead of the negatively-charged sugar-phosphate backbone of DNA. Figure 2.3 shows the comparison of structures between PNA and DNA structures. The nucleobases are attached to the backbone via tertiary amide linker. PNA offers great affinity and specificity in binding to the target DNA/RNA [41]. One of the most impressive feature of PNA is the stronger binding between complementary PNA/DNA strands than between complementary DNA/DNA strands at low to medium ionic strength. This is attributed to the lack of charge repulsion between the PNA strand and the DNA strand [18]. Interestingly, not only is the affinity higher for PNA/DNA duplexes, but the specificity was also higher. PNA has therefore been widely applied as a biomolecular probe for DNA/RNA sensing applications.

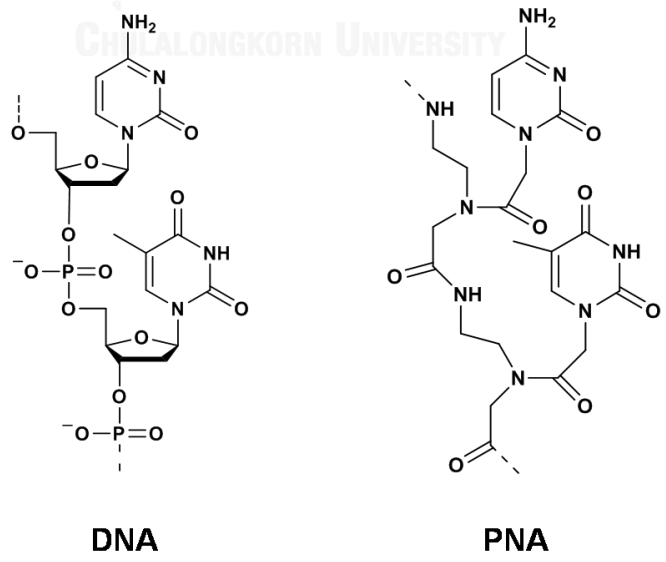

Figure 2.3 The comparison of structures between DNA and PNA [42].

Recently, Vilaivan's group [22] proposed a new conformationally pyrrolidinyl PNA system (known as acpcPNA) which possesses an α,β-peptide backbone deriving from D-proline/2-aminocyclopentanecarboxylic acid (Figure 2.4). The conformational constraints controlled by the pyrrolidine ring and the β-amino acid are key requirements determining the binding efficiency.

AcpcPNA exhibits a strong binding affinity and a high specificity towards a complementary target DNA, RNA and also self-hybridization. This ability is affected by its structure and stereochemistry of the PNA backbone. AcpcPNA binds to DNA with outstanding affinity and sequence specificity of (2′R,4′R)-proline/(1S,2S)-2 aminocyclopentanecarboxylic backbone. acpcPNA also binds to RNA in a highly sequence-specific fashion, even if with lower affinity than to DNA. In addition, acpcPNA provides high specificity of antiparallel binding to DNA and a low tendency for self-hybridize. These properties make acpcPNA as a promising probe for various biological applications.

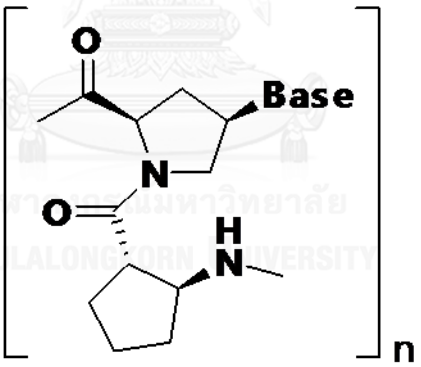

Figure 2.4 The structure of acpcPNA.

2.3 Paper-based analytical device

The traditional paper-based platform, such as a pregnancy strip test and a diabetes strip test, has been widely used and commercially available. The basic concept of these devices depends on the specificity between antigens and antibodies. The qualitative analysis can be observed by the visible color changed when the antigen flows and binds to the gold conjugated antibody. The results

provide only “yes” or “no” answer which is insufficient for diagnosis owing to the level of analytes may be linked to the degree of treatment. Paper-based analytical devices (PADs) are therefore introduced as a quantitative analysis device.

In 2007, Whitesides et al. [43] created the first PADs for quantitative analysis of glucose and protein using colorimetric assay. The level of glucose and protein were monitored via the intensity of color measured by digitizing in each assay zone which is proportional to the glucose and protein concentration as shown in Figure 2.5.

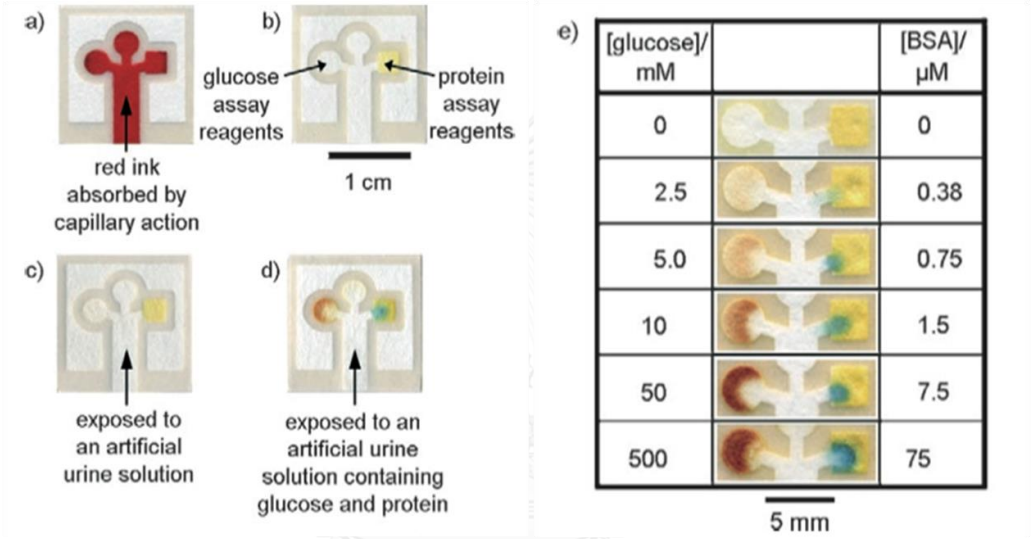

Figure 2.5 PADs for determination of glucose and protein concentrations in an artificial urine solution [43].

Nowadays, PADs has continuously gained interests as alternative analytical device since it offers great promising to be a point-of-care sensor. The material used for fabrication of this device platform is paper which provided numerous advantages as follow [44];

1. Can be made for the cost effective device due to its inexpensiveness and abundance.
2. Solution can flow naturally through paper via capillary force.
3. Can be chemically modified since it provides a plenty of –OH on the cellulose surface.
4. Convenient to observe the colorimetric tests due to being usually white so

it provides a strong contrast between a colored reaction and the background.

5. Flammable and biodegradable which is suitable to use as a disposable and environmentally friendly device.

Of these attractive and useful properties, PADs have been extensively used for applications ranging from environmental analysis to clinical diagnostic assays [45].

2.4 Fabrication method

The fabrication method has also played an important role in term of cost effectiveness and mass production of PADs. There are several methods for fabricating PADs including photolithography, plotting, plasma etching, inkjet etching, cutting and wax printing as summarized below;

Table 2.1 Fabrication methods of PADs.

Method	Advantages	Disadvantages
Photolithography [46, 47]	A wide variety of paper up to 360 μm in width.	Channels are exposed to polymers and solvents.
Plotting [48]	- Channels are not exposed to polymers or solvents. - Hydrophobic barriers are flexible.	Requires a customized plotter.
Plasma etching [49]	Useful for laboratories equipped with a plasma cleaner	- Metal masks must be made for each pattern. - Cannot produce arrays of free-standing hydrophobic patterns.
Inkjet printting [50]	Reagents can be printed directly into the test zones using the printer.	Hydrophilic channels are exposed to polymers and solvents.
Cutting [51]	Hydrophilic channels are not exposed to polymers or solvents.	Devices must be encased in tape.

Method	Advantages	Disadvantages
Wax printing [52]	- Rapid - Hydrophilic channels are not exposed to polymers or solvents.	Requires only a commercially available printer and hot plate.

Recently, the wax printing has been extensively used for rapid mass production of PADs. For wax printing method, the hydrophobic pattern is printed onto the paper surface using a commercial wax printer. The wax-printed paper is then heated to allow the penetration of wax into the paper generating a hydrophobic barrier. The wax printing method is shown in Figure 2.6.

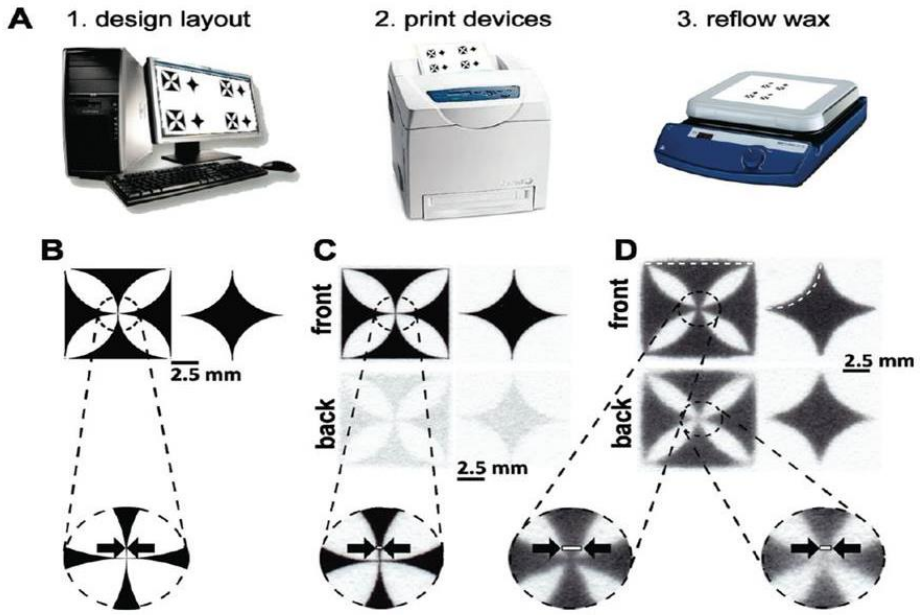

Figure 2.6 Patterning wax patterned PADs by wax printing method [53].

2.5 Detection method

Various techniques have been reported as a detection mode incorporating with PADs including electrochemistry [28, 54], colorimetry [26, 33], fluorescene [55, 56] and mass spectrometry [57, 58]. These techniques provide outstandingly sensitive

and selective detection. However, high equipment cost and difficulty to use for on-site analysis is the major obstacle. In this dissertation, electrochemical and colorimetric detection were selected as the detection mode to couple with PADs since they offer a combination of simplicity, low-cost and portable.

2.5.1 Electrochemical detection

Electrochemical detection has been extensively integrated with PADs due to its high sensitivity, easy to use, low cost and portable. This technique can be divided in five major groups including potentiometry, voltammetry, coulometry, conductometry, and dielectrometry [59]. Votammetry such as cyclic voltammetry (CV) and square-wave votammetry (SWV) were used as the electrochemical sensing in this dissertation. Moreover, electrochemical impedance spectroscopy (EIS) was also performed to achieve the electrochemical characterization of modified electrode and the quantitative analysis for label-free based sensor.

2.5.1.1 Cyclic votammetry

Cyclic voltammetry (CV) [60] is the most widely used technique for obtaining qualitative information of electrochemical reactions. It is generally used to study the electrochemical properties of an analyte in solution. CV consists of scanning linear potential sweeping using a triangular potential waveform, as shown in Figure 2.7A. During the potential sweep, the current resulting from the applied potential was measured. The relationship between current and potential plot is termed as cyclic voltammogram.

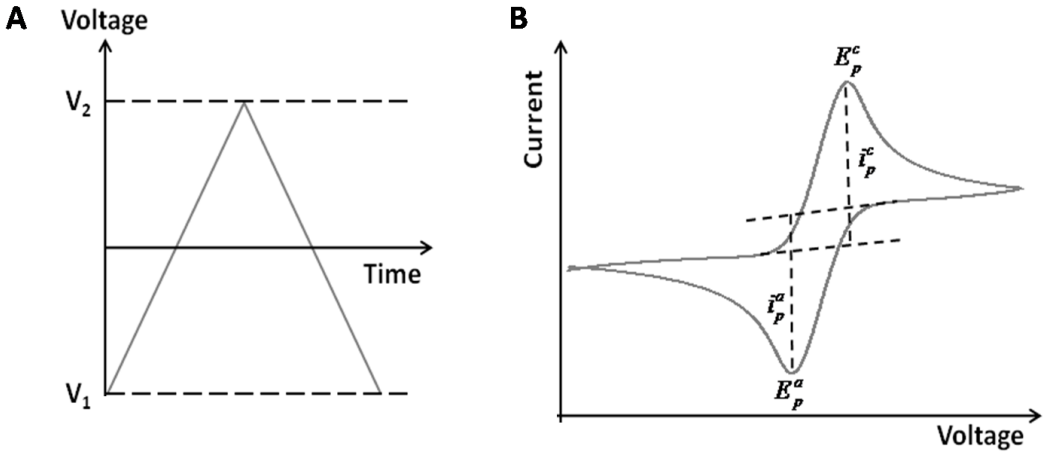

Figure 2.7 (A) Potentail-time excitation wave forms for cyclic voltammetry and (B) its output.

Figure 2.7B demonstrate the cyclic votammogram which plotted as current (i) vs. potential (E). CV measurements were characterized by a peak potential. E_p is the potential at which the current reaches its maximum value; i_p is the value that is called the peak current. The $i_{p,a}$ and $E_{p,a}$ are the anodic peak current and anodic peak potential, respectively. The $i_{p,c}$ and $E_{p,c}$ are the cathodic peak current and cathodic peak potential, respectively.

There are two general systems of CV including reversible and irreversible system. The shapes of these two systems are shown in Figure 2.8. The peak current for a reversible couple is given by the Randles-Sevcik equation below:

$$i_p = 2.69\times10^5 n^{3/2} A D^{1/2} C \nu^{1/2} \quad \text{at } 25^\circ\text{C} \qquad \text{(Equation 2.1)}$$

Where *n:* The number of electron

A: The electrode area (cm^2)

D: The diffusion coefficient ($cm^2 \cdot s^{-1}$)

C: The concentration of electroactive species ($mol \cdot cm^3$)

ν: The potential scan rate ($V \cdot s^{-1}$)

For irreversible processes, the individual peaks are reduced in size and widely separated. The peak current given by

$$i_p = (2.99\times10^5)n(\infty n_a)^{1/2}ACD^{1/2}\boldsymbol{\nu}^{1/2} \quad \text{at } 25^\circ\text{C} \quad \text{(Equation 2.2)}$$

Where *n:* The number of electron

A: The electrode area (cm^2)

D: The diffusion coefficient ($cm^2 \cdot s^{-1}$)

C: The concentration of electroactive species ($mol \cdot cm^3$)

$\boldsymbol{\nu}$: The potential scan rate ($V \cdot s^{-1}$)

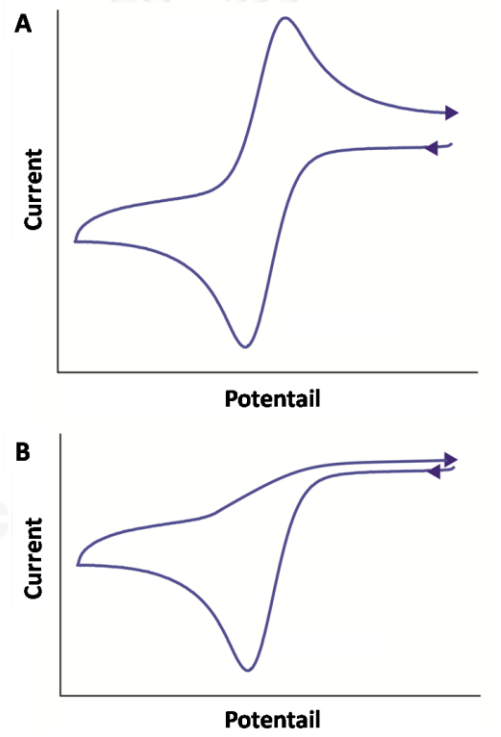

Figure 2.8 Typical shape of (A) reversible and (B) irreversible cyclic voltammogram.

2.5.1.2 Square-wave voltammetry

Square-wave voltammetry (SWV) [60] is a large-amplitude differential technique. Its waveform imposed on a symmetric staircase potentail as shown in Figure 2.9. The forward pulse is coincident with the staircase step in time

while the reverse cycle decrease the half way of the staircase step. The current is measured twice during square-wave cycle at the end of the forward (t_1) and reverse pulse (t_2). The difference between the two measurements plotted versus the base staircase potential is termed as square-wave voltammogram.

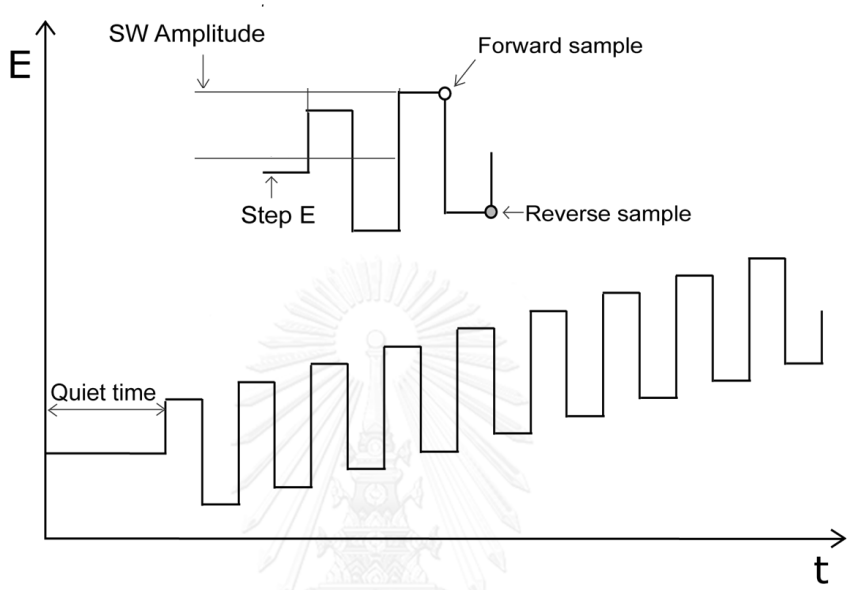

Figure 2.9 Potentail excitation waveforms for square-wave voltammetry.

The electrochemical responses of the forward, reverse, and difference currents are given in Figure 2.10. The resulting peak-shaped voltammogram is symmetric about the half-wave potential, and the peak current is proportional to the concentration. Excellent sensitivity accrues from the fact that the net current is larger than either the forward or reverse components.

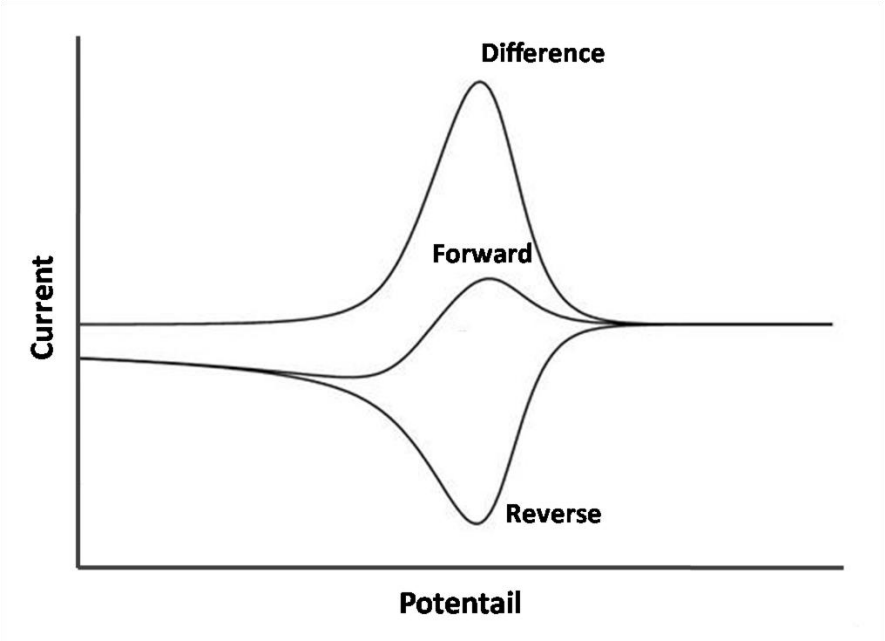

Figure 2.10 Electrochemical responses for square-wave voltammetry.

2.5.1.3 Electrochemical impedance spectroscopy

Electrochemical impedance spectroscopy (EIS) [60] has been employed as a sensitive technique to monitor the electrical response of a solid/liquid system which provides information concerning the solid/liquid interface. EIS is a non-destructive steady-state technique that is capable of probing the relaxation phenomena over a range of frequencies.

EIS is an analysis method of the complex electrical resistance. This method is sensitive to surface phenomena and changes of bulk properties. The impedance (Z) is generally observed by applying a voltage perturbation with small amplitude and detecting the current response. The impedance is a complex value, since the current can differ not only in terms of the amplitude but it can also show a phase shift ϕ compared to the voltage-time function. The Z value can be described by the real part (Zr) and the imaginary part (Zi) of the impedance as shown in Figure 2.11.

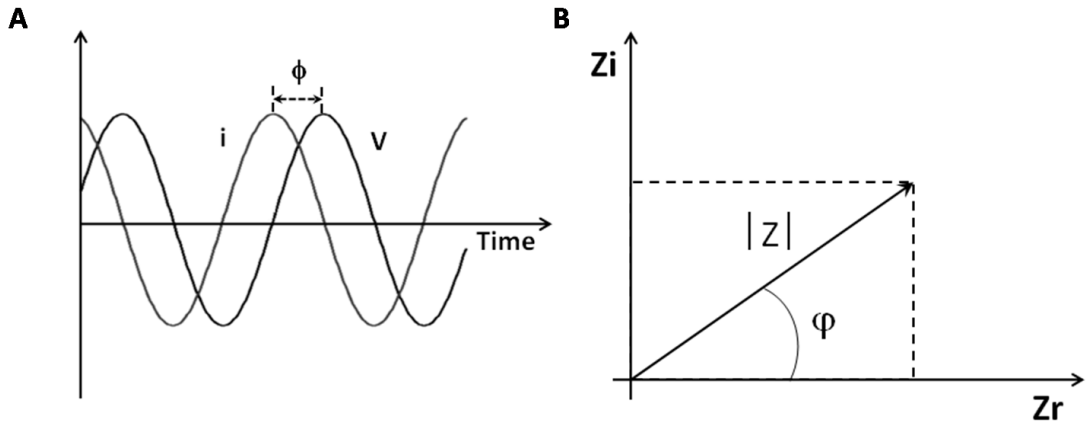

Figure 2.11 (A) Response of sinusoidal current in a linear system. (B) The expression of Z.

The results of an impedance measurement can be illustrated in two different ways: a Nyquist plot and a Bode plot. For the Nyquist plot, the impedance (Figure 2.12A) can be represented as a vector (arrow) of length |Z |. The angle between this vector and x-axis, commonly called the phase angle, is ϕ (=argZ). This plot results from electrical circuit of Figure 2.12B.

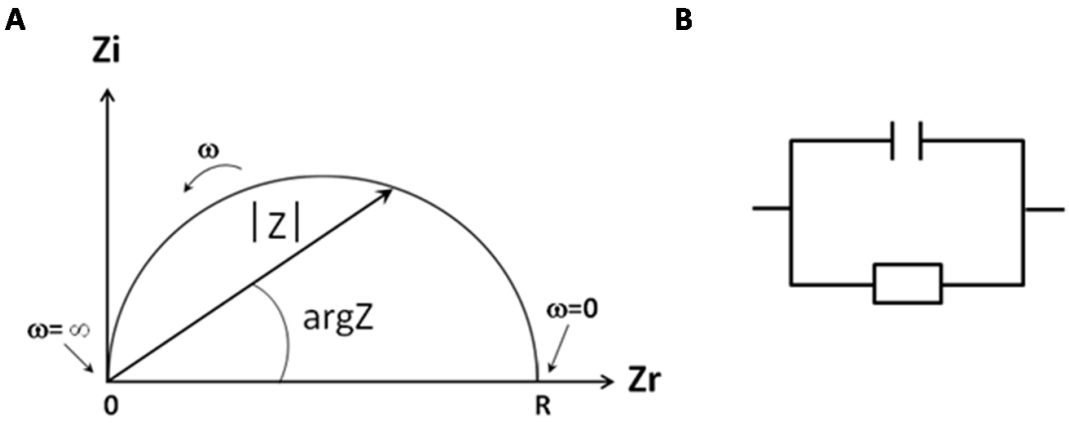

Figure 2.12 (A) Nyquist plot with impedance vector and (B) equivalent circuit with one time constant.

Another popular representation method is the Bode plot. The impedance is plotted with log frequency on the x-axis and both the absolute values of the impedance ($|Z| = Z_0$) and the phase-shift on the x-axis.

In the typical biosensor application of EIS, the biological component is immobilized on the working electrode and the interaction with an analyte molecule is detected. The impedance of the sensing electrode (the working electrode modified with the biological component) controls the overall impedance.

2.5.2 Colorimetric detection

Colorimetric detection is a method for determining the chemical compound in a solution using the change of a color reagent. The change in color intensity which is proportional to the concentration of the analyte can be determined by using a digital camera or scanner [31, 34]. Figure 2.13 illustrates the procedure of the quantitative analysis. Scanner or camera-based optical detection was used to record the color intensity. The mean intensity of recorded image is observed by readily available software such as Adobe Photoshop or Image J. This detection mode provides the benefits of simplicity, rapidity and inexpensiveness. In addition, the image from the field analysis can be transmitted electronically and digitally to the laboratory and the analyzed results can be returned in real-time to the testing site.

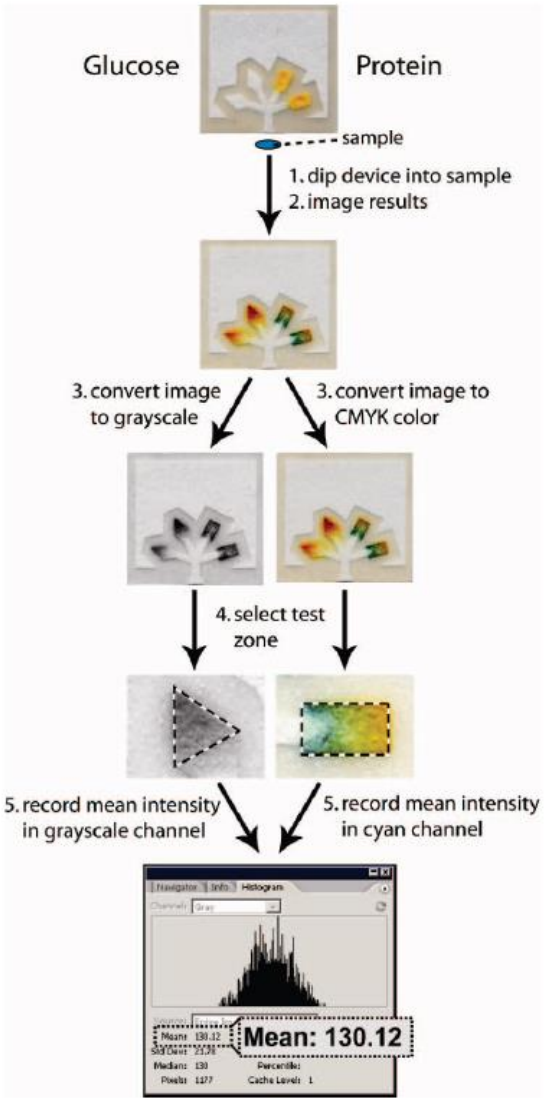

Figure 2.13 Procedure for quantifying of colorimetric detection using the Adobe Photoshop program [61].

CHAPTER III

DEVELOPMENT OF DNA SENSORS USING PAPER-BASED ANALYTICAL DEVICE COUPLED WITH ELECTROCHEMICAL DETECTION

3.1 Electrochemical paper-based peptide nucleic acid biosensor for detecting human papillomavirus

Prinjaporn Teengam[a], Weena Siangproh[b], Adisorn Tuantranont[c], Charles S. Henry[d], Tirayut Vilaivan[e], Orawon Chailapakul[f,g,*]

[a]Program in Petrochemistry, Faculty of Science, Chulalongkorn University, Pathumwan, Bangkok, 10330, Thailand

[b]Department of Chemistry, Faculty of Science, Srinakharinwirot University, Bangkok, 10110, Thailand

[c]Nanoelectronics and MEMS Laboratory, National Electronics and Computer Technology Center, Pathumthani, 12120, Thailand

[d]Department of Chemistry, Colorado State University, Fort Collins, Colorado, 80523, United States

[e]Organic Synthesis Research Unit, Department of Chemistry, Faculty of Science, Chulalongkorn University, Pathumwan, Bangkok, 10330, Thailand

[f]Electrochemistry and Optical Spectroscopy Research Unit, Department of Chemistry, Chulalongkorn University, Pathumwan, Bangkok, 10330, Thailand

[g]Nanotec-CU Center of Excellence on Food and Agriculture, Bangkok, 10330, Thailand

[*]Corresponding author

Analytica Chimica Acta 952 (2017) 32-40.

ABSTRACT

A novel paper-based electrochemical biosensor was developed using an anthraquinone-labeled pyrrolidinyl peptide nucleic acid (acpcPNA) probe (AQ-PNA) and graphene-polyaniline (G-PANI) modified electrode to detect human papillomavirus (HPV). An inkjet printing technique was employed to prepare the paper-based G-PANI-modified working electrode. The AQ-PNA probe baring a negatively charged amino acid at the N-terminus was immobilized onto the electrode surface through electrostatic attraction. Electrochemical impedance spectroscopy (EIS) was used to verify the AQ-PNA immobilization. The paper-based electrochemical DNA biosensor was used to detect a synthetic 14-base oligonucleotide target with a sequence corresponding to human papillomavirus (HPV) type 16 DNA by measuring the electrochemical signal response of the AQ label using square-wave voltammetry before and after hybridization. It was determined that the current signal significantly decreased after the addition of target DNA. This phenomenon is explained by the rigidity of PNA-DNA duplexes, which obstructs the accessibility of electron transfer from the AQ label to the electrode surface. Under optimal conditions, the detection limit of HPV type 16 DNA was found to be 2.3 nM with a linear range of 10-200 nM. The performance of this biosensor on real DNA samples was tested with the detection of PCR-amplified DNA samples from the SiHa cell line. The new method employs an inexpensive and disposable device, which easily incinerated after use and is promising for the screening and monitoring of the amount of HPV-DNA type 16 to identify the primary stages of cervical cancer.

Keywords: Graphene, Polyaniline, Paper-based electrochemical DNA biosensor, acpcPNA, Electrochemical detection, Human papillomavirus

3.1.1. Introduction

The most important factors for diagnostic devices, especially for developing countries, are low cost, simplicity and speed of results for early screening and monitoring of disease biomarkers. To achieve this goal, paper-based analytical devices (PADs) have been widely used as an alternative device design for point-of-care (POC) applications [31, 62, 63]. Two detection modes that have been most frequently used with PADs include colorimetric and electrochemical detections. Since first reported by Dungchai et al. [54], PADs with electrochemical detection (ePADs) have increasingly attracted attention as they offer a combination of simplicity, low power requirements, low limits of detection, and ease of quantitation [28, 64-66]. ePADs are therefore an ideal platform for developing sensitive, selective DNA biosensors for point-of-care applications.

In electrochemical DNA biosensors, many different electrode types have been used, including a gold [67-69], hanging mercury drop (HMDE) [70, 71] and various carbon-based materials [72-75]. Carbon is considered a good electrode material due to its low cost, wide potential range, chemical inertness and low background current. Furthermore, carbon electrodes have a fast response time and can be easily fabricated in different configurations. These features make carbon suitable for use in ePAD DNA biosensors. However, the use of micro-scale electrodes as part of ePAD is a major obstacle due to limited sensitivity. To overcome this problem, graphene (G) has been used as a carbon-based nanomaterial and has achieved significant popularity due to the large specific surface area and unique electrochemical properties of G [76-78]. G-based electrodes exhibited superior performance compared to other carbon-based electrodes in terms of their electro-catalytic activity and electrical conductivity [79, 80]. G has also been used in combination with various types of functional materials to fabricate high-performance electrodes. Among them, polyaniline (PANI) is a useful conducting polymer that has been widely used for electronic, optical and electrochemical applications such as enzyme-based biosensors and

DNA assays due to its excellent environmental stability and unusual doping/dedoping chemistry [81-83]. Moreover, PANI improves the dispersion and reduces the agglomeration of the planar sp2-carbon of G [81, 84]. PANI also possesses free amino groups, which can act as a handle for the covalent immobilization of suitable detection probes via amide bonds [85, 86]. Finally, doped PANI possesses the positive charge of the amino group, which can immobilize negatively-charged probes via electrostatic interactions. Thus, it is a challenge to evaluate alternative systems for immobilization of various bio-recognition elements via electrostatic interaction.

For most electrochemical DNA biosensors, a probe that is designed to detect a specific sequence of target DNA is first immobilized on the electrode. Then, the electrochemical signal of an electroactive species, which was either covalently attached to the probe or added later as an indicator, is recorded and compared before and after the hybridization with the complementary DNA target [70, 87]. The probe is a key parameter that determines the detection selectivity. While most DNA biosensors employ short oligodeoxynucleotide probes, several alternative probes have been used with great success. Peptide nucleic acid (PNA) [18, 88], a synthetic DNA mimic with a peptide-like backbone of repeating N-(2-aminoethyl)-glycine units replacing the sugar-phosphate in natural DNA or RNA, has attracted increasing interest as the probe for electrochemical DNA biosensors [70, 89-91] due to its sequence-specific binding to DNA or RNA, resistance to nuclease and protease enzymes, and strong binding to the target DNA. Recently, Vilaivan's group [20-22] proposed a new conformationally constrained pyrrolidinyl PNA system (known as acpcPNA) that possesses an α,β-peptide backbone derived from D-proline/2-aminocyclopentanecarboxylic acid. This new acpcPNA demonstrates a stronger binding affinity and higher specificity towards complementary DNA compared to DNA and Nielsen’s PNA, and there are several applications of acpcPNA as a probe for DNA biosensors [23, 24, 92].

Human papillomavirus or HPV is the common virus that can be passed through any type of sexual contact. There are some high-risk types of HPV including type 16 and 18, which can cause abnormal changes to the cells of the cervix. These changes can lead to cervical cancer which, is one of the most important health problems for woman. The mortality occurring from cervical cancer has continuously increased especially in developing countries that have limited medical facilities [93].

In our previous work [92], the electrochemical sensor based-on acpcPNA probe for HPV detection was reported. Although the good limit of detection (LOD) was achieved, the use of PVC-based sensor was costly and the procedure relies on covalent method for probe immobilization was complicated and time-consuming. Cost is the most critical challenge for disposable POC electrochemical sensors. In this work, using PAD has potential to address all of challenges of disposable sensor in term of low-cost and simple fabrication. Electrostatic immobilization is also a key step of this work. This method eliminated the complicate steps of covalent process and significantly reduced time. Moreover, inkjet printing used for electrode modification step is advantageous due to it provided electrode reproducibility and high pattern resolution [94]. Inkjet-printing is scalable of mass production, while small amount of modifier is wasted in the modification process.

Here, we aim to develop a novel paper-based electrochemical DNA biosensor using an AQ-labeled acpcPNA probe in combination with a G-PANI modified electrode. In this new DNA biosensor, the acpcPNA probe labeled with anthroquinone (AQ) was first incorporated onto a G-PANI-modified ePAD using electrostatic immobilization. In the absence of complementary DNA, a strong signal was observed for the AQ. Hybridization with the complementary DNA target resulted in a decrease of the electrochemical signal that linearly correlated with the concentration of the target. The application of the biosensor to the sensitive detection of HPV DNA type 16 is demonstrated. The proposed method is applicable to the screening and monitoring of HPV-DNA

type 16 in the primary stage of cervical cancer, a disease that leads to the death of women around the world, particularly in developing countries that have limited resources for public healthcare.

3.1.2. Materials and methods

3.1.2.1 Chemicals and materials

Graphene (G) was purchased from A.C.S (Medford, USA). Polyaniline, camphor-10-sulfonic acid ($C_{10}H_{16}O_4S$), glutamic acid and N-methyl-2-pyrrolidone (NMP) were ordered from Sigma Aldrich (St.Louis, USA). Carbon and silver/silver chloride ink were obtained from Gwent group (Torfaen, United Kingdom). The screen-printed block was made by Chaiyaboon Co. Ltd. (Bangkok, Thailand). The labeling electroactive spices, 4-(anthraquinone-2-oxy)butyric acid**,** was synthesized as described previously [23]. Analytical grade reagents, including NaCl, KH_2PO_4, Na_2HPO_4 and KCl, were purchased from Merck and used without further purification. Synthetic oligonucleotides which correspond to partial sequences of HPV type 16 and other types of high risk HPV (HPV types 18, 31 and 33) used in the specificity test, were obtained from Pacific Science (Bangkok, Thailand). The sequences of the DNA oligonucleotides used are shown in Table 3.1.1.

Table 3.1.1 List of oligonucleotides

Oligonucleotide	Sequence (5'-3')
Complementary DNA (HPV type 16)	5'-GCTGGAGGTGTATG-3'
Non-complementary DNA 1 (HPV type 18)	5'-GGATGCTGCACCGG-3'
Non-complementary DNA 2 (HPV type 31)	5'-CCAAAAGCCCAAGG-3'
Non-complementary DNA 3 (HPV type 33)	5'-CACATCCACCCGCA-3'

The forward (5'-CACTATTTTGGAGGACTGGA-3') and reverse primer (5'-GCCTTAAATCCTGCTTGTAG-3') used for the PCR cell-line samples were purchase from Pacific Science (Bangkok, Thailand). The cervical cancer cell-lines with (SiHa) HPV types 16 were obtained from the Human Genetics Research Group, Department of Botany, Faculty of Science, Chulalongkorn University.

3.1.2.2 Apparatus

The electrochemical measurements using square-wave voltametry (SWV) were performed using a CHI1232A electrochemical analyzer (CH Instruments, Inc., USA). A three electrode system was used and the working electrode was a G-PANI-modified screen-printed carbon electrode (4 mm in diameter). The electrochemical impedance spectroscopy (EIS) was carried out using PGSTAT 30 potentiostat (Metrohm Siam Company Ltd., Switzerland) in a solution of 0.1 M PBS with the frequency range from 0.1 to 10^{-5} Hz. The Dimatix™ Materials Printer (DMP-2800, FUJIFILM Dimatix, Inc., Santa Clara, USA) was used for the electrode modification. JEM-2100 transmission electron microscope (Japan Electron Optics Laboratory Co., Ltd, Japan) was used for characterization of G-PANI composites. MALDI-TOF MS spectra was performed on a Microflex MALDI-TOF mass spectrometer (Bruker Daltonik GmbH, Bremen, Germany).

3.1.2.3 Fabrication of a paper-based electrochemical DNA sensor

A paper-based electrochemical DNA sensor was fabricated using the wax-printing method [95, 96]. Initially, the patterned paper was designed using Adobe Illustrator and printed onto the filter paper (Whatman No.1) using a wax printer (Xerox Color Qube 8570, Japan). The printed paper was then placed on a hot plate (175 ºC, 50 s) to melt the wax and create a hydrophobic barrier. For electrode fabrication, three electrode systems were prepared using an in-house screen-printing method. First, carbon ink was screened as a working electrode

(WE) and counter electrode (CE). Afterward, silver/silver chloride was screened as a reference electrode (RE) and conductive pad. The basic design of the paper-based electrochemical DNA biosensor was shown in Figure 3.1.1.

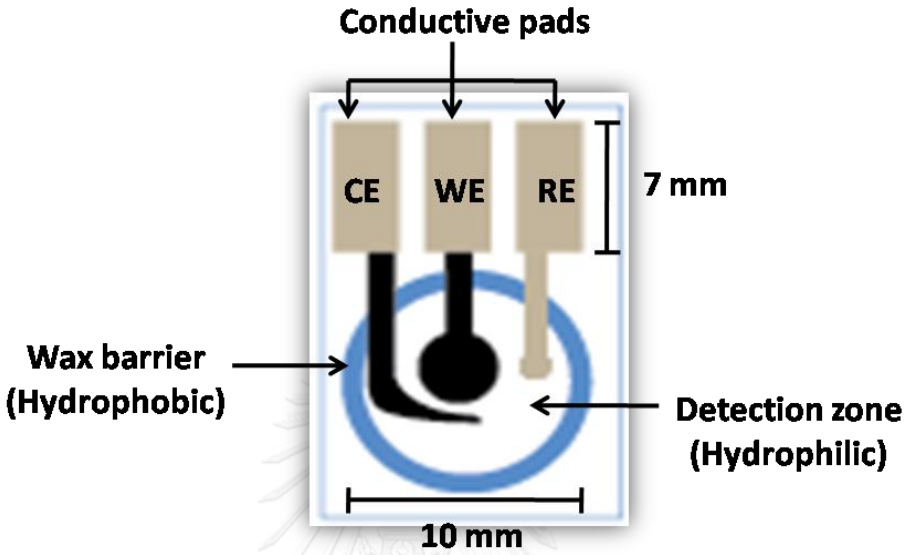

Figure 3.1.1 The basic design of paper-based electrochemical DNA biosensor consisting of WE, working electrode (4 mm i.d.); RE, reference electrode and CE, counter electrode.

3.1.2.4 Inkjet-printing of a G-PANI composite modified paper-based electrochemical DNA biosensor

Prior to electrode modification, a G-PANI composite was prepared using a physical mixing method following procedures extracted from relevant literature [97]. Graphene powder (10 mg) was dispersed in N-methyl-2-pyrrolidone (NMP) and sonicated for 20 h at room temperature. Subsequently, 20 mg of PANI (emeraldine base) was doped with 25 mg of camphor-10-sulfonic acid (CSA) to generate a positively charged amino group and also dissolved in 10 mL of NMP. For the preparation of the G-PANI conductive ink, the solutions of G and PANI were mixed together and stirred for 1 h. The mixture was centrifuged at 5000 rpm and filtered through a 0.43 μm filter membrane before

use. The morphology of G-PANI conductive ink was characterized by transmission electron microscopy (TEM).

For electrode modification, the G-PANI composite solution was used as the ink for inkjet printing. The G-PANI conductive ink was loaded into a cartridge and printed onto the working electrode of the paper-based electrochemical DNA sensor using a Dimatix™ Materials Printer (DMP-2800, FUJIFILM Dimatix, Inc., Santa Clara, USA) at 30 °C, 20 V of applied voltage and 25 µm of drop spacing. Modification of the electrode is shown in Figure 3.1.2A. Six layers of G-PANI composite solution were printed onto the surface area of the working electrode. Next, the modified electrode was heated at 65 °C for 30 min to dry the solvents from the G-PANI conductive ink.

3.1.2.5 Synthesis and labeling of the acpcPNA probe

The acpcPNA probe with the sequence Ac-$(Glu)_3$-CATACACCTCCAGC-Lys(AQ)NH_2 (written in the N⟶C direction, Ac = acetyl; AQ = anthraquinone; Glu = glutamic acid; Lys = lysine) was designed to detect 14 base synthetic oligonucleotide target with a sequence corresponding to human papillomavirus (HPV) type 16. The probe, referred to as AQ-PNA, was synthesized by solid-phase peptide synthesis using Fmoc chemistry as previously described [20]. The probe was modified with three glutamic acid residues at the N-terminus to incorporate the negative charge, which was followed by end-capping with an acetyl group. At the C-terminus, the acpcPNA probe was labeled with anthraquinone (AQ) via 4-(anthraquinone-2-oxy) butyric acid to the amino side chain of a C-terminal lysine residue. The progress of the reaction was monitored by MALDI-TOF-MS analysis on a Microflex MALDI-TOF mass spectrometer (Bruker Daltonik GmbH, Bremen, Germany). The modified PNA on the solid support was treated with 1:1 (v/v) aqueous ammonia:dioxane in a sealed tube at 60 °C overnight to remove the nucleobase protecting groups. Following cleavage from the solid support with trifluoroacetic acid (TFA), the AQ-PNA was purified by reverse-phase HPLC (C18 column, 0.1% (v/v) TFA in

H_2O-MeOH gradient). The identity of AQ-PNA was verified by MALDI-TOF MS analysis, and the purity was confirmed to be >90% by reverse-phase HPLC.

3.1.2.6 Immobilization and hybridization of the PNA probe

First, the AQ-PNA probe (3 µL, 125 nM) was immobilized onto the G-PANI modified screen-printed carbon electrode surface by the drop-casting method and incubated for 15 min at room temperature. Next, 50 µL of PBS was placed onto the electrode surface. After immobilization of the probe, the AQ-PNA/G-PANI/SPCE modified electrode was hybridized with 3 µL of target DNA for 15 min. Then, the electrochemical signal response was measured using square-wave voltammetry. The immobilization and hybridization procedures are illustrated in Figure 3.1.2B.

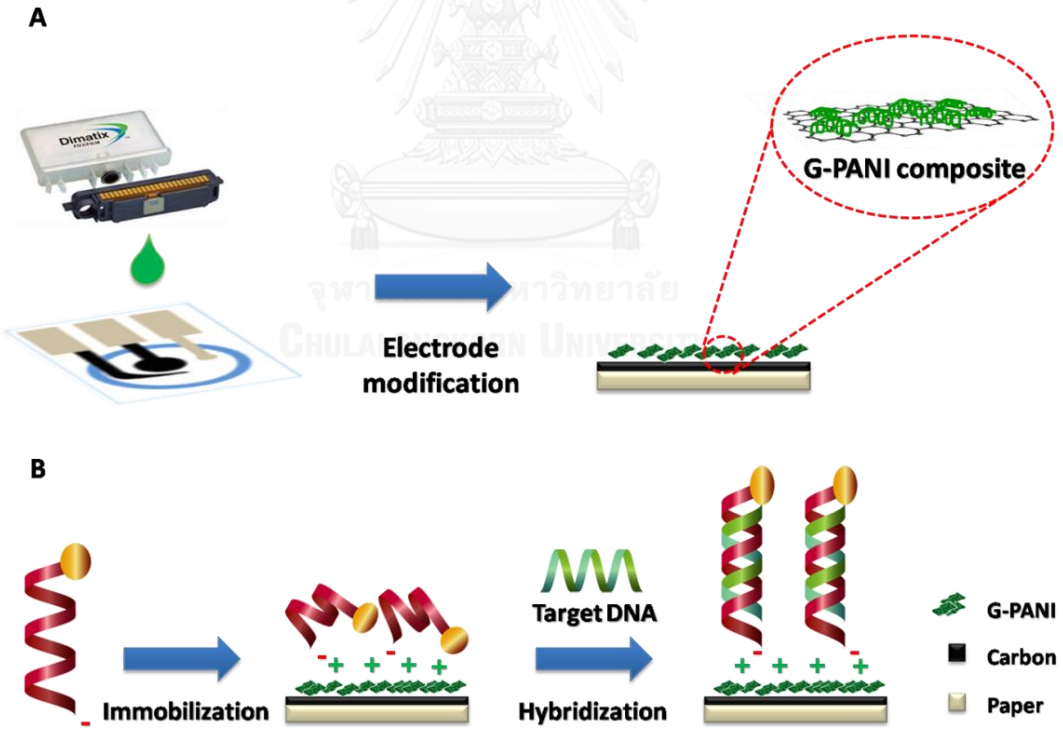

Figure 3.1.2 Schematic illustration of (A) electrode modification and (B) immobilization and hybridization steps of paper-based electrochemical DNA biosensor.

3.1.2.7 PCR amplification of the cell line DNA sample

The SiHa (HPV type 16 positive) cell line DNA sample was amplified using PCR as previously reported [92]. Briefly, the amplification mixture containing 0.2 mM deoxynucleotide triphosphate mixture, 1x buffer (KCl, Tris) + 1.5 mM $MgCl_2$, 0.5 U of Taq polymerase, 0.4 µM of each of the primers and 100 ng/µL of the cell line DNA sample was amplified at 95 ºC for 10 min, follow by 30 cycles at 52 ºC for 30 s and finally 72 ºC for 7 min. The success of the PCR was confirmed by gel electrophoresis in 2% (w/v) agarose TBE gel followed by staining with ethidium bromide and visualization under a UV-transilluminator.

3.1.2.8 Electrochemical measurement

For electrochemical measurements, the square-wave voltammetry was used throughout the experiment using a potentiostat (CHI1232A). After the immobilization process, 50 µL of PBS was dropped onto the modified working electrode, followed by adding the DNA target. Hybridization with AQ-PNA probe was done for 15 min. The electrochemical detection was performed under the optimal parameters including a frequency of 20 Hz, an amplitude of 100 mV and a step potential of 20 mV. The electrochemical signal after the hybridization was measured and compared with the signal in the absence of the DNA sample.

3.1.3 Results and Discussion

3.1.3.1 Characterization of the G-PANI conductive ink

To confirm the success of the preparation of the G-PANI conductive ink, the morphology of the ink was characterized by transmission electron microscopy (TEM). Figure 3.1.3A shows a TEM image of the G-PANI composite, which indicates a strong dispersion of G inside the composites without aggregation. Moreover, the electron diffraction pattern of G (Figure 3.1.3B) matches very well with the standard, single crystal graphene.

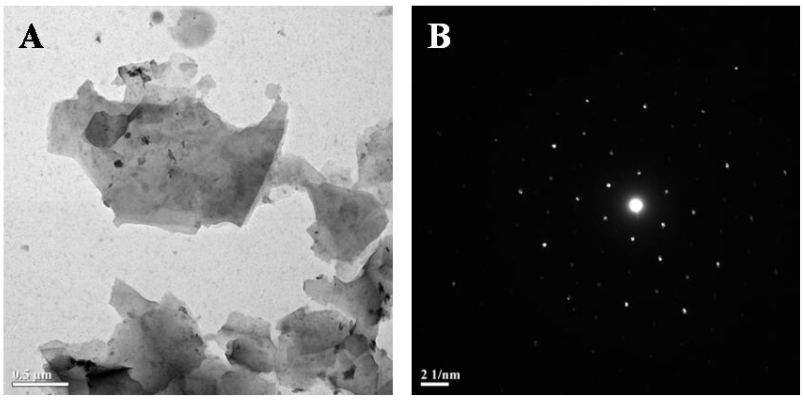

Figure 3.1.3 (A) TEM image of G-PANI (B) Electron diffraction of G.

The influence of the G-PANI ratio on the electrochemical conductivity of the modified electrodes was investigated. The anodic current of 1.0 mM $[Fe(CN)_6]^{3-/4-}$ in a 0.1 M KCl solution was measured using different proportions of G and PANI. Interestingly, the anodic peak current of 1.0 mM $[Fe(CN)_6]^{3-/4-}$ increased with an increasing G:PANI ratio. The highest anodic current of $[Fe(CN)_6]^{3-/4-}$ was observed with the G-PANI modified electrode at the ratio of 1:2 indicating the optimal sensitivity of the modified sensor (Figure 3.1.4).

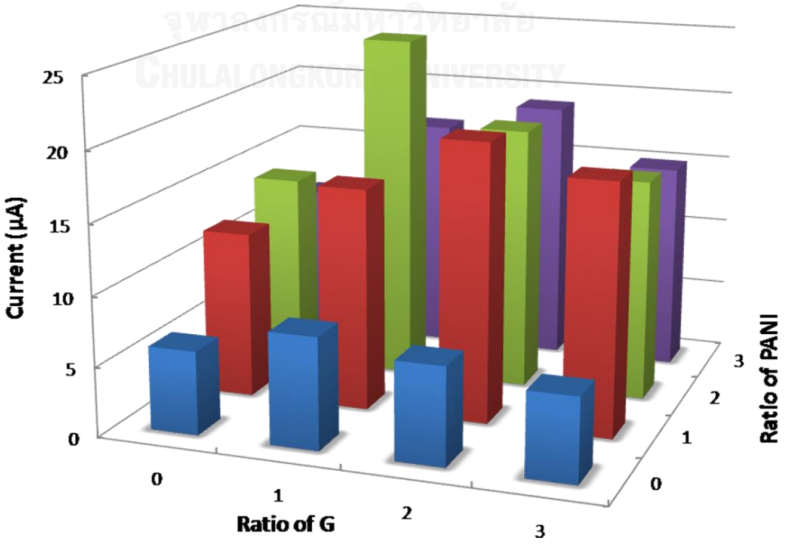

Figure 3.1.4 Comparison of anodic current of 1.0 mM $[Fe(CN)_6]^{3-/4-}$ in different ratio between graphene and polyaniline.

In addition, the peak currents gradually decrease for the higher G:PANI ratio, which could be due to the agglomeration of G within the G-PANI modifier [97]. Moreover, the effect of the number of printed G-PANI layers was also investigated as shown in Figure 3.1.5. The anodic peak current of 1.0 mM $[Fe(CN)_6]^{3-/4-}$ tends to increase with an increase in the number of G-PANI layers. However, the current of the printed G-PANI modified electrode slightly decreased over 6 printing layers. We also believe that this phenomenon arises from the aggregation of excess G on the modified electrode surface causing a decrease in the anodic current response.

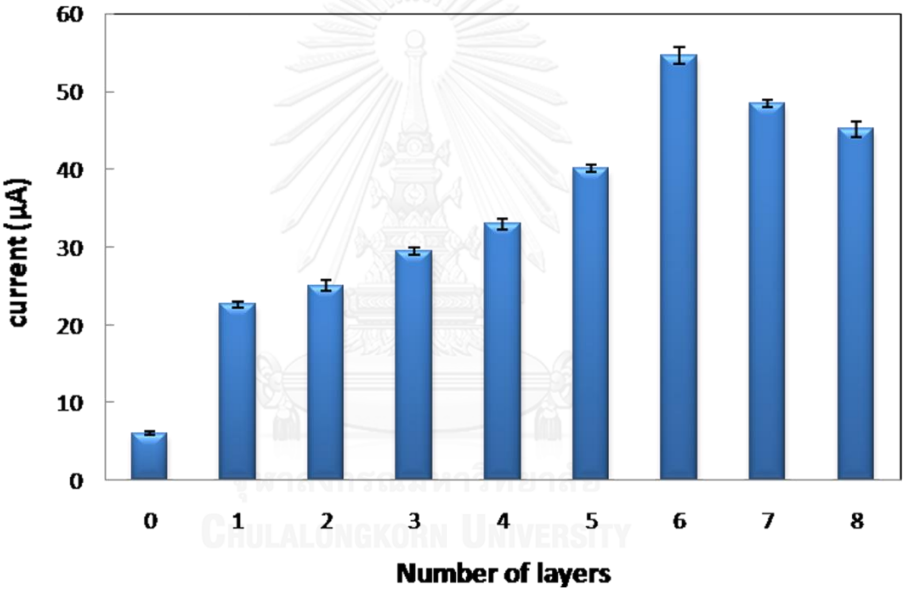

Figure 3.1.5 The effect of number of inkjet-printed layer on anodic current of 1.0 mM $[Fe(CN)_6]^{3-/4-}$.

Next, the electroactive surface area (A) of SPCE and G-PANI modified electrode were determined to illustrate that the G-PANI conductive ink increases the surface area of the SPCE by solving the Randles-Sevcik equation (equation 3.1.1):

$$I_p = (2.69 \times 10^5)\, n^{3/2} A C D^{1/2} v^{1/2} \qquad \text{(equation 3.1.1)}$$

Where I_p = current, n = number of electron transfer, C = concentration of electroactive species (mol cm^{-3}), D = diffusion coefficient (cm^2 s^{-1}) and v = scan rate (v s^{-1}). As shown in Figure 3.1.6, the cyclic voltamograms of 5.0 mM $[Fe(CN)_6]^{3-/4-}$ in a 0.1 M KCl solution for SPCE and G-PANI modified electrode were obtained. The current (i_p) is directly proportional to the square root of scan rate. According to the Randles-Sevcik equation, an approximate value of A was calculated to be 0.041 cm^2 and 0.222 cm^2 for SPCE and G-PANI modified electrode, respectively. This result provided a 5.4 times increase of electrode-electroactive surface area, thus, G-PANI conductive ink can improve the surface area of electrode, leading to enhance the sensitivity. As a result, the six G-PANI-layered modified electrode and the 1:2 ratio of G:PANI were considered to be the optimal conditions and were used for subsequent experiments.

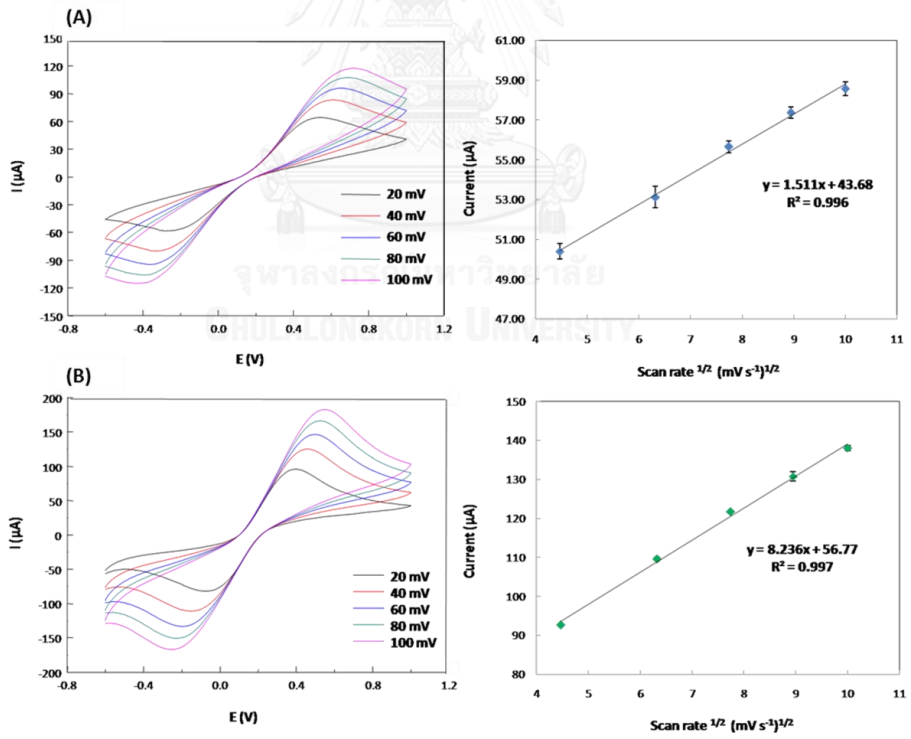

Figure 3.1.6 Cyclic voltamograms and the relationship between current and square root scan rate of (A) unmodified SPCE and (B) G-PANI modified electrode in 5.0 mM $[Fe(CN)_6]^{3-/4-}$ in a 0.1 M KCl at different scan rates.

3.1.3.2 Characterization of acpcPNA-labeled probe

In order to confirm the success of the synthesis and labeling of the AQ-PNA probe, MALDI-TOF mass spectrometry was used to characterize the unlabeled and labeled acpcPNA probes. The 14-mers unlabeled acpcPNA showed a mass peak at 4754 m/z. After labeling, the mass increased to 5477 m/z. This increase of 723 m/z coincides with the mass of AQ and three glutamic acid residues plus an acetyl group. Therefore, the labeling of the acpcPNA probe with the electroactive species and the negatively charged polyglutamate was confirmed.

3.1.3.3 Electrochemical characterization

Electrochemical impedance spectroscopy (EIS) was used to characterize the AQ-PNA probe immobilization onto the working electrode. In general, the shape of the semicircle portion obtained from the EIS spectrum relates to either the electron transfer limited process or electron transfer resistance. Figure 3.1.7A shows the Nyquist plots obtained from SPCE, G-PANI/SPCE and AQ-PNA/G-PANI/SPCE before and after hybridization with the target DNA in a solution of 1.0 mM $[Fe(CN)_6]^{3-/4-}$. Figure 3.1.7A (inset) shows the Nyquist curve of unmodified SPCE (red line) with an R_{ct} value of 27.5 kΩ. This value is larger than that obtained from G-PANI/SPCE, and indicates that the unmodified SPCE has a higher charge-transfer resistance. Therefore, the decrease in R_{ct} to 5.08 kΩ of G-PANI/SPCE (blue line) indicates that G-PANI improves the electron transfer rates. After the immobilization step (Figure 3.1.7A), the semicircular portion of AQ-PNA/G-PANI/SPCE (pink line) dramatically decreased with the R_{ct} value of 2.67 kΩ. This result can be explained theoretically as AQ is electroactive and can improve conductivity. Thus, the AQ-labeled PNA probe, which was immobilized onto the electrode surface, can facilitate the electron transfer process at the interface between the G-PANI/SPCE surface and the electrolyte. For this reason, the Nyquist curve of AQ-PNA/G-PANI/SPCE should have

possessed the smallest semicircular portion. In order to confirm the success of the immobilization of the AQ-PNA probe, the heterogeneous electron-transfer rate constant (K_{et}) value was obtained from equation (3.1.2), which shows the relationship between R_{ct} and K_{et}.

$$K_{et} = \frac{RT}{n^2F^2R_{et}AC_{redox}} \qquad \text{(equation 3.1.2)}$$

Where n = number of electron transfer, F = faraday's constant (KJ mol^{-1}), A = electrode surface area (cm^2), C_{redox} = concentration of the redox couple (mol cm^{-3}). From the equation, the K_{et} values for SPCE, G-PANI/SPCE and AQ-PNA/G-PANI/SPCE were calculated to be 7.45 x 10^{-5} cm s^{-1}, 40.28 x 10^{-5} cm s^{-1} and 76.70 x 10^{-5} cm s^{-1}, respectively. The increasing of K_{et} values inferred that the electron transfer process on AQ-PNA/G-PANI/SPCE is easier and faster than that on G-PANI/SPCE and SPCE. These results indicate that the negatively charged AQ-PNA probe was successfully immobilized onto the positively charged G-PANI modified electrode surface through electrostatic attraction.

Next, the electrochemistry of the immobilized AQ-PNA/G-PANI/SPCE probe before and after hybridization with the DNA target were investigated using square-wave voltammetry (SWV), (Figure 3.1.7B). The immobilization of the AQ-PNA/G-PANI/SPCE probe displayed a redox peak at approximately –0.65 V. After hybridization with an equimolar quantity of the complementary target DNA, the electrochemical response significantly decreased due to the increased rigidity of the PNA-DNA duplex relative to the native PNA probe. The rigidity hinders the electron transfer between the redox-active label (AQ) and the electrode surface [98, 99].

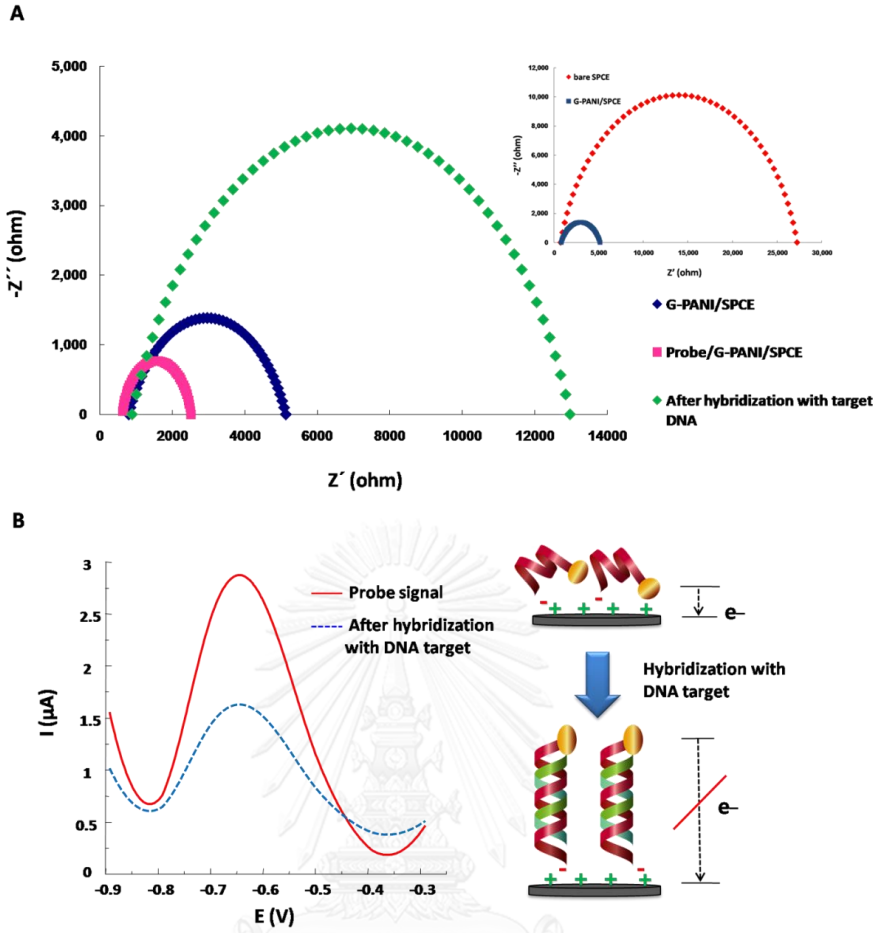

Figure 3.1.7 (A) Nyquist plot of SPCE (inset), G-PANI/SPCE (inset), AQ-PNA/G-PANI/SPCE before and after hybridization with target DNA in 0.1 M $[Fe(CN)_6]^{3-/4-}$. (B) Square-wave voltammograms of immobilized AQ-PNA probe on G-PANI/SPCE before and after hybridization with an equimolar concentration of target DNA.

3.1.3.4 Optimization of experimental variables

The experimental conditions were optimized next. The effect of AQ-PNA probe concentration on AQ electrochemical oxidation was investigated first. The oxidation current obtained for different concentrations of the AQ-PNA probe measured by square wave voltammetry are shown in Figure 3.1.8. The current continuously increased up to 125 nM. Above 125 nM, the current decreased significantly. The decrease in peak current at high AQ-PNA

concentrations can potentially be caused do to an increased thickness of the organic layer [100, 101], which leads to a lower electron transfer between AQ and the working electrode surface. Hence, the probe concentration of 125 nM was selected as the optimal concentration for further experiments.

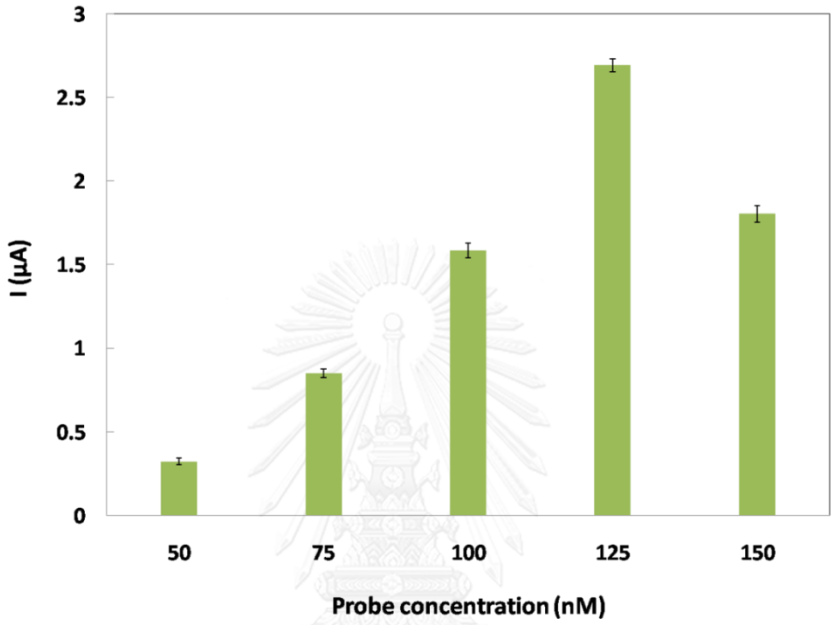

Figure 3.1.8 The effect of AQ-PNA probe concentration on AQ electrochemical oxidation during the immobilization step.

For electrochemical detection using SWV, the variable parameters including frequency, step potential and amplitude were optimized using a 125 nM AQ-PNA probe concentration without DNA target shown in Figure 3.1.9. The optimal parameters for electrochemical detection of this system was found to be 20 Hz of frequency, 100 mV of amplitude and 20 mV of step potential.

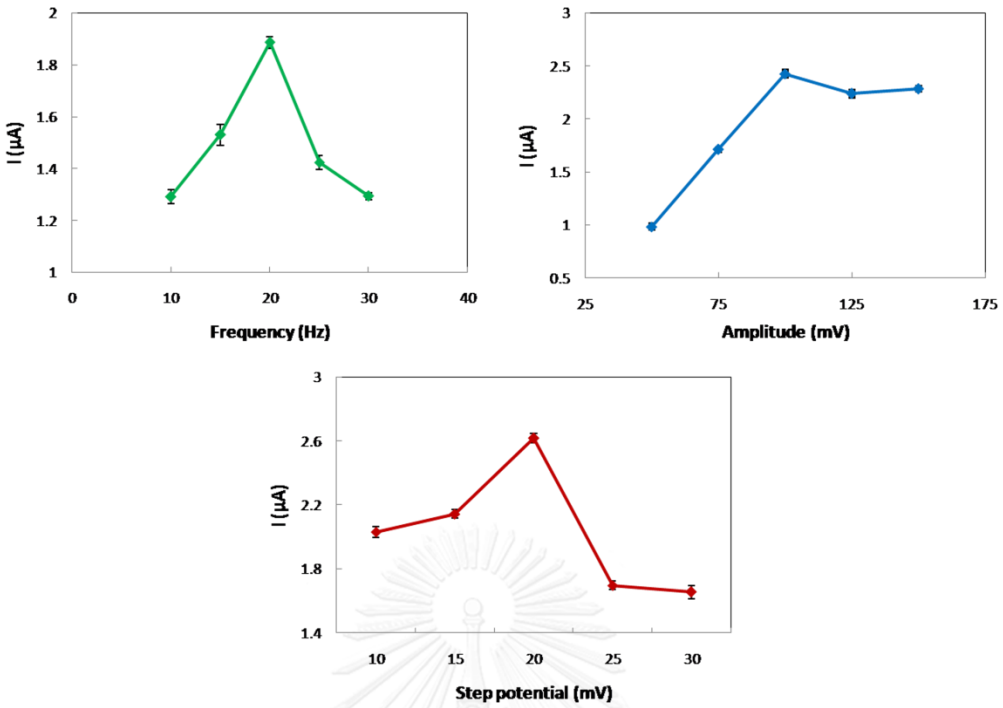

Figure 3.1.9 The optimal parameters for electrochemical detection using a 125 nM AQ-PNA probe concentration.

3.1.3.5 Analytical performance

To evaluate the analytical performance of the AQ-PNA/G-PANI/SPCE modified electrode, different concentrations of DNA target were determined using SWV analysis. Figure 3.1.10 shows the voltammograms as well as the calibration curve (inset) as a function of target DNA concentrations. The calibration curve provided a linear range from 10 nM to 200 nM with a correlation coefficient of 0.997. The limit of detection (LOD) and limit of quantitation (LOQ), which were calculated as the concentration that produced a signal at 3 times and 10 times of the standard deviation of the blank (N=5) [54], were found to be 2.3 nM and 7.7 nM, respectively. Our proposed method provides a wide linear range and sufficiently low detection limit for HPV detection. Table 3.1.2 shows a comparison of electrochemical performance between AQ-PNA/G-PANI/SPCE and the other modified electrodes used for HPV detection. It can be seen that a sufficiently low detection limit for HPV

detection could be obtained from our proposed method. Importantly, this ePAD DNA biosensor can be easily and inexpensively prepared compared to the other HPV DNA biosensors [92, 100, 102].

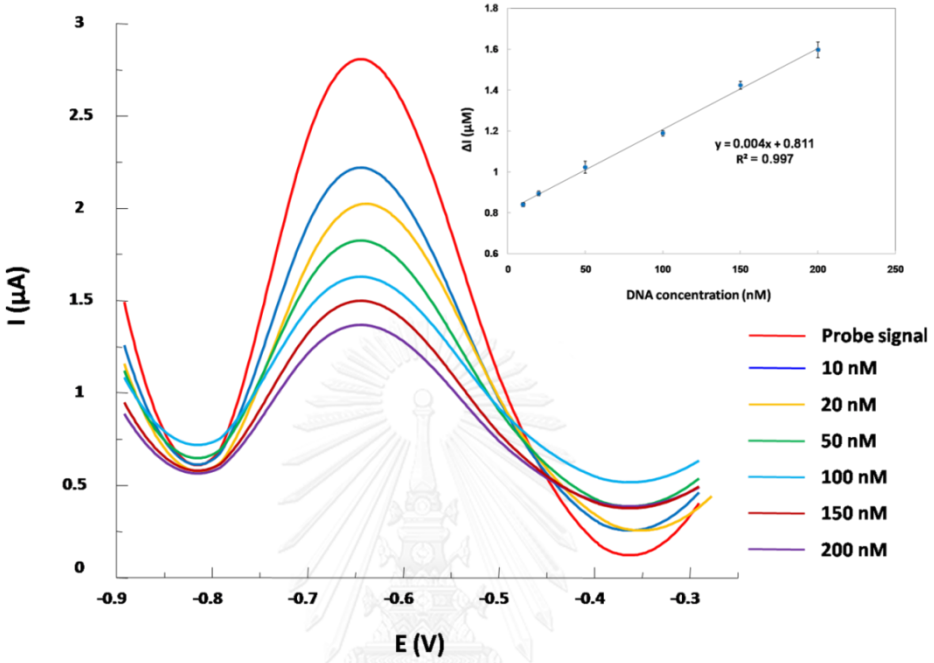

Figure 3.1.10 Square-wave voltamograms of AQ-PNA/G-PANI/SPCE after hybridize with the target DNA in the concentration range of 10-200 nM and the calibration plots of the change in the probe electrochemical current (ΔI) versus the target DNA concentration (inset) at optimal condition; 125 nM of AQ-PNA probe concentration, a frequency of 20 Hz, an amplitude of 100 mV and a step potential of 20 mV.

Table 3.1.2 Comparison of various electrochemical DNA biosensors for HPV detection.

Modified electrode	Probe	Method of probe immobilization	Linear range (nM)	LOD (nM)	Reference
PANI/MWCNTs/PtE	aptamer	covalent	10-50	0.49	[102]
L-Cysteine/AuE	DNA	covalent	18.75-250	18.13	[100]
Thionine/G/AuE	DNA	covalent	0.001-100	1.26×10^{-4}	[103]
G/AuNRs/PT/GCE	DNA	covalent	1×10^{-4}-10	0.4×10^{-4}	[104]
Ch/SCPE	acpcPNA	covalent	20-12×10^{3}	4.00	[92]
G-PANI/SCPE	acpcPNA	electrostatic	10-200	2.33	This work

3.1.3.6 Selectivity of the HPV type 16 detection

In order to investigate the selectivity of the acpcPNA probe, the current response obtained from the 14-nucleotide oligomer HPV type 16 DNA target was compared to non-complementary 14-nucleotide oligomers, which originate from the other types of high risk HPV (types 18, 31 and 33), under the same experimental conditions. As shown in Figure 3.1.11, a significantly different current was only obtained from the complementary DNA relative to the non-complementary DNA. Therefore, the immobilized AQ-PNA probe selectively binds to the HPV type 16 DNA target sequences. Accordingly, the proposed DNA biosensor demonstrated high selectivity to HPV type 16 DNA.

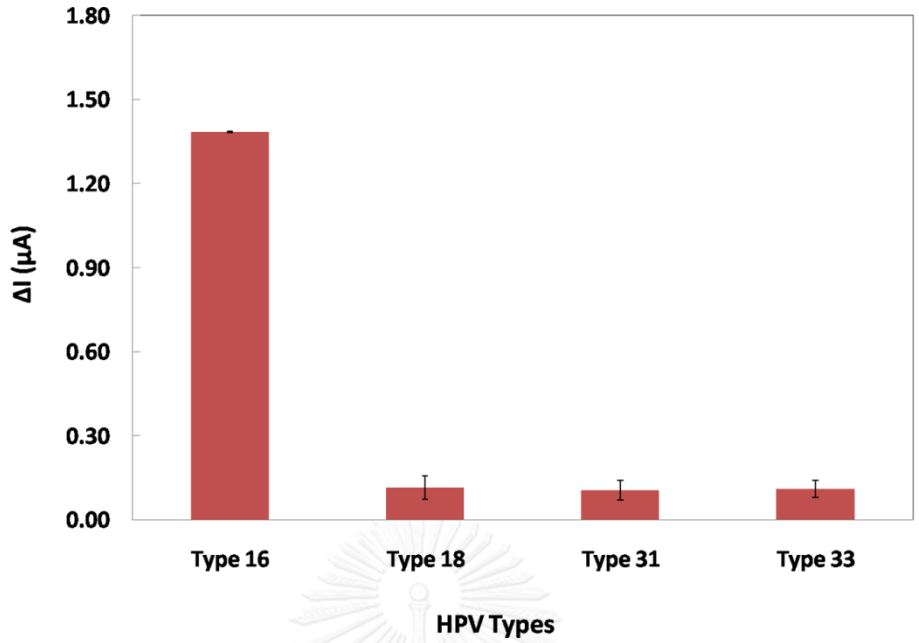

Figure 3.1.11 The electrochemical signal response derived from AQ-PNA/G-PANI/SPCE probe after hybridized with various HPV types.

3.1.3.7 Reproducibility and stability of the paper-based electrochemical DNA biosensor

The electrode-to-electrode reproducibility and stability of the paper-based electrochemical DNA biosensor was examined. The relative standard deviations (RSDs) of five electrodes were tested in the concentration range of 10-200 nM. The % RSDs was determined to be between 2.16% and 7.79%. These results indicate that the proposed DNA biosensor offers acceptable reproducibility. Moreover, the storage stability is another important parameter for DNA biosensor development. The ePAD DNA biosensor was stored at room temperature (25 °C) for 2 weeks before recording the current response to 10 nM target DNA. It was determined that 90.2% of the initial current response was retained in the aged sensor compared to the response obtained from the freshly prepared sensor. The stability of this DNA sensor is mainly attributed to the environmental stability of PANI.

3.1.3.8 Detection of the PCR DNA sample

To test the ePAD biosensor, DNA was extracted from the SiHa cell line, HPV type 16 and amplified using PCR. Figure 3.1.12A shows the SWV response of the proposed DNA biosensor in the presence of positive PCR products. It was observed that the current response decreased in the presence of the PCR product from the HPV type 16-positive cell line. Moreover, the current response decreased with increasing amounts of sample, as shown in Figure 3.1.12B. These results indicate that the paper-based electrochemical DNA biosensor has potential for detecting HPV type 16 DNA in PCR samples in clinical samples in future work.

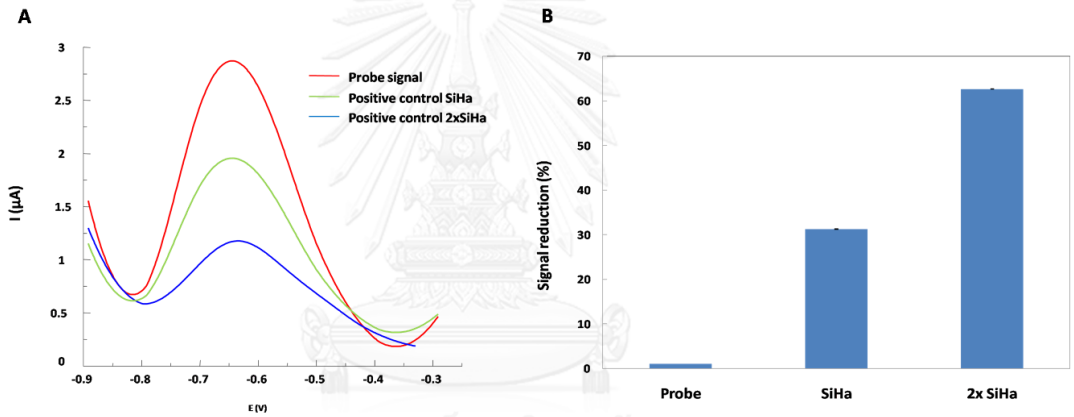

Figure 3.1.12 Square-wave voltammograms of AQ-PNA/G-PANI/SPCE probe in the presence of PCR-amplified HPV type 16 positive sample from SiHa cell-line.

3.1.4 Conclusions

A novel paper-based electrochemical DNA biosensor was developed and used for the determination of high-risk HPV type 16 using AQ-PNA probe immobilized on a G-PANI/SPCE modified electrode. The AQ-PNA probe was modified with negatively charged amino acids at the C-terminus to enable electrostatic immobilization on the cationic G-PANI electrode. Using SWV, the electrochemical current decreased after hybridization with the complementary

target DNA. Under optimal conditions, a linear range of 10-200 nM was obtained and the limit of detection was determined to be 2.3 nM. The proposed DNA sensor also exhibited very high selectivity against non-¬complementary 14-base oligonucleotides, including HPV types 18, 31 and 33 DNA. Finally, this sensing system was successfully applied to detect the PCR amplified DNA from HPV type 16 positive SiHa cells. As was demonstrated, several features make this highly sensitive ePAD DNA biosensor suited as an alternative tool for the diagnostic screening and detection of cervical cancer. First, the ePAD can provide a low-cost, disposable sensor for this POC application. Second, the immobilization through electrostatic attraction using G-PANI modified electrode is attractive relative to covalent immobilization because of its inherent simplicity. Third, the inkjet printing method for electrode modification process provides the potential for mass production while helping to reduce the variation among individual sensors, which is crucial for disposable sensor.

3.2 Electrochemical impedance-based sensor using pyrrolidinyl peptide nucleic acids for tuberculosis detection

Prinjaporn Teengam[†], Weena Siangproh[‡], Adisorn Tuantranont[§], Tirayut Vilaivan[‖], Orawon Chailapakul[#, ¶, *] and Charles S. Henry[¥,*]

[†]Program in Petrochemistry, Faculty of Science, Chulalongkorn University, Pathumwan, Bangkok, 10330, Thailand

[‡]Department of Chemistry, Faculty of Science, Srinakharinwirot University, Bangkok, 10110, Thailand

[§]Nanoelectronics and MEMS Laboratory, National Electronics and Computer Technology Center, Pathumthani, 12120, Thailand

[‖]Organic Synthesis Research Unit, Department of Chemistry, Faculty of Science, Chulalongkorn University, Pathumwan, Bangkok, 10330, Thailand

[#]Electrochemistry and Optical Spectroscopy Center of Excellence, Department of Chemistry, Chulalongkorn University, Pathumwan, Bangkok, 10330, Thailand

[¶]National Center of Excellence for Petroleum, Petrochemicals, and Advanced Materials, Chulalongkorn University, Pathumwan, Bangkok, 10330, Thailand

[¥]Department of Chemistry, Colorado State University, Fort Collins, Colorado 80523

*Corresponding authors

ACS Sensors (2017): Submitted manuscript.

ABSTRACT

A label-free electrochemical DNA sensor based on pyrrolidinyl peptide nucleic acid (acpcPNA)-immobilized paper-based analytical device (PAD) was developed. Unlike previous PNA-based electrochemical PAD (ePAD) sensors where the capture element was placed directly on the electrode, acpcPNA was covalently immobilized onto partially oxidized cellulose paper. As an example application, a sensor probe was designed for *Mycobacterium tuberculosis* (MTB) detection. The ePAD DNA sensor was used to quantify a synthetic 15-base oligonucleotide of MTB by measuring the fractional change in the charge transfer resistance (R_{ct}) obtained from electrochemical impedance spectroscopy (EIS). The R_{ct} of $[Fe(CN)_6]^{3-/4-}$ before and after hybridization with the target DNA could be clearly distinguished. Cyclic voltammetry (CV) was used to verify the EIS results, and showed an increase in peak potential splitting in a similar stepwise manner for each immobilization step. Under optimal conditions, a linear calibration curve in the range of 2-200 nM and the limit of detection 1.24 nM were measured. The acpcPNA probe exhibited very high selectivity for the complementary oligonucleotides over the single-base-mismatch, two-base-mismatch and non-complementary DNA targets. Moreover, ePAD DNA sensor platform was successfully applied to detect the PCR-amplified MTB DNA extracted from clinical samples. The proposed paper-based electrochemical DNA sensor has potential to be an alternative device for low-cost, simple, label-free, sensitive and selective DNA sensor.

Keywords: Paper-based electrochemical DNA biosensor, acpcPNA, Electrochemical impedance spectroscopy, Mycobacterium tuberculosis

3.2.1 Introduction

Tuberculosis (TB) is one of the top 10 causes of death worldwide. The current increasing in TB incidence rate and mortality become the crucial global health problems. In 2015, the World Health Organization (WHO) reported that 10.4 million people fell ill with TB and 1.8 million people died from this disease. In humans, TB is caused by mycobacteria, *M. tuberculosis* (MTB). Standard TB diagnostic methods rely on the identification of MTB and mainly employ sputum smear microscopy, culture of bacilli and/or polymerase chain reaction (PCR) [105-110]. Although these methods are sensitive, they have limitations. Sputum smear tests require trained personnel and use of a microscope to identify MTB. Bacillus culture and PCR are complicated and time-consuming methods. The requirement of highly trained personnel, sophisticated instrumentation and multiple detection steps limits the feasibility of applying these methods for routine diagnosis of TB in developing countries.

Detecting specific DNA sequences has attracted increasing attention for disease diagnosis. Many detection methods for point of care assays, including fluorescent [111], electrochemiluminescence [112], enzymatic [113], surface plasmon resonance [114] and electrochemical [25, 74, 90] have been proposed. Among the existing approaches, electrochemical DNA sensors have become an interesting option as they offer simplicity, portability and low-cost. Generally, electrochemical DNA sensors rely on oligonucleotide probes immobilized on an electrode surface. After exposure to a sample containing the specific complementary target sequence, the electrochemical response is monitored upon DNA hybridization by either direct or indirect methods. Although direct detection based on guanine (G) and/or adenine (A) oxidation allows a simple and reagentless process, the oxidation signal depends on the number of electroactive bases as well as their distance from the electrode, impacting sensitivity and detection limit. On the other hand, indirect methods require additional electroactive labels or indicators, including redox couples such as methylene blue [89, 115], daunomycin [116] or anthraquinone [23, 25, 117]

metal ion complexes with osmium or ruthenium [118-120] or nanoparticles [121] to generate sensitive electrochemical signal. However, strategies involving labels are time-consuming and complicate the detection process.

A label-free assay would be preferable for reducing time and complexity in DNA diagnostics [122, 123]. Electrochemical impedance spectroscopy (EIS) is a particularly useful detection mode for DNA diagnostics because it does not require labels or indicators [124-127]. The resistance to charge transfer (R_{ct}) at the electrode surface is a sensitive indicator for monitoring the change of interfacial surface properties following DNA hybridization. Label-free detection based on EIS is therefore an ideal platform for developing sensitive, low-cost detection when combined with portable instrumentation for point-of-care applications.

In field of electrochemical DNA sensors, one of the key components to achieve specific DNA detection is the probe. Vilaivan's group proposed a new conformational pyrrolidinyl PNA system (known as acpcPNA) which possesses an α,β-peptide backbone deriving from D-proline/2-aminocyclopentanecarboxylic acid [20, 22]. Compared to the original aegPNA [19], acpcPNA exhibits a stronger affinity and higher sequence specificity binding to DNA and RNA. It also provides the characteristic selectivity of antiparallel/parallel binding to the target and a low tendency for self-hybridization. Moreover, it can be modified at nucleobase or backbone to incorporate diverse functionalities. These properties allow acpcPNA to be widely used as a probe for biological application [23, 25, 92, 128].

Paper-based analytical devices (PADs) have continuously received the significant interest as a point-of-care sensor. Because PADs are simple, inexpensive, portable and disposable [27, 28, 45, 54, 95, 129], they can act as a preliminary screening tool for diagnostics in developed and developing countries alike. Additionally, paper is typically made of cellulose which is compatible for biological samples and can be chemically modified with a variety of functional groups [28]. In 2015, Jirakittiwut et al. [24] proposed a

fabrication of paper-based DNA sensor by covalently attaching of the cellulose paper with acpcPNA probe. The presence of DNA was determined by the visual color of cationic colorimetric dyes bound to DNA by electrostatic interaction. This new colorimetric DNA assay concept offers a low-cost fabrication with great specificity way for DNA detection. More recently, a paper-based device for multiplex detection of DNA oligonucleotides based on electrostatic interaction between acpcPNA and silver nanoparticles leading to distinct color change in the absence and presence of DNA was developed [26].

Here, we report a label-free electrochemical PAD (ePAD) for DNA detection using acpcPNA as a probe and electrochemical impedance spectroscopy (EIS) as the detection motif. Unlike previous examples of PNA sensors, the acpcPNA probe was covalently immobilized onto cellulose paper. The quantification of DNA was performed by monitoring the change in the charge transfer resistance using EIS before and after the acpcPNA-DNA hybrid is formed. The proposed concept was used for detection of a MTB oligonucleotide and successfully applied with PCR-amplified DNA from a clinical sample. This simple-to-fabricate label-free electrochemical paper-based DNA sensor has the potential to be developed as an alternative diagnostic device for simple, low-cost, sensitive and selective DNA and RNA detection.

3.2.2 Experimental

3.2.2.1 Chemicals and materials

Analytical grade reagents, including LiCl from Wako Pure Chemicals Industry (Japan), $NaIO_4$ from CARLO ERBA reagents (Italy), 2,4-dinitrophenyl hydrazine (2,4-DNP) from H&W (USA), $NaCNBH_3$ from Acros Organics (USA), NaCl, KH_2PO_4, Na_2HPO_4 and KCl from Merck (Germany), potassium ferricyanide and potassium ferrocyanide from Sigma-Aldrich (Singapore), were used without further purification. 18 M Ωcm^{-1} resistance water was obtained from a Millipore Milli-Q water system. Dimethylformamide and acetonitrile were products of

Merck. Carbon graphene and silver/silver chloride ink were obtained from Gwent group (United Kingdom). The screen-printed block was made by Chaiyaboon Co. Ltd. (Thailand). Synthetic oligonucleotides were obtained from Pacific Science (Thailand). The sequences of the oligonucleotides used in this study are shown in Table 3.2.1.

Table 3.2.1 List of oligonucleotides

Oligonucleotide	Sequence (5'-3')
Complementary DNA	5'-ATAACGTGTTTCTTG-3'
Single-base-mismatch	5'-ATAACGTCTTTCTTG-3'
Two-base-mismatch	5'-ATAACGTCTCTCTTG-3'
Non-complementary DNA	5'-CACTTGCCTACACCA-3'

The forward (5'-CCTGCGAGCGTAGGCGTCGG-3') and reverse DNA primers (5'-CTCGTCCAGCGCCGCTTCGG-3') were used for the PCR samples. The clinical sample of MTB was obtained from Asst. Prof. Chaniya Leepiyasakulchai, Department of Clinical Microbiology and Applied Technology, Faculty of Medical Technology, Mahidol University and was collected using university human subjects board approved procedures.

3.2.2.2 Synthesis of acpcPNA

The acpcPNA probe was designed to be complementary to the synthetic oligonucleotide MTB targets with a sequence of CAAGAAACACGTTAT (written in the N⟶C direction). The acpcPNA probe was synthesized by solid-phase peptide synthesis using Fmoc chemistry as previously described.[20] L-lysinamide was included at the C-terminus to provide a handle for subsequent immobilization via the ε-amino group. The progress of the reaction was monitored by MALDI-TOF-MS analysis on a Microflex MALDI-TOF mass spectrometer (Bruker Daltonik GmbH, Bremen, Germany). The acpcPNA on the

solid support was treated with 1:1 (v/v) aqueous ammonia:dioxane in a sealed tube at 60 ºC overnight to remove the nucleobase protecting groups. The PNA was cleaved from the solid support with trifluoroacetic acid (TFA) and purified by reverse-phase HPLC (C18 column, 0.1% (v/v) TFA in H_2O-MeOH gradient). The identity of the acpcPNA was verified by MALDI-TOF MS analysis, and the purity was confirmed to be >90% by reverse-phase HPLC.

3.2.2.3 Fabrication of 3D paper-based electrochemical DNA sensor

A 3D ePAD DNA sensor was fabricated using the wax-printing technique.[53] The patterned paper was designed using Adobe Illustrator based on the origami concept[130] and printed onto the filter paper (Whatman No.1) using a wax printer (Xerox Color Qube 8570, Japan). The printed paper was subsequently melted on a hot plate (175 ºC, 50 s) to generate a hydrophobic barrier. For electrode fabrication, three-electrode systems were prepared using an in-house screen-printing method. Carbon graphene ink was used as a working electrode (WE) and counter electrode (CE). Reference electrode (RE) and conductive pad were screen printed using silver/silver chloride ink. The design and operation of the paper-based electrochemical DNA sensor was shown in Figure 3.2.1. As shown in Figure 3.2.1A, the sensor consists of two layers: layer A and layer B. Layer A contains CE and RE while layer B contain WE. The sample reservoir is punched in layer A to allow a solution connection directly from the top to the bottom layer when the 3D DNA sensor was fully assembled by folding layer A over layer B.

3.2.2.4 Immobilization of acpcPNA

Covalent immobilization of acpcPNA on the paper WE was carried out according to previous reports [131-133] with slight modification. The immobilization process is shown in Figure 3.2.1B. First, 2.10 M of LiCl in $NaIO_4$

(0.04 M) was spotted onto the back of WE. The reaction was allowed to proceed in the dark at room temperature for 15 min to generate the aldehyde groups on the surface of the cellulose paper [44]. Next, the WE was washed with Milli-Q water to remove the inorganic salts and allowed to dry at room temperature. For covalent immobilization of the acpcPNA, a solution of acpcPNA (2 µM) containing $NaBH_3CN$ (1 mg/mL) in DMF was prepared. 3 µL of acpcPNA solution was dropped onto the aldehyde modified paper and allowed to react for 12 hr in the dark and humid condition. Afterward, the acpcPNA-immobilized paper was washed for 30 min with Milli-Q water:acetronitrile (1:1) and allowed to dry at room temperature. Finally, the 3D DNA sensor was stored at 4°C prior to use.

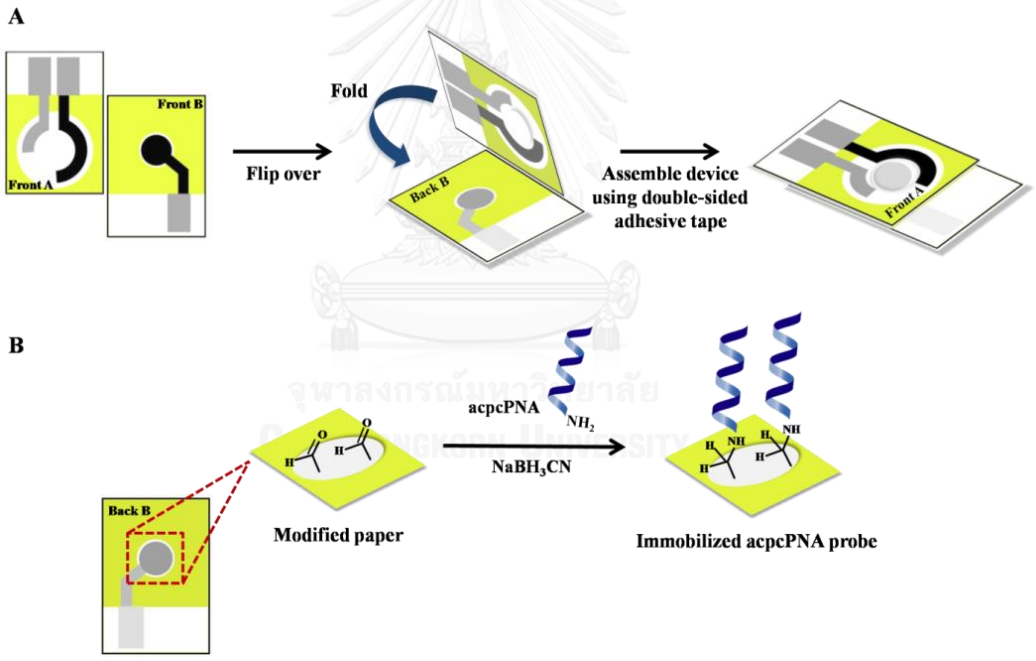

Figure 3.2.1 Schematic drawing of (A) Design and operation of 3D electrochemical paper-based DNA sensor. (B) The process of acpcPNA covalent immobilization.

3.2.2.5 Hybridization of DNA

The solution of MTB DNA oligonucleotide target was dropped onto the acpcPNA-immobilized WE and incubated for 15 min at room temperature.

Then, the non-hybridized sequence was removed from the WE by washing with 0.1 M PBS (pH 7.4). The same procedure was applied for the selectivity test with single-base mismatch, two-base mismatch and non-complementary targets.

3.2.2.6 PCR-amplified MTB analysis in real sample

The extracted DNA from clinical sample was amplified using PCR [134]. The amplification reaction was performed using Thermus aquaticus (Taq) polymerase and the following condition: 1 μM each of AmpliTaq DNA polymerase, nucleotides, 10X reaction buffer and primer were mixed together. Subsequently, 5 μL of the extracted DNA was added. The sample was denatured at 94 ºC for 5 min and then 25 cycles of amplification were performed. The cycle consisted of denaturation at 94 ºC for 2 min, annealing at 68 ºC for 2 min and extension at 72 ºC for 2 min. The PCR product was visualized by electrophoresis in a 2% agarose gel containing ethidium bromide under UV light.

3.2.2.7 Electrochemical measurement

For electrochemical measurements, the EIS was used throughout the experiment using a PGSTAT30 potentiostat (Metrohm Siam Company Ltd., Switzerland) and CV was performed on a CHI1232A electrochemical analyzer (CH Instruments, Inc., USA). All electrochemical experiments were carried out in 5 mM $[Fe(CN)_6]^{3-/4-}$. After the immobilization and hybridization process, 100 μL of $[Fe(CN)_6]^{3-/4-}$ was added onto the modified working electrode. EIS was recorded in the frequency range of 0.01 Hz – 100 kHz with the potential at 0.1 V. The R_{ct} after the hybridization was measured and compared with the R_{ct} in the absence of the DNA target.

3.2.3 Results and Discussion

3.2.3.1 Characterization of acpcPNA - covalently immobilized electrode

In order to confirm the success of covalent immobilization of acpcPNA, the change of R_{ct} in EIS was monitored in a stepwise electrode modification using 5 mM $[Fe(CN)_6]^{3-/4-}$. The semicircle of the Nyquist curve represents the electron transfer resistance and the R_{ct} derived from a diameter of semicircle portion of the Nyquist plots can indicate the efficiency of electron transfer from electrode surface to the redox couple solution. First, the electron transfer resistance of bare electrode and modified paper electrode without the immobilization of acpcPNA probe was measured (Figure 3.2.2). The bare and modified paper electrodes provided Nyquist curves giving R_{ct} values of 34.00 (±0.08) and 34.16 (±1.25), respectively, indicating that the electron transfer of electrode surface is not affected by the paper modification process.

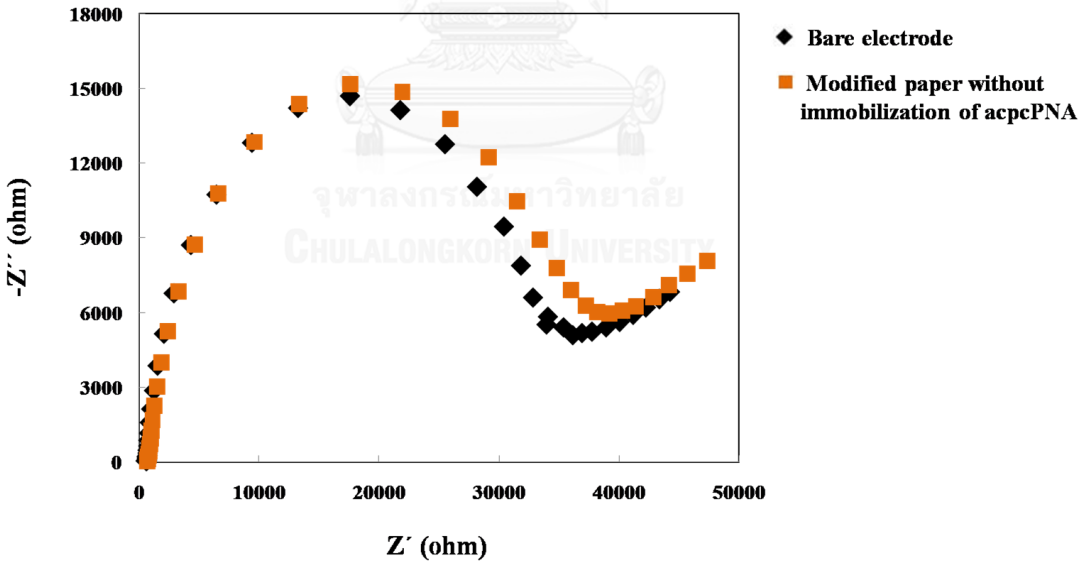

Figure 3.2.2 Nyquist plot of bare electrode and modified paper without immobilization of acpcPNA in 0.5 M $[Fe(CN)_6]^{3-/4-}$.

Figure 3.2.3A shows the Nyquist plots obtained from bare electrode and acpcPNA-covalently immobilized on the electrode before and after hybridization with the DNA target. It can be seen that the bare electrode has the largest semicircle with an R_{ct} of 34.00 (±0.08) kΩ. After the acpcPNA was immobilized on electrode, the R_{ct} value (18.95 (±0.35) kΩ) decreased, indicating that the acpcPNA modified electrode provided a lower charge transfer resistance and higher electron transfer to the electrode. We believe the increased electron transfer was due to the electroactivity of guanine (G) and adenine (A) bases in the acpcPNA probe sequence as has been suggested previously [135-137]. When the acpcPNA modified electrode was hybridized with the DNA target, the R_{ct} value increases to 27.05 (±0.15) kΩ due to the increase in electrostatic repulsion between the negatively charged DNA and redox probe.

CV was also used to further verify electrode modification. As shown in Figure 3.2.3B, cyclic voltammogram shows a significant shift in the peak potential and the increasing of anodic peak current after acpcPNA immobilization. The ΔE_p of bare electrode was 0.67 (±0.01) V, while the ΔE_p of acpcPNA modified electrode was 0.35 (±0.02) V. Also, the current response of bare electrode (7.13 (±0.26) μA) was higher than acpcPNA-modified electrode (28.89 (±0.95) μA). This result suggests that G and A bases of acpcPNA probe have ability to accelerate the electron transfer process. Upon the hybridization of DNA target, the ΔE_p slightly shifted to 0.44 (±0.01) V, while the anodic peak current (19.94 (±0.76) μA) decreased, which implied that the electron transfer is low due to the electrostatic repulsion phenomenon of PNA-DNA duplexes and redox couple. According to the characterization evidences, the change of R_{ct} in EIS, ΔE_p and peak current in CV clearly indicate successful covalent immobilization of acpcPNA on the electrode.

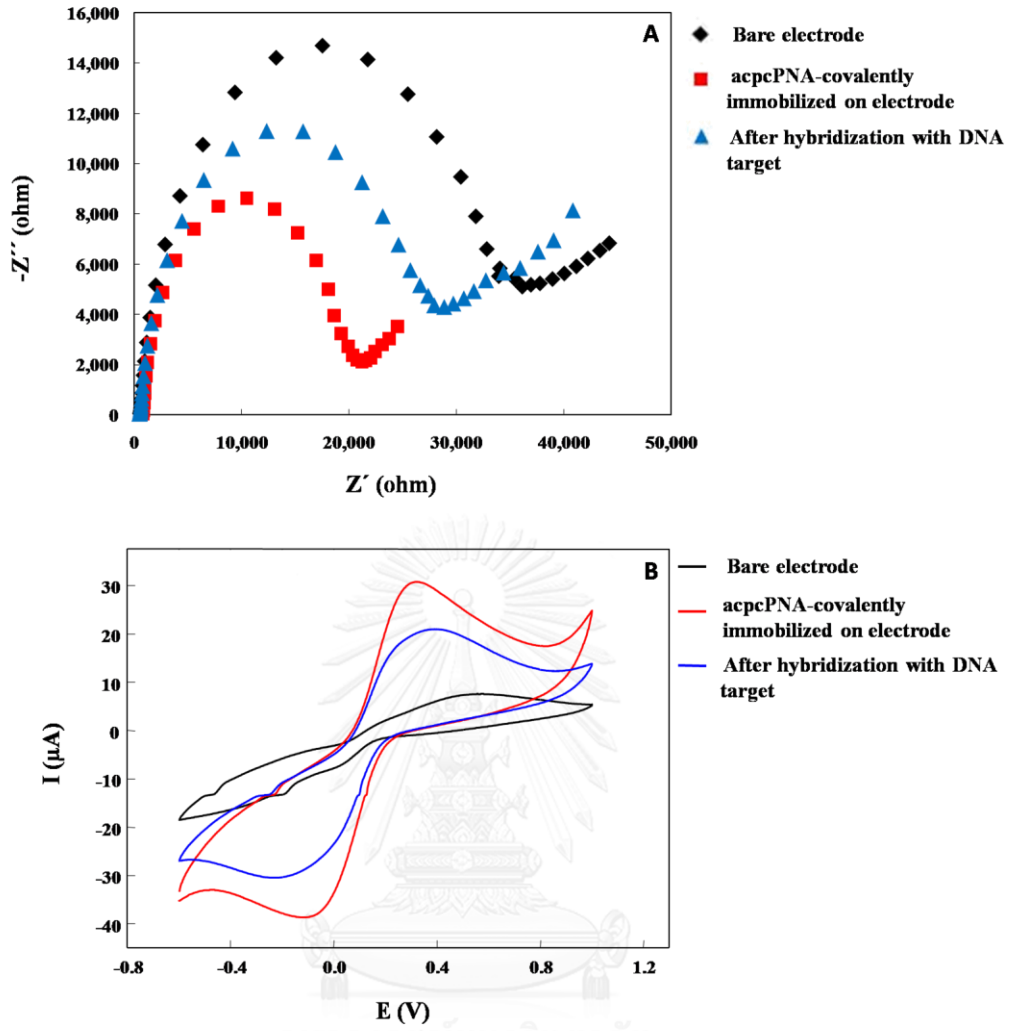

Figure 3.2.3 (A) Nyquist plot and (B) cyclic voltammogram of bare electrode, acpcPNA-covalently immobilized on electrode before and after hybridization with an equimolar concentration of target DNA in 0.5 M $[Fe(CN)_6]^{3-/4-}$.

3.2.3.2 Optimization of experimental variables

3.2.3.2.1 acpcPNA probe concentration

The effect of acpcPNA probe concentration on R_{ct} obtained from EIS was investigated as shown in Figure 3.2.4A. As the PNA concentration increased, R_{ct} for acpcPNA functionalized electrode decreased until a plateau was reached at a concentration of 2 µM.

Increasing the PNA concentration will increase the PNA surface density, which leads to a lower accessibility of redox molecules to reach the working electrode surface, which results in a constant R_{ct}. Therefore, a 2 μM of the acpcPNA probe concentration was selected for further studies.

3.2.3.2.2 Hybridization time

The influence of DNA hybridization time on electrode impedance was studied next. The DNA target was incubated with the acpcPNA-modified electrode for different times before washing with PBS (0.01 M, pH 7.4). In Figure 3.2.4B, ΔR_{ct} obtained after hybridization of DNA target increases with the increasing hybridization time, and the largest ΔR_{ct} was obtained at 15 min. This result indicated that increasing hybridization time provided higher efficiency of the binding between the acpcPNA probe and the DNA target, leading to an increase in charge-transfer resistance. Accordingly, the hybridization time at 15 min was selected as the optimal condition.

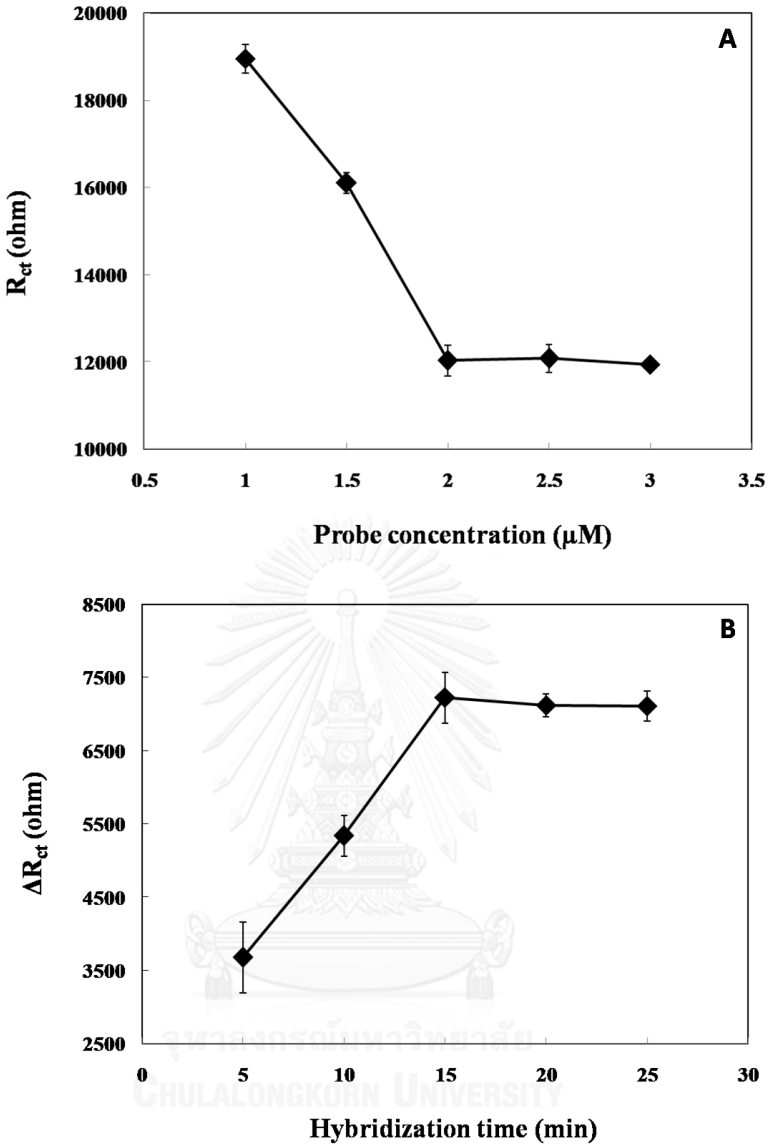

Figure 3.2.4 The effect of (A) acpcPNA probe concentration and (B) hybridization time of DNA target on the R_{ct} value.

3.2.3.3 Analytical performance

The analytical performance of 3D paper-based electrochemical DNA sensor for MTB determination was evaluated. To assess the detection limit and linear range, ΔR_{ct} as a function of DNA target concentration was determined (Figure 3.2.5). The calibration curve (inset Figure 3.2.5), which was plotted as a function of logarithmic DNA concentration and ΔR_{ct}, provided a linear relationship from 2 nM to 200 nM with a correlation coefficient of 0.997. The limit of detection (LOD, S/N=3) and limit of quantitation (LOQ, S/N=10) were found to be 1.24 nM and 3.69 nM, respectively. The wide linear range and low detection limit suggest that our proposed method is useful for MTB DNA detection after amplification.

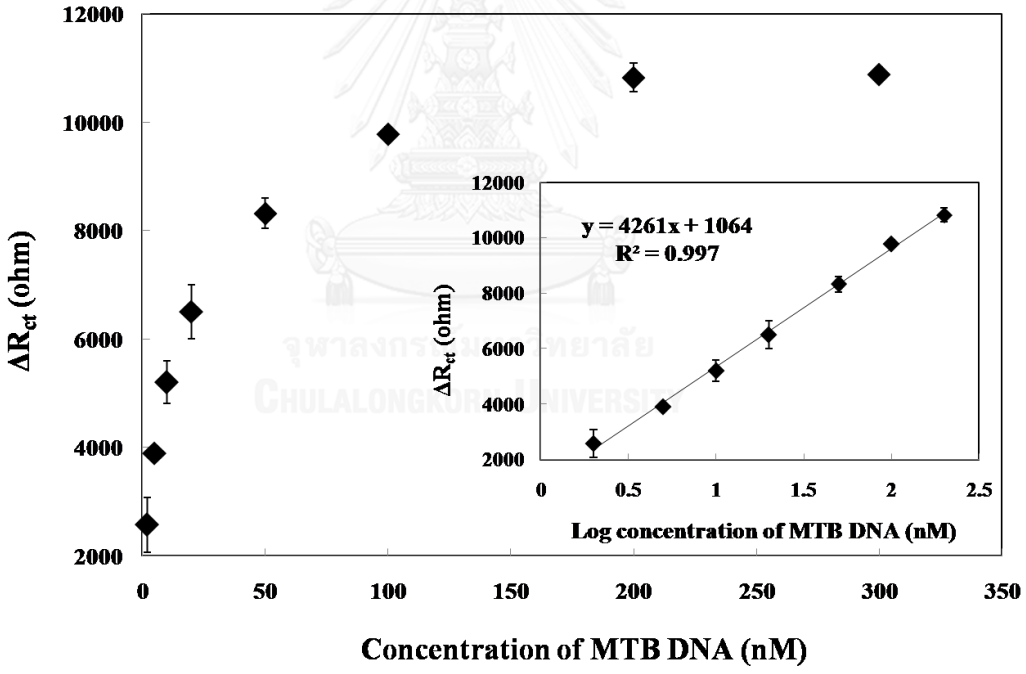

Figure 3.2.5 The change of R_{ct} (ΔR_{ct}) versus DNA target concentration and calibration curve between ΔR_{ct} and log DNA target concentration (inset) for MTB detection in 0.5 M $[Fe(CN)_6]^{3-/4-}$, frequency 0.01 Hz-100 kHz, potential 0.1 V.

3.2.3.4 Selectivity

In order to evaluate the selectivity of the sensor, the R_{ct} obtained from MTB DNA target was compared to single-base mismatch (DNA_{m1}), two-base mismatch (DNA_{m2}) and non-complementary DNA (DNA_{nc}). In the presence of DNA_{com}, the R_{ct} increased dramatically; whereas the R_{ct} did not change for DNA_{m1}, DNA_{m2} and DNA_{nc} as shown in Figure 3.2.6. These results indicated that there was no significant interference by the mismatched and non-complementary DNA targets. Thereby, the proposed DNA sensor provided high selectivity for MTB detection, which re-emphasizes the usefulness of acpcPNA probes.

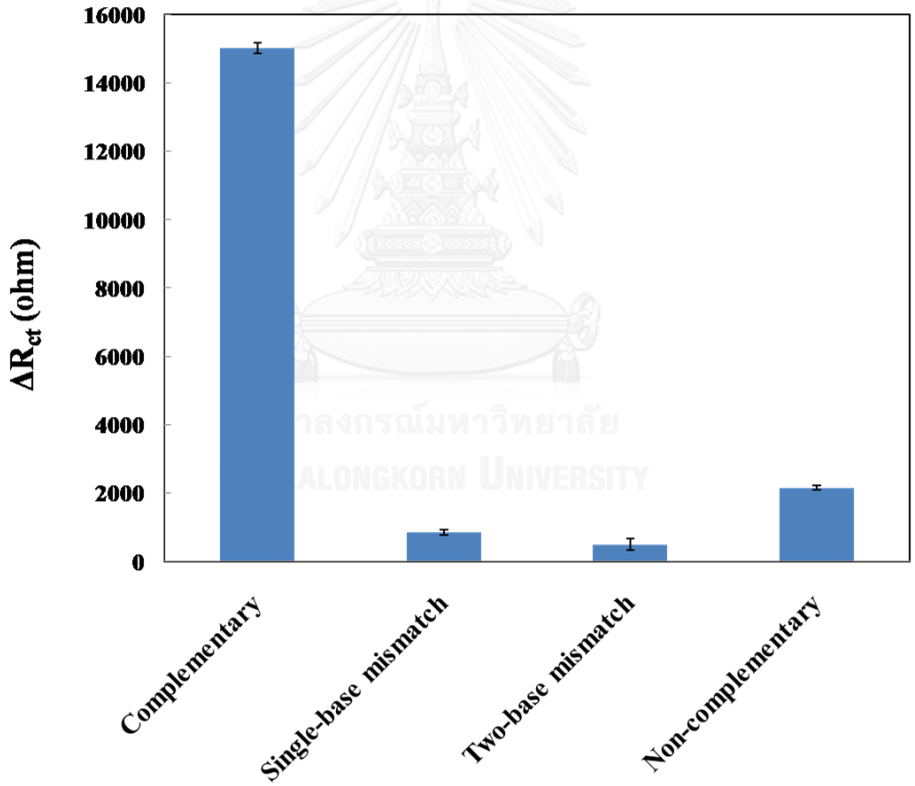

Figure 3.2.6 The ΔR_{ct} in electrochemical impedance spectroscopy of MTB detection after hybridization of DNA_{m1}, DNA_{m2} and DNA_{nc}.

3.2.3.5 Stability and reproducibility

To investigate the stability of the proposed label-free DNA biosensor, the sensor was stored at 4 °C in dry environment over one month before testing the R_{ct} response before and after hybridization with 20 nM DNA target. It was observed that the change of R_{ct} decreased to 96.25% and 94.13% of the initial response for acpcPNA-covalently immobilized on electrode before and after hybridization with DNA target, respectively (Figure 3.2.7). The electrode-to-electrode reproducibility of the DNA biosensor was also examined. The relative standard deviations (RSDs) of five electrodes were tested in the concentration range of 2-200 nM. The %RSDs was determined to be between 0.58% and 3.46%. These results indicate that the proposed DNA biosensor offers acceptable stability and reproducibility.

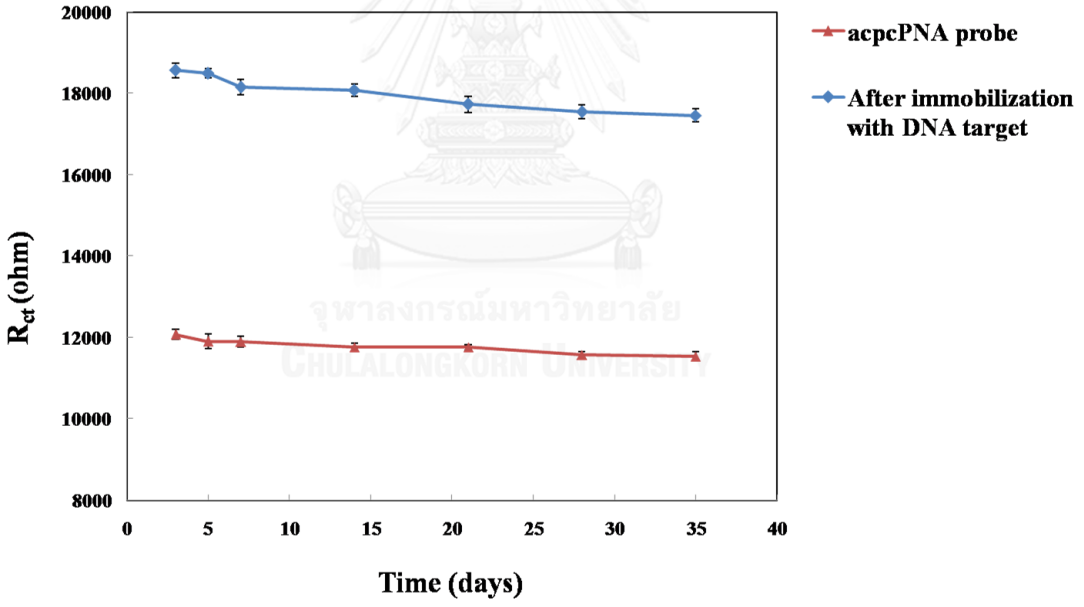

Figure 3.2.7 The R_{ct} of acpcPNA-covalently immobilized on electrode before and after hybridization with DNA target in 0.5 M $[Fe(CN)_6]^{3-/4-}$.

3.2.3.6 Real sample analysis

To evaluate the efficiency of the proposed method, the developed label-free DNA biosensor was used to detect MTB in PCR-amplified DNA from a blood sample. It was observed that the R_{ct} was increased in the presence of positive sample of MTB (Figure 3.2.8), which confirmed the occurrence of hybridization in the proposed system.

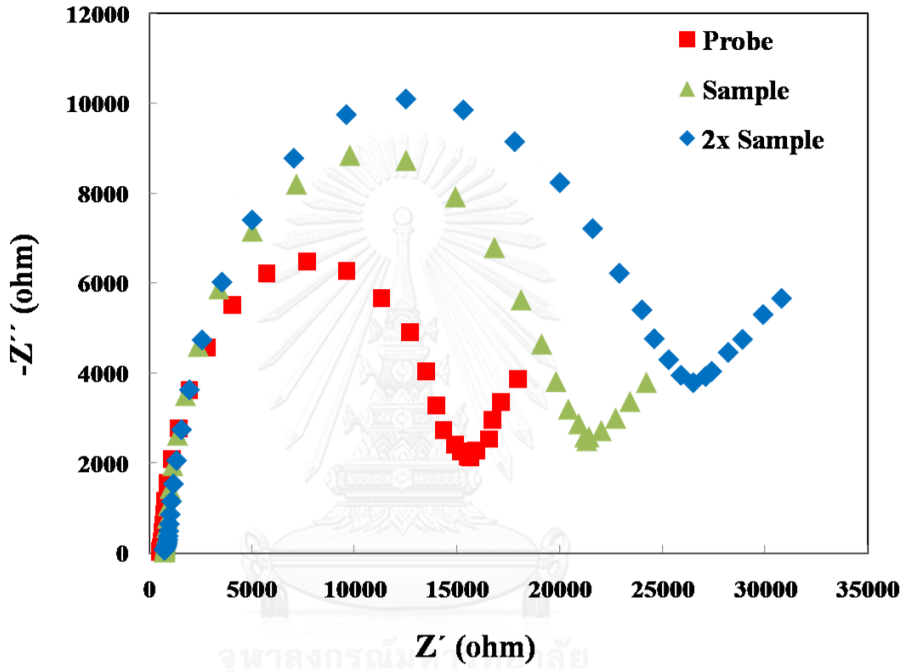

Figure 3.2.8 Nyquist plot of acpcPNA probe, acpcPNA probe in the presence of PCR sample and acpcPNA probe in the presence of 2x PCR sample in 0.5 M $[Fe(CN)_6]^{3-/4-}$.

In addition, the increasing of PCR sample was also observed by the incubation of 2-fold amount of sample onto electrode surface. It was found that the R_{ct} increased with the increasing of amount of PCR positive sample as shown in Figure 3.2.9. Therefore, it clearly shows that this label-free DNA biosensor platform is applicable for determining MTB in a blood sample.

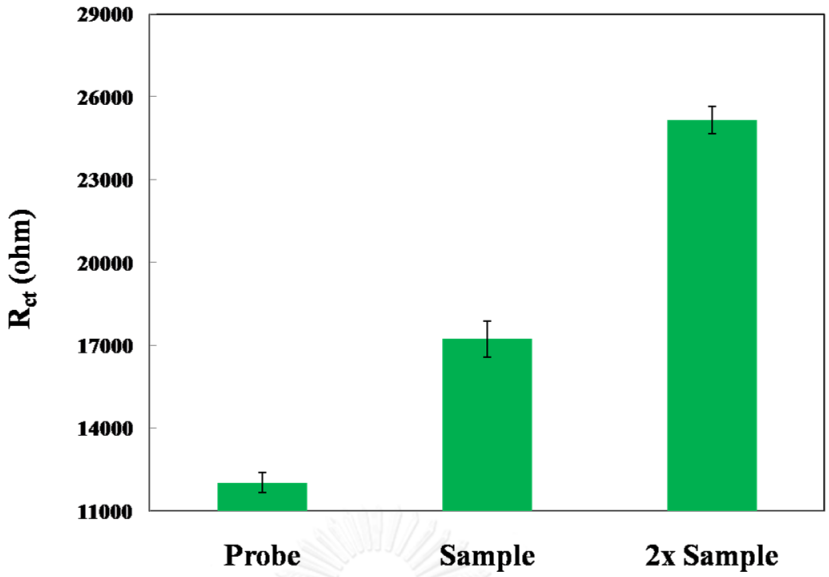

Figure 3.2.9 R_{ct} response of the label-free DNA biosensor in the presence of PCR-amplified MTB positive sample from clinical sample.

3.2.4 Conclusions

A new label-free electrochemical DNA biosensor platform using acpcPNA as a probe was successfully developed for MTB detection by measuring changes in resistance to charge transfer. The acpcPNA probe was covalently immobilized onto partially oxidized cellulose paper by reductive alkylation unlike previous methods that required direct electrode modification. The change of surface resistance in the presence of target DNA monitored by EIS was used to achieve the quantitative measurement. The label-free system offers the advantage over the more widely used electroactive indicators or labels since it eliminates the complicated and time consuming steps for labeling or adding indicators without compromising the performance in terms of detection limit and linearity range. The proposed DNA sensor demonstrated very high selectivity of acpcPNA against single-base mismatch, two-base mismatch and non-complementary DNA targets. This sensing system can be employed to determine the PCR amplification of MTB from clinical sample. As a result, this ePAD DNA sensor is well suited as an alternative platform since it

provides a promising system to fabricate simply and cost-effective to achieve a rapid for screening detection.

CHAPTER IV

DEVELOPMENT OF DNA SENSORS USING PAPER-BASED ANALYTICAL DEVICE COUPLED WITH COLORIMETRIC DETECTION

4.1 Multiplex paper-based colorimetric DNA sensor using pyrrolidinyl peptide nucleic acid-induced AgNPs aggregation for detecting MERS-CoV, MTB and HPV oligonucleotides

Prinjaporn Teengam[†], Weena Siangproh[‡], Adisorn Tuantranont[§],Tirayut Vilaivan[‖], Orawon Chailapakul[#, ¶, *] and Charles S. Henry[¥,*]

[†]Program in Petrochemistry, Faculty of Science, Chulalongkorn University, Pathumwan, Bangkok, 10330, Thailand

[‡]Department of Chemistry, Faculty of Science, Srinakharinwirot University, Bangkok, 10110, Thailand

[§]Nanoelectronics and MEMS Laboratory, National Electronics and Computer Technology Center, Pathumthani, 12120, Thailand

[‖]Organic Synthesis Research Unit, Department of Chemistry, Faculty of Science, Chulalongkorn University, Pathumwan, Bangkok, 10330, Thailand

[#]Electrochemistry and Optical Spectroscopy Research Unit, Department of Chemistry, Chulalongkorn University, Pathumwan, Bangkok, 10330, Thailand

[¶]National Center of Excellence for Petroleum, Petrochemicals, and Advanced Materials, Chulalongkorn University, Pathumwan, Bangkok, 10330, Thailand

[¥]Departments of Chemistry and Chemical and Biological Engineering, Colorado State University, Fort Collins, Colorado 80523

*Corresponding authors

Analytical Chemistry 89 (2017) 5428-5435.

ABSTRACT

The development of simple fluorescent and colorimetric assays that enable point-of-care DNA and RNA detection has been a topic of significant research because of the utility of such assays in resource limited settings. The most common motifs utilize hybridization to a complementary detection strand coupled with a sensitive reporter molecule. Here, apaper-based colorimetric assay for DNA detection based on pyrrolidinyl peptide nucleic acid (acpcPNA)-induced nanoparticle aggregationis reported as an alternative to traditional colorimetric approaches. PNA probes are an attractive alternative to DNA and RNA probes because they are chemically and biologically stable, easily synthesized, and hybridize efficiently with the complementary DNA strands. The acpcPNA probe contains a single positive charge from the lysine at C-terminus and causes aggregation of citrate anion-stabilized silver nanoparticles (AgNPs) in the absence of complementary DNA. In the presence of target DNA, formation of the anionic DNA-acpcPNA duplex results in dispersion of the AgNPs as a result of electrostatic repulsion, giving rise to a detectable color change. Factors affecting the sensitivity and selectivity of this assay were investigated, including ionic strength, AgNPs concentration, PNA concentration, and DNA strand mismatches. The method was used for screening of synthetic Middle East respiratory syndrome coronavirus (MERS-CoV), mycobacterium tuberculosis (MTB) and human papillomavirus (HPV) DNA based on a colorimetric paper-based analytical device developed using the aforementioned principle. The oligonucleotide targets were detected by measuring the color change of AgNPs, giving detection limits of 1.53 nM (MERS-CoV), 1.27 nM (MTB) and 1.03 nM (HPV).The acpcPNA probe exhibited high selectivity for the complementary oligonucleotides over single-base-mismatch, two-base-mismatch and non-complementary DNA targets. The proposed paper-based colorimetric DNA sensor has potential to be an alternative approach for simple, rapid, sensitive and selective DNA detection.

Keywords: Paper-based colorimetric DNA sensor, acpcPNA, Middle East respiratory syndrome coronavirus, Mycobacterium tuberculosis, Human papillomavirus

4.1.1 Introduction

Infectious diseases represent a major threat to human health in developed and developing countries alike. DNA alterations contribute to different types of diseases; therefore, the detection of specific DNA sequences plays a crucial role in the development method for early stage treatment and monitoring of genetic-related diseases. DNA diagnostics can provide sequence-specific detection, especially for single-nucleotide polymorphisms (SNPs) [138], which critical for a range of applications including the diagnosis of human diseases and bacterial/viral infections.

Middle East respiratory syndrome (MERS), tuberculosis (TB) and cervical cancers related to human papilloma virus (HPV) are examples of infectious diseases caused by bacterial and viral infections that benefit greatly from DNA detection. TB is an infectious disease caused by mycobacteria, usually *M. tuberculosis* (MTB) in humans [139]. HPV has been shown to be a major cause of cervical cancer [140]. Middle East Respiratory Syndrome coronavirus (MERS-CoV) has recently emerged as an infectious disease with a high fatality rate in humans [141]. Diagnostic methods developed for these infectious diseases include reverse transcription polymerase chain reaction (RT-PCR) for MERS-CoV [142], sputum smear microscopy, culture of bacilli and molecular species diagnostics for MTB [105-110] and Digene Hybrid Capture assay (HC2) and Pap smear test for HPV [143, 144]. While these techniques have been used for successful detection, they are difficult to implement in point-of-care clinical diagnostics particularly in developing countries lacking specialized medical facilities and skilled personnel. Therefore, simple, rapid, low-cost and highly accurate on-site diagnostic platforms amenable to nucleic acid detection remain a challenge for early detection of infectious diseases for better patient management and infection control. Although DNA amplification is still needed with the current method to provide high sensitivity, we seek to further improve selectivity and assay simplicity to give immediate and quantitative responses in resource limited settings.

Paper-based analytical devices (PADs) are a point-of-use technology that recently received renewed interest because they are simple, inexpensive, portable and disposable [27, 43, 145]. To date, PADs have been extensively used for applications ranging from environmental analysis to clinical diagnostic assays [27, 28, 146]. Colorimetric assays are particularly attractive when coupled with PADs due to their ease-of-use, lack of complicated external equipment and ability to provide semi-quantitative results [29, 30, 33]. Moreover, quantitative analysis of colorimetric assays can be accomplished using simple optical technologies such as digital cameras [31, 32, 147] and office scanners [33, 34] combined with image processing software to carry out color, hue, and/or intensity measurements. In the field of clinical diagnostics, the advantages of simplicity, sensitivity and low-cost are key reasons that make PADs coupled with colorimetric detection an effective diagnostic tool relative to traditional methods.

Colorimetric assays based on the aggregation of silver (AgNPs) and gold nanoparticles (AuNPs) have attracted increasing attention in biomedical applications. The optical properties of these nanomaterials depend on their size and shape [148-153]. AgNPs are known to have a higher extinction coefficient compared to AuNPs [154-156], leading to improved optical sensitivity. Chemical reduction of silver salts is frequently used to synthesize AgNPs; while specific control of shape and size distribution is achieved by varying the reducing agents and stabilizers [157-159]. Among stabilizing agents, negatively-charged citrate has been widely used [160, 161]. Recently, colorimetric assays based on AgNPs aggregation for DNA detection has been reported [156]. Colorimetric DNA detection using AgNPs usually involves modifying the particles with a DNA probe and mixing them with the DNA target containing the complementary sequence. When the hybridization of probe and target DNA occurs, the AgNPs aggregate and change color [155, 156]. The assay principal has been further adopted using charge-neutral peptide nucleic acids (PNA) [19, 162] as the hybridization agent. PNA causes aggregation of metal

nanoparticles in solution without immobilization, thus simplifying the assay [163, 164]. Finally, PNA-based nanoparticle aggregation assays also provide a high hybridization efficiency of PNA-DNA duplexes leading to a rapid color change [164].

Recently, Vilaivan's group proposed a new conformationally constrained pyrrolidinyl PNA system which possesses an α,β-peptide backbone derived from D-proline/2-aminocyclopentanecarboxylic acid (known as acpcPNA) [20, 22]. Compared to Nielsen's PNA [19], acpcPNA exhibits a stronger affinity and higher sequence specificity binding to DNA. acpcPNA exhibits the characteristic selectivity of antiparallel binding to the target DNA and low tendency to self-hybridize. Moreover, the nucleobases and/or backbone of acpcPNA can be modified to increase molecular functionality. These combined properties make acpcPNA an attractive candidate as a probe for biological applications [23, 24, 92].

Here, the multiplex colorimetric PAD for DNA detection based on the aggregation of AgNPs induced by acpcPNA is reported. acpcPNA bearing a positively-charged lysine modification at C-terminus was designed as the probe. The cationic PNA probe can interact with the negatively-charged AgNPs leading to nanoparticle aggregation and a significant color change. This proposed sensor was used for simultaneous detection of MERS-CoV, MTB and HPV. The developed paper-based DNA sensor has potential as an alternative diagnostic device for simple, rapid, sensitive and selective DNA/RNA detection.

4.1.2 Experimental

4.1.2.1 Chemicals and Materials

Analytical grade reagents, including $AgNO_3$, $NaBH_4$ and sodium citrate from Sigma-Aldrich, KH_2PO_4 and KCl from Fisher Scientific, Na_2HPO_4 from Mallinckrodt and NaCl from Macron, were used without further purification. 18 M Ωcm^{-1} resistance water was obtained from a Millipore Milli-Q water system.

Synthetic DNA oligonucleotides were obtained from Biosearch Technologies. The sequences of DNA oligonucleotides are shown in Table 4.1.1.

Table 4.1.1 List of oligonucleotide used in this study

Oligonucleotide	Sequence (5'-3')
MERS-CoV	
Complementary DNA	5′-CGATTATGTGAAGAG -3′
Two-base-mismatch	5′-CGATTATCTGAGGAG -3′
Non-complementary DNA	5′-TTCGCACAGTGGTCA -3′
MTB	
Complementary DNA	5′-ATAACGTGTTTCTTG -3′
Single-base-mismatch	5′-ATAACGTCTTTCTTG -3′
Non-complementary DNA 1	5′-TGGCTAGCCGCTCCT-3′
Non-complementary DNA 2	5′-CACTTGCCTACACCA -3′
HPV	
Complementary DNA (HPV type 16)	5'-GCTGGAGGTGTATG-3'
Non-complementary DNA 1 (HPV type 18)	5'-GGATGCTGCACCGG-3'
Non-complementary DNA 2 (HPV type 31)	5'-CCAAAAGCCCAAGG-3'
Non-complementary DNA 3 (HPV type 33)	5'-CACATCCACCCGCA-3'

4.1.2.2 Synthesis of AgNPs

The AgNPs were synthesized using the citrate-stabilization method.[165] Briefly, 4 mL of 12.6 mM sodium citrate and 50 mL of 0.3 mM $AgNO_3$ was mixed together. Then, 1 mL of 37 mM $NaBH_4$ was added to the mixture under vigorous stirring and the solution turned yellow. The formation of AgNPs and their size distribution were verified by dynamic light scattering measurement, and the average size of AgNPs was found to be 19 nm (Figure 4.1.1.).

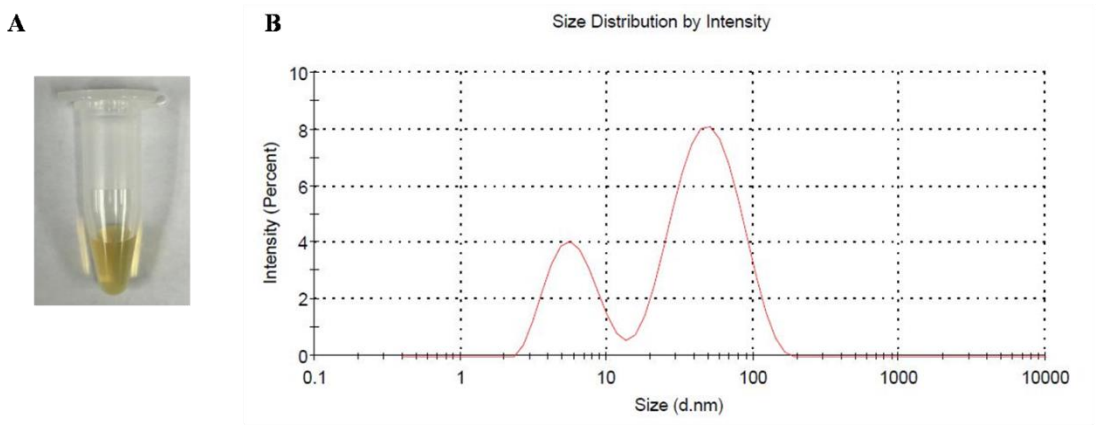

Figure 4.1.1 (A) Photograph and (B) dynamic light scattering result of the synthesized AgNPs.

4.1.2.3 Synthesis of acpcPNA probes

The acpcPNA probeswere designed to detect the synthetic oligonucleotide targets with sequences corresponding to MERS-CoV, MTB and HPV type 16. The sequences of acpcPNA probes are as follows:

MERS-CoV: CTCTTCACATAATCG-LysNH_2

MTB: CAAGAAACACGTTAT-LysNH_2

HPV type 16: CATACACCTCCAGC-LysNH_2

*(written in the N⟶C direction)

The acpcPNA probe was synthesized by solid-phase peptide synthesis using Fmoc chemistry, as previously described [20]. At the C-terminus, lysinamide was included as a positively charged group that could induce nanoparticle aggregation. All PNA were purified by reverse-phase HPLC (C18 column, 0.1% (v/v) trifluoroacetic acid (TFA) in H_2O-MeOH gradient). The identity of the acpcPNA was verified by MALDI-TOF MS analysis (Figure 4.1.2.), and the purity was confirmed to be >90% by reverse-phase HPLC.

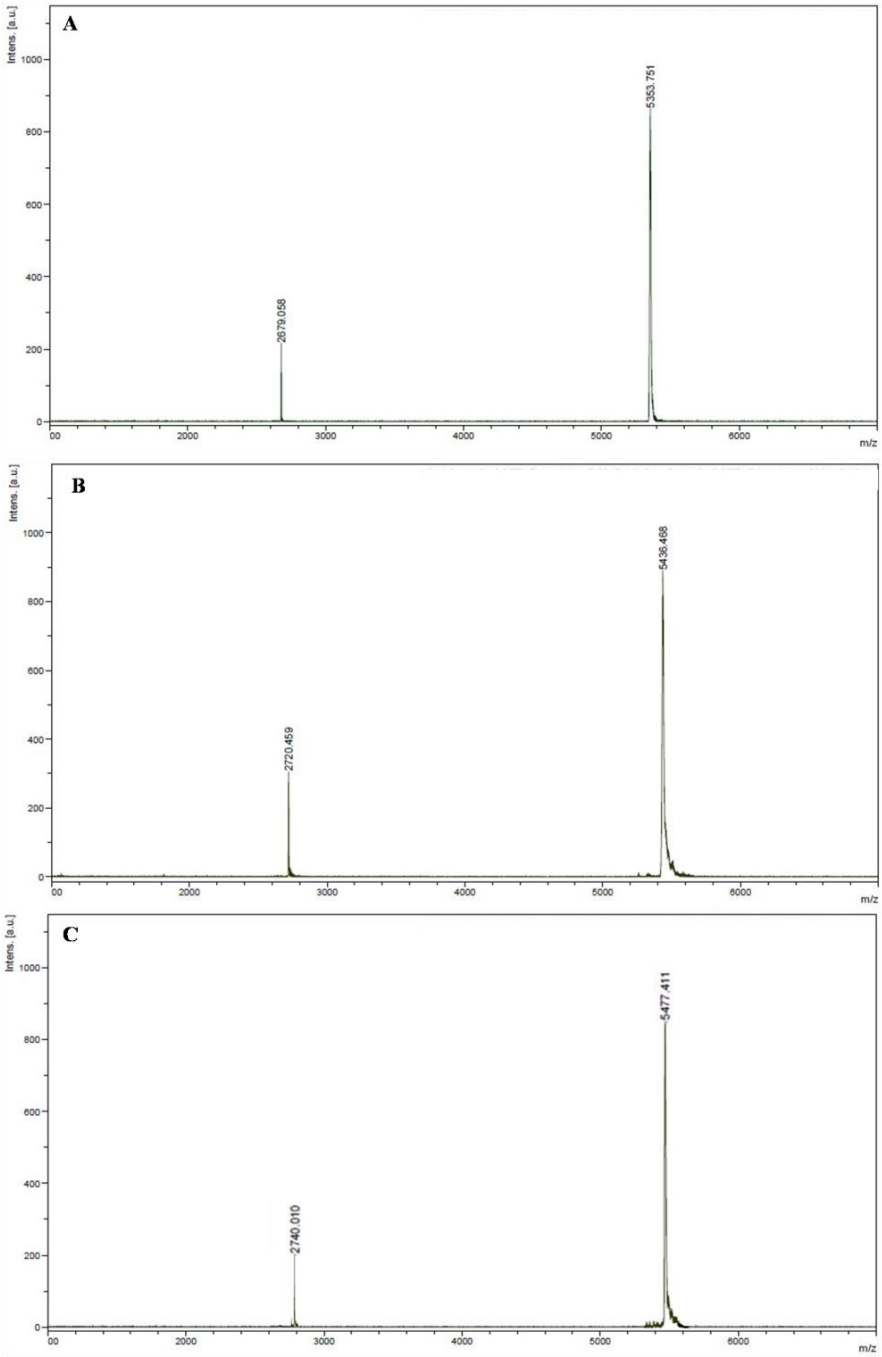

Figure 4.1.2 MALDI-TOF mass spectra of (A) MERS-CoV (B) MTB and (C) HPV acpcPNA probe.

4.1.2.4 Design and operation of paper-based multiplex DNA sensor

A wax-printing technique was used to create PADs [53]. The sensor was designed using Adobe Illustrator. The wax colors were selected to be complementary to the colorimetric reactions to enhance visualization. For paper-based device fabrication, the wax design was printed onto Whatman Grade 1 filter paper (VWR) using a wax printer (Xerox Phaser 8860). The wax pattern was subsequently melted at 175 °C for 50 s to generate the hydrophobic barriers and hydrophilic channels. The sensor was based on Origami concept consisting of two layers [130, 166]. As shown in Figure 4.1.3A, the base layer contains four wax-defined channels extending outward from the sample reservoir (6 mm i.d.) and the top layer contains four detection and control zones (4 mm i.d.). Figure 4.1.3B illustrates operation of the multiplex sensor. First, the sample reservoir of the top layer was punched to provide a solution connection directly from the top to the bottom layer, and then the device was assembled by folding the top layer over the base layer to create the three-dimension origami paper-based device. A polydimethylsiloxane (PDMS) lid was used for holding the two layers together. The lid consisting of one 6 mm-diameter hole over the sample reservoir and eight 4 mm-diameter holes over the colorimetric detection and control zones was aligned over the device to provide consistent pressure across the surface of the device. Next, the acpcPNA probe and AgNPs solution were added onto the detection and control zones. Finally, the sample solution was added onto the sample reservoir and flow through the channels to wet the colorimetric detection zones.

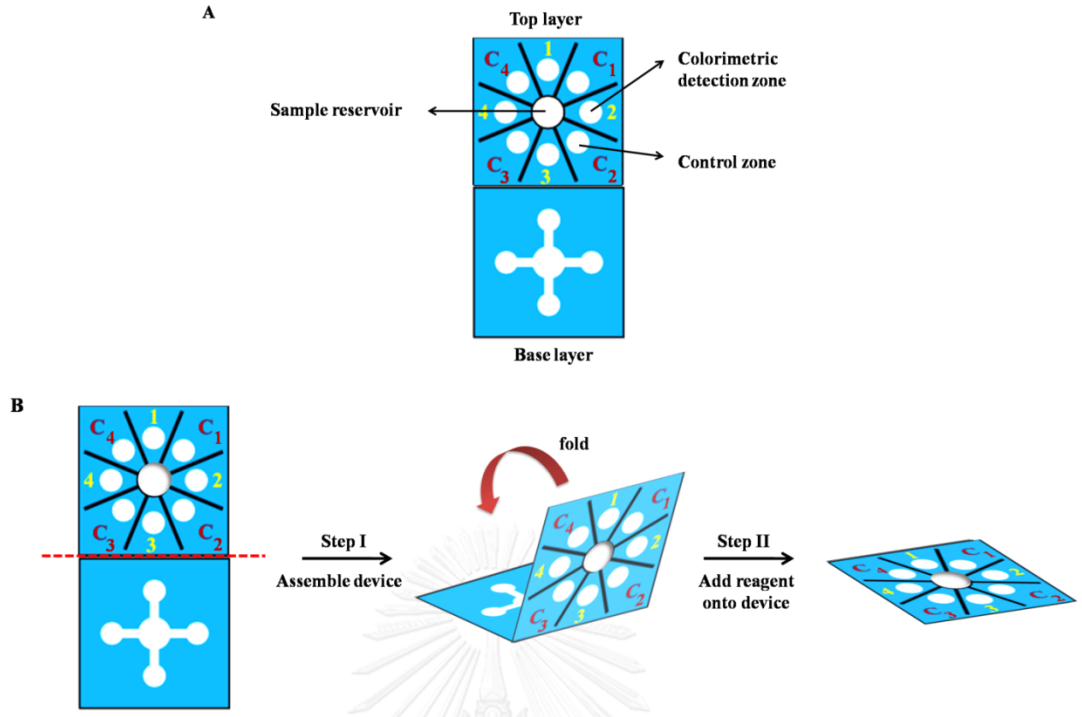

Figure 4.1.3 Schematic drawing of (A) Design and (B) operation of multiplex paper-based colorimetric device.

4.1.2.5 Colorimetric detection of MERS-CoV, MTB and HPV DNA target

According to the concept of PNA-induced AgNPs aggregation [163, 164], acpcPNA was designed as a specific probe for quantitative detection of synthetic MERS-CoV, MTB and HPV DNA targets. For colorimetric detection, the detection zone was prepared by adding 10 µL of AgNPs in 0.1 M phosphate buffer saline (PBS) pH 7.4 in a ratio of 5:1 (AgNPs: PBS), followed by 1 µL of specific acpcPNA probe. Control zones were prepared using the same conditions as the colorimetric detection zones. Next, 25 µL of DNA target was added to the open sample reservoir. Upon sample addition, solution moved outward through the channels to wet the colorimetric detection zone of the top layer. Finally, the AgNPs aggregation occurred and the color intensity was measured.

4.1.2.6 Image processing

The detection images were recorded using a scanner (XEROX DocuMate 3220) and saved in JPEG format at 600 dpi. ImageJ software (National Institutes of Health) was used to analyze the mean intensity of the color for each colorimetric reaction zone by applying a color threshold window for removing the blue background. Images were then inverted and the mean intensity was measured [33, 95].

4.1.3 Results and discussion

4.1.3.1 acpcPNA-induced AgNPs aggregation

The process of acpcPNA-induced AgNPs aggregation is shown in Figure 4.1.4. The anionic AgNPs are initially well dispersed due to electrostatic repulsion. On addition of the cationic acpcPNA, the electrostatic repulsion is shielded resulting in nanoparticle aggregation. When complementary DNA (DNA_{com}) is present, the specific PNA-DNA interaction outcompetes the less specific PNA-AgNPs interaction resulting in a negatively charged PNA-DNA_{com} duplex and de-aggregation of the anionic nanoparticles. Upon addition of non-complementary DNA (DNA_{nc}), the acpcPNA should remain bound to the AgNPs and no color change occurs. To prove the concept, we designed and synthesized acpcPNA probes to detect synthetic oligonucleotide targets with sequences corresponding to MERS-CoV, MTB and HPV type 16. The photographs of the results are shown in Figure 4.1.5. The yellow AgNPs turned red when the acpcPNA was added. When the solution contained of the acpcPNA and DNA_{nc}, the color also changed to red due to aggregation of the AgNPs. On the other hand, the color changed from red (aggregated) to yellow (non-aggregated) in the presence of DNA_{com}, with the intensity dependent on the DNA concentration.

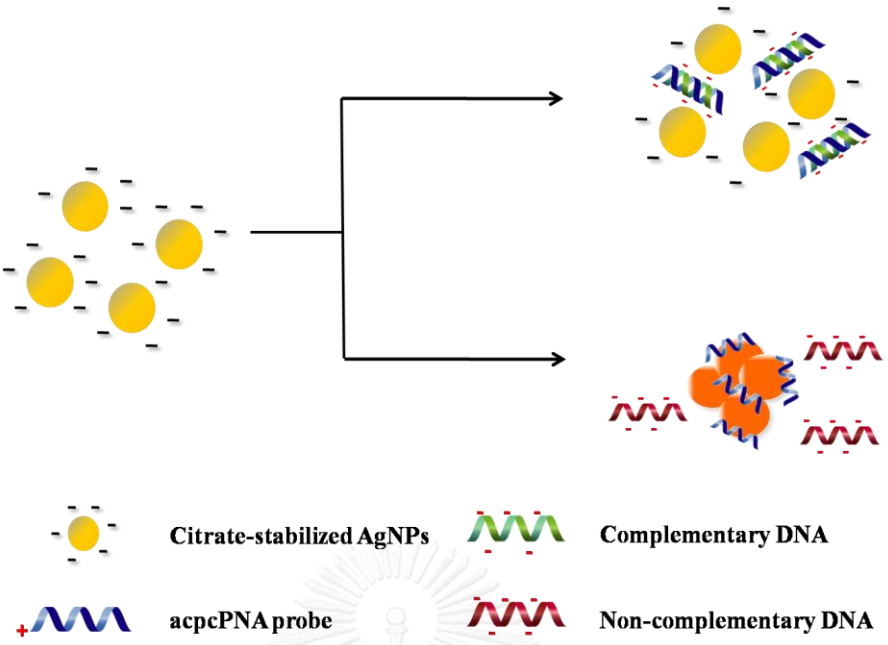

Figure 4.1.4 The process of acpcPNA-induced AgNP aggregation in the presence of DNA_{com} and DNA_{nc}.

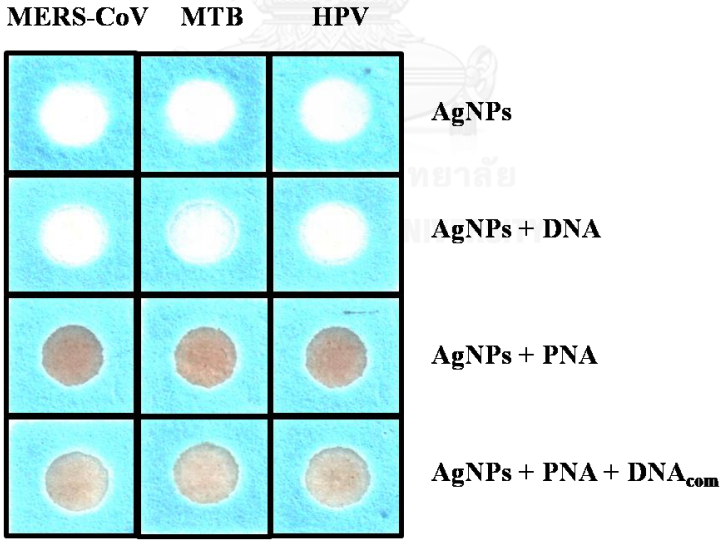

Figure 4.1.5 Photograph of visual color changes obtained from detection of MERS-CoV, MTB and HPV in the presence of DNA_{com}.

Next, the sequence of adding the PNA probe and DNA target was investigated. As shown in Figure 4.1.6, when equimolar DNA_{com} was added either before or after the addition of acpcPNA probe into the AgNPs, the same color intensities were obtained indicating that the sequence of adding acpcPNA and DNA_{com} did not impact the final signal.

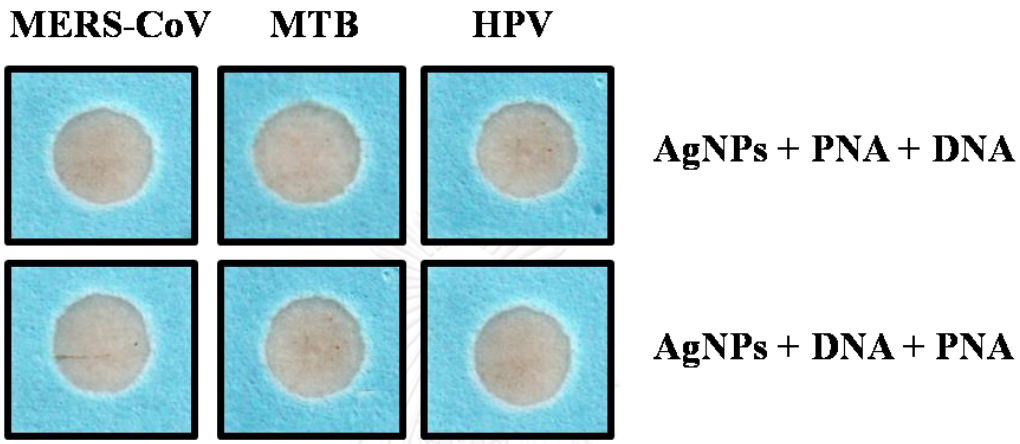

Figure 4.1.6 Photograph of visual color changes obtained from different sequence of adding probe and DNA target for the detection of MERS-CoV, MTB and HPV.

4.1.3.2 Critical coagulation concentration (CCC)

The influence of electrolyte solution on the aggregation behavior of citrate-stabilized AgNPs was investigated based on the CCC [167]. The CCC represents the electrolyte concentration required to cause aggregation of the nanoparticles in the absence of acpcPNA. In Figure 4.1.7, the color intensity of citrate-stabilized AgNPs in the absence of acpcPNA probe is shown as a function of NaCl concentration. The intensity, and therefore the degree of aggregation, increased with the concentration of NaCl, indicating that increasing ionic strength led to enhanced aggregation [168]. We believe that the ionic strength can decrease the electrostatic repulsion of citrate-stabilized AgNPs as a result of shielding, accelerating the AgNPs dissolution. The CCC was obtained when the degree of aggregation reached a maximum and became independent of NaCl concentration. In this experiment, the CCC of citrate-stabilized AgNPs was

found to be 30 mM. Above this concentration, PNA-induced aggregation was not observed.

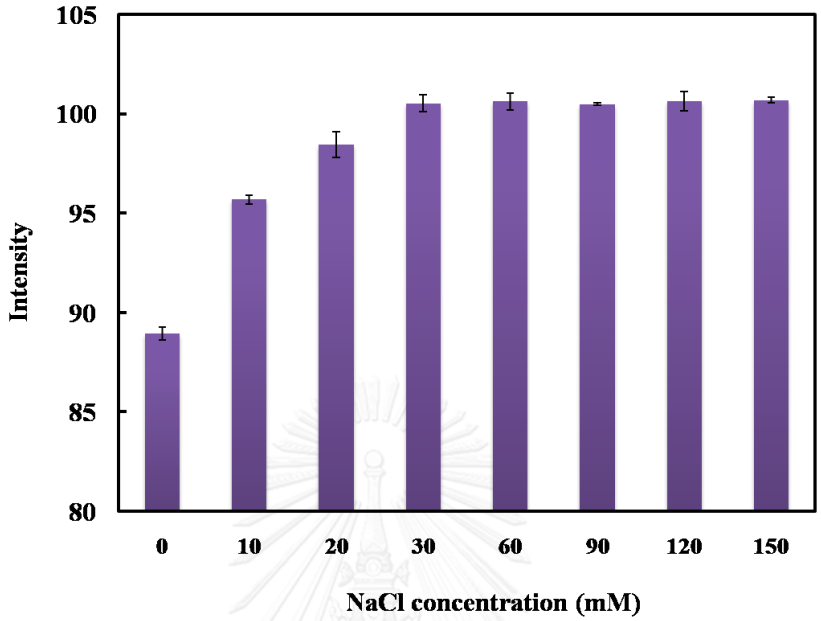

Figure 4.1.7 The color intensity of citrate-stabilized AgNPs as a function of NaCl concentrations.

4.1.3.3 Optimization of assay parameters

For a colorimetric assay based on acpcPNA-induced AgNPs aggregation, assay parameters including 0.1 M PBS (pH 7.4) ratio and acpcPNA concentration were optimized using a simple paper-based design. The degree of AgNPs aggregation was determined by measuring the color intensity of the resulting solution in the presence of acpcPNA without target DNA. First, the impact of the PBS concentration on AgNPs aggregation was measured. The differential color intensity (Δ intensity, ΔI) obtained before and after addition of acpcPNA as a function of AgNPs to PBS ratio is shown in Figure 4.1.8A. ΔI increased until the ratio of AgNPs:PBS reached 5:1 and then decreased until it plateaued at 5:2. Thus, the ratio of 5:1 AgNPs:PBS was selected as the optimal condition because it gave the largest ΔI. Another important aspect for the DNA assay is probe concentration. The influence of acpcPNA probe concentration on absolute

intensity was studied. As shown in Figure 4.1.8B, the acpcPNA concentration was varied within a range of 0-2.5 μM and the highest aggregation was obtained at the concentration of 1.0 μM. At this concentration, the aggregation became independent of acpcPNA concentration, which was desirable for simplifying the assay. Higher concentrations of AgNPs were not tested in order to minimize reagent consumption. As a result, the optimal conditions consisting of AgNPs:PBS ratio of 5:1 and acpcPNA concentration of 1.0 μM were selected for further experiments.

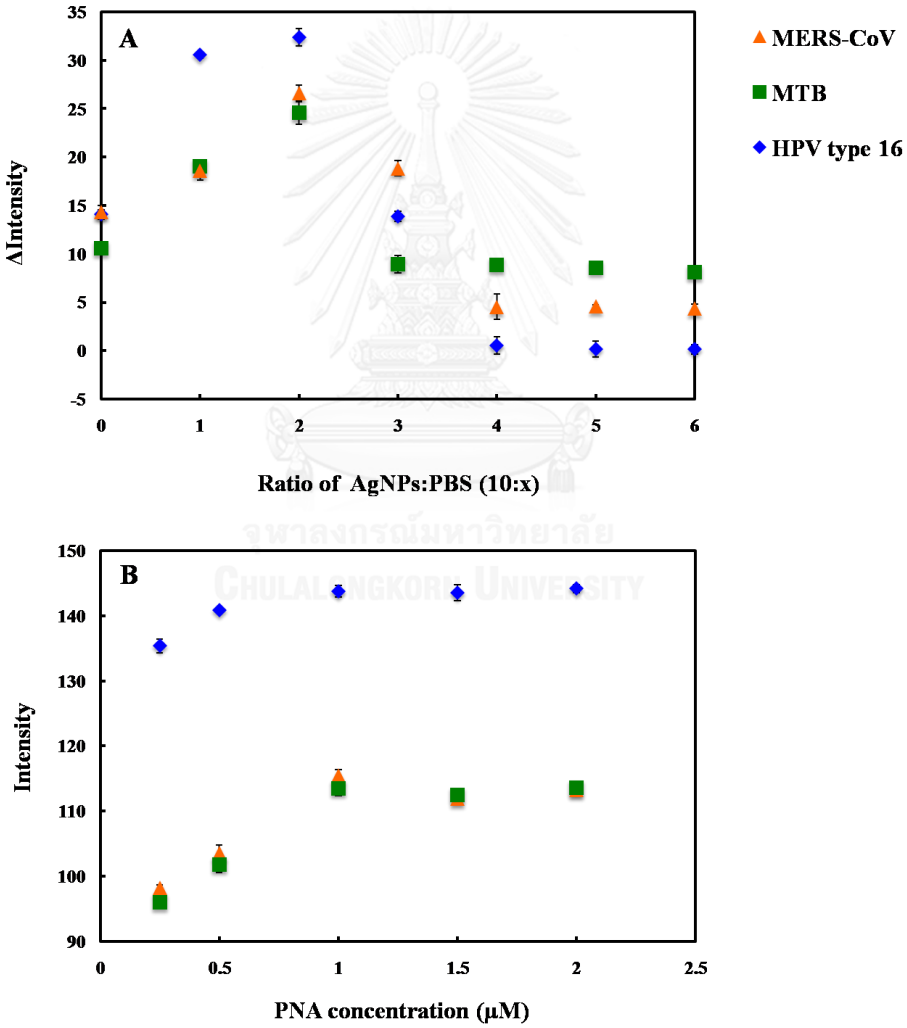

Figure 4.1.8 Influence of (A) AgNP:PBS ratio and (B) acpcPNA probe concentration on color intensity for MERS-CoV, MTB and HPV detection. The error bars represent one standard deviation (SD) obtained from three independent measurements (n=3).

4.1.3.4 Selectivity of MERS-CoV, MTB and HPV detection

To investigate the selectivity of this system, the color intensity obtained from the DNA_{com} of MERS-CoV, MTB and HPV was compared to that of single-base mismatch (DNA_{m1}), two-base mismatch (DNA_{m2}) and DNA_{nc} sequences. The color intensity decreased significantly in the presence of DNA_{com}; whereas the intensity did not change for the mismatched and non-complementary targets (Figure 4.1.9). We believe the affinity of PNA-DNA hybridization was reduced due to the contribution of one- and two-base mismatches, leaving free PNA to aggregate the nanoparticles. PNA-DNA_{com} complex can retard the ability of PNA to induce AgNPs aggregation as discussed above and result in different color intensities. These results suggest that the fully complementary DNA selectively hybridized the acpcPNA probe and yielded measurable signals.

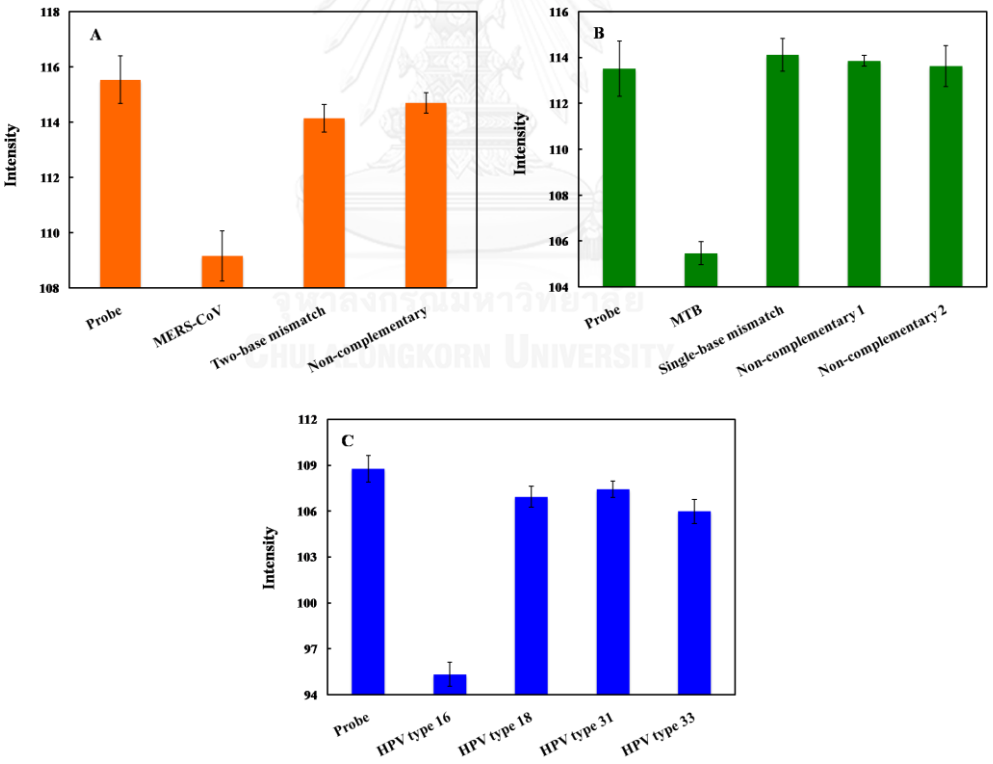

Figure 4.1.9 The color intensity of (A) MERS-CoV, (B) MTB and (C) HPV detection after hybridization of DNA_{m1}, DNA_{m2} and DNA_{nc}. The error bars represent one standard deviation (SD) obtained from three independent measurements (n=3).

In addition, bovine serum albumin (BSA), which is commonly used in cell culture protocols, was used to investigate the protein interference of the proposed system. The DNA target was prepared in the presence of 3% BSA solution. It was observed that the color intensities of the DNA targets for MERS-CoV, MTB and HPV in 3% BSA solution were statistically identical to the ones without BSA (Figure 4.1.10). Hence, common proteins should not negatively affect the analysis of this system.

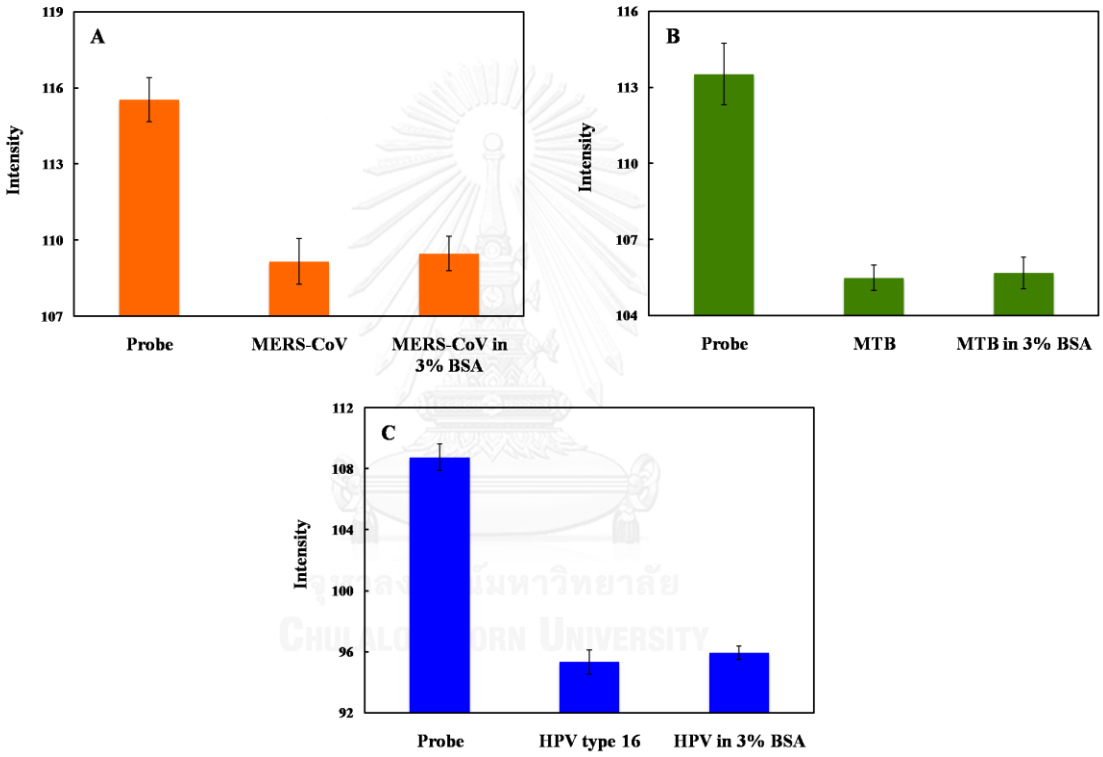

Figure 4.1.10 The color intensity of (A) MERS-CoV, (B) MTB and (C) HPV detection in the presence of BSA.

4.1.3.5 Analytical performance

To assess the sensitivity of the proposed method for DNA quantification, the intensity as a function of the target DNA concentration was determined. The color intensity decreases with the target DNA concentration. The calibration curves for each species are shown in Figure 4.1.11A, B and C for MERS-CoV, MTB

and HPV, respectively. The linear range for each DNA target using a logarithmic DNA concentration and color intensity (Figure 4.1.11 inset) was also obtained.

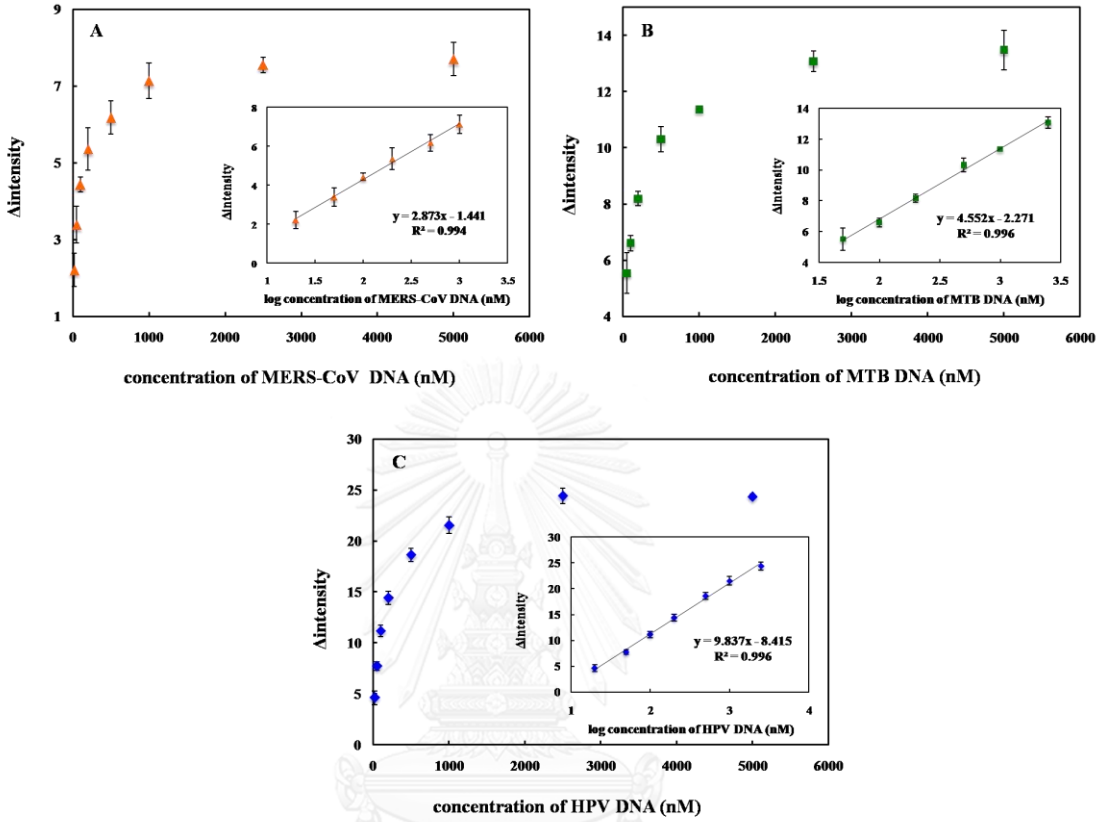

Figure 4.1.11 The change of probe color intensity versus DNA target concentration (ΔI) and calibration graph between ΔI and log DNA target concentration (inset) for (A) MERS-CoV, (B) MTB and (C) HPV detection. The error bars represent standard deviation (SD) obtained from three independent measurement (n=3).

The analytical performances for all three DNA targets are summarized in Table 4.1.2. It can be seen that a sufficiently low detection limit could be obtained for MERS-CoV, MTB and HPV detection without the need for multiple PCR cycles. Moreover, this multiplex system can provide sensitive and selective detection for simultaneous analysis of multiple DNA targets in a single device, which simplifies the analysis compared to traditional diagnostics [108, 169-172].

Table 4.1.2 Summarized analytical performance of the Multiplexed 3DPAD for colorimetric DNA assay.

DNA target	Linearity	LOD	%RSD (*n*=3)
MERS-CoV	20-1000 nM	1.53 nM	0.17-0.50
MTB	50-2500 nM	1.27 nM	0.12-0.67
HPV	20-2500 nM	1.03 nM	0.43-0.93

4.1.3.6 Device design

Next, a multiplex device (Figure 4.1.3) was designed for simultaneous detection of MERS-CoV, MTB and HPV. The top layer contained four detection zones and four control zones. Each zone contained AgNPs with a single acpcPNA probe to provide selectivity for DNA. The base layer contained four wax-defined channels extending outward from a sample inlet. After the device was folded and stacked together, the channels of the base layer were connected to four detection zones of the top layer. Upon sample addition, the solution moved outward through the channels of the base layer to wet the colorimetric detection zones of the top layer and lead to color change. Figure 4.1.12 illustrates the ability of the proposed sensor for detection of 100 nM MERS-CoV, MTB and HPV. Only the colorimetric detection zones that contained the selective probes changed color compared to their control zones. This result indicated that the multiplex paper-based colorimetric sensor is promising for simultaneous determination of MERS-CoV, MTB and HPV.

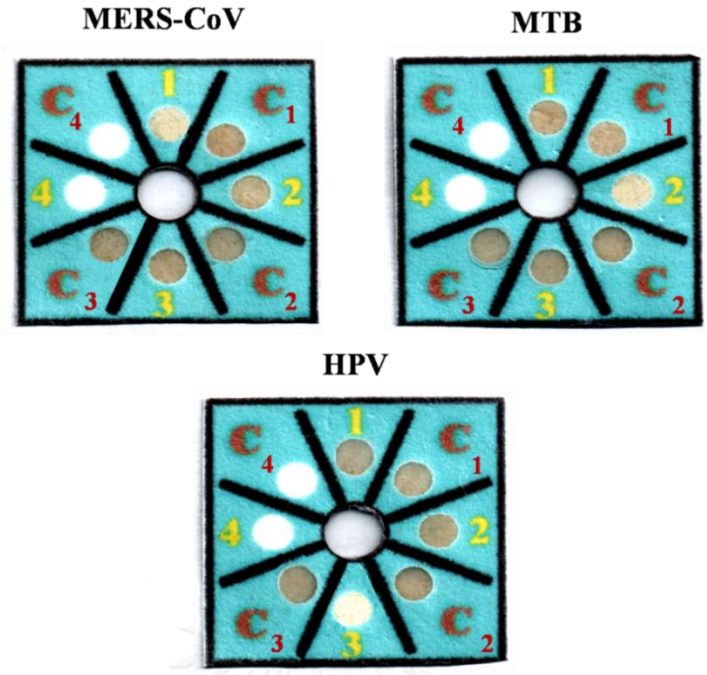

Figure 4.1.12 The selectivity of 100 nM MERS-CoV, MTB and HPV detection using multiplex colorimetric PAD. (1,C_1= AgNPs+MERS-CoV acpcPNA probe; 2,C_2= AgNPs+MTB acpcPNA probe; 3,C_3= AgNPs+HPV acpcPNA probe)

4.1.4 Conclusions

A multiplex colorimetric PAD was developed for simultaneous detection of DNA associated with viral and bacterial infectious diseases, including Middle East respiratory syndrome coronavirus (MERS-CoV), mycobacterium tuberculosis (MTB) and human papillomavirus (HPV). AgNPs were used as a colorimetric reagent for DNA detection based on acpcPNA-induced nanoparticle aggregation. This colorimetric DNA sensor exhibited high selectivity against single-base mismatch, two-base mismatch and non-complementary target DNA. Under the optimized condition, the limit of detection for MERS-CoV, MTB and HPV were found to be 1.53, 1.27 and 1.03 nM, respectively. As a result, this developed multiplex colorimetric PAD could be a low-cost and disposable alternative tool for rapid screening and detecting in infectious diagnostics.

CHAPTER V
CONCLUSIONS AND FUTURE PERSPECTIVE

5.1 Conclusions

This dissertation is aimed to develop paper-based DNA sensor integrated with electrochemical/colorimetric detection for the determination of clinically-relevant disease biomarkers. Various outstanding characteristics for each proposed system can be concluded as following;

5.1.1 Electrochemical paper-based peptide nucleic acid biosensor for detecting human papillomavirus

A novel paper-based electrochemical DNA biosensor was developed and used for the determination of high-risk HPV type 16 using the AQ-PNA probe immobilized on G-PANI/SPCE modified electrode. The AQ-PNA probe was modified with negatively charged amino acids at the C-terminus and immobilized onto the G-PANI modified electrode surface through electrostatic interaction with positive charges of the amino group of doped PANI. By using SWV, the electrochemical response was dramatically decreased after hybridization with the complementary target DNA. Under the optimum condition, the linear range of 10-200 nM was obtained and the low limit of detection was found to be 2.33 nM. The proposed DNA sensor also exhibited very high selectivity against non-complementary 14-base oligonucleotide, including HPV types 18, 31 and 33 DNA. In addition, this sensing system was successfully applied to detect the PCR amplification of HPV type 16 from SiHa cell line. Therefore, this sensitive paper-based electrochemical DNA biosensor could be an alternative tool with the uncomplicated preparation, low cost, disposability and simplicity for screening in cervical cancer diagnostic.

5.1.2 Electrochemical impedance-based DNA sensor using pyrrolidinyl peptide nucleic acid for MTB detection

A new impedance-based electrochemical DNA biosensor using acpcPNA was successfully developed for MTB detection. acpcPNA was covalently immobilized on cellulose paper to serve as a probe. The change of surface resistance in the presence of DNA target monitored by EIS was used to achieve the quantitative measurement. The proposed system offers the advantage over the general used of electroactive indicators in terms of the elimination of the complicated steps for indicator labeling leads to reduce time. Under optimal conditions, a linear calibration curve in the range of 2-200 nM and the limit of detection 1.24 nM were obtained. The proposed DNA sensor demonstrated very high selectivity of acpcPNA against single-base mismatch, two-base mismatch and non-complementary DNA targets. This sensing system can be employed to determine the PCR amplification of MTB from clinical sample. As a result, this developed DNA sensor is well suited as an alternative platform since it provides a promising system to fabricate simply and cost-effective to achieve a rapid for screening detection.

5.1.3 Multiplex paper-based colorimetric DNA sensor using pyrrolidinyl peptide nucleic acid-induced AgNPs aggregation for detecting MERS-CoV, MTB and HPV oligonucleotides

A multiplex colorimetric PAD was successfully developed for simultaneous detection of viral and bacterial infectious diseases, including MERS-CoV, MTB and HPV. AgNPs was used as a colorimetric reagent for DNA detection based on acpcPNA - induced the nanoparticles aggregation. This colorimetric DNA sensor exhibited very high selectivity against single-base mismatch, two-base mismatch and non-complementary DNA targets. Under the optimal condition, the limit of detection for MERS-CoV, MTB and HPV were found to be 1.53, 1.27 and 1.03 nM, respectively. As a result, this developed multiplex colorimetric PAD could be an alternative tool with the low cost and

disposability for simple screening and detecting in infectious diagnostics.

5.2 Future perspective

Paper-based DNA sensors using acpcPNA probe coupled with electrochemical and colorimetric detection offer a great promise for future clinical applications on all aspects. The simple-to-fabricate, low-cost, sensitive and selective DNA biosensor has potential to be developed as an alternative device in the field of clinical diagnostics. These analytical platforms can be further applied as a screening tool of other disease biomarker, especially for critical infectious diseases.

REFERENCES

[1] Rogers, K.R. Biosensors for environmental applications. Biosensors and Bioelectronics 10(6) (1995): 533-541.

[2] Rodriguez-Mozaz, S., Alda, M.J.L.d., Marco, M.-P., and Barceló, D. Biosensors for environmental monitoring: A global perspective. Talanta 65(2) (2005): 291-297.

[3] Rogers, K.R. Recent advances in biosensor techniques for environmental monitoring. Analytica Chimica Acta 568(1–2) (2006): 222-231.

[4] Arora, P., Sindhu, A., Dilbaghi, N., and Chaudhury, A. Biosensors as innovative tools for the detection of food borne pathogens. Biosensors and Bioelectronics 28(1) (2011): 1-12.

[5] Ercole, C., Del Gallo, M., Mosiello, L., Baccella, S., and Lepidi, A. Escherichia coli detection in vegetable food by a potentiometric biosensor. Sensors and Actuators B: Chemical 91(1–3) (2003): 163-168.

[6] Torun, Ö., Hakkı Boyacı, İ., Temür, E., and Tamer, U. Comparison of sensing strategies in SPR biosensor for rapid and sensitive enumeration of bacteria. Biosensors and Bioelectronics 37(1) (2012): 53-60.

[7] Sin, M.L.Y., Mach, K.E., Wong, P.K., and Liao, J.C. Advances and challenges in biosensor-based diagnosis of infectious diseases. Expert review of molecular diagnostics 14(2) (2014): 225-244.

[8] Malhotra, B.D. and Chaubey, A. Biosensors for clinical diagnostics industry. Sensors and Actuators B: Chemical 91(1–3) (2003): 117-127.

[9] Gruhl, F.J., Rapp, B.E., and Länge, K. Biosensors for diagnostic applications. in Seitz, H. and Schumacher, S. (eds.),Molecular Diagnostics, pp. 115-148. Berlin, Heidelberg: Springer Berlin Heidelberg, 2013.

[10] Blonder, R., Ben-Dov, I., Dagan, A., Willner, I., and Zisman, E. Photochemically-activated electrodes: application in design of reversible immunosensors and antibody patterned interfaces. Biosensors and Bioelectronics 12(7) (1997): 627-644.

[11] Blonder, R., Levi, S., Tao, G., Ben-Dov, I., and Willner, I. Development of amperometric and microgravimetric immunosensors and reversible immunosensors using antigen and photoisomerizable antigen monolayer electrodes. Journal of the American Chemical Society 119(43) (1997): 10467-10478.

[12] Drummond, T.G., Hill, M.G., and Barton, J.K. Electrochemical DNA sensors. Nat Biotech 21(10) (2003): 1192-1199.

[13] Arora, K., Prabhakar, N., Chand, S., and Malhotra, B.D. Ultrasensitive DNA hybridization biosensor based on polyaniline. Biosensors and Bioelectronics 23(5) (2007): 613-620.

[14] Prabhakar, N., Arora, K., Singh, S.P., Pandey, M.K., Singh, H., and Malhotra, B.D. Polypyrrole-polyvinyl sulphonate film based disposable nucleic acid biosensor. Analytica Chimica Acta 589(1) (2007): 6-13.

[15] Berdat, D., Marin, A., Herrera, F., and Gijs, M.A.M. DNA biosensor using fluorescence microscopy and impedance spectroscopy. Sensors and Actuators B: Chemical 118(1–2) (2006): 53-59.

[16] Sharma, S.K., Sehgal, N., and Kumar, A. Biomolecules for development of biosensors and their applications. Current Applied Physics 3(2–3) (2003): 307-316.

[17] Berney, H., West, J., Haefele, E., Alderman, J., Lane, W., and Collins, J.K. A DNA diagnostic biosensor: development, characterisation and performance. Sensors and Actuators B: Chemical 68(1–3) (2000): 100-108.

[18] Egholm, M., et al. PNA hybridizes to complementary oligonucleotides obeying the Watson-Crick hydrogen-bonding rules. Nature 365(6446) (1993): 566-8.

[19] Nielsen, P., Egholm, M., Berg, R., and Buchardt, O. Sequence-selective recognition of DNA by strand displacement with a thymine-substituted polyamide. Science 254(5037) (1991): 1497-1500.

[20] Vilaivan, T. and Srisuwannaket, C. Hybridization of pyrrolidinyl peptide nucleic acids and DNA: selectivity, base-pairing specificity, and direction of binding. Organic Letters 8(9) (2006): 1897-1900.

[21] Vilaivan, C., et al. Pyrrolidinyl peptide nucleic acid with α/β-peptide backbone: A conformationally constrained PNA with unusual hybridization properties. Artificial DNA, PNA & XNA 2(2) (2011): 50-59.

[22] Vilaivan, T. Pyrrolidinyl PNA with α/β-dipeptide backbone: from development to applications. Accounts of Chemical Research 48(6) (2015): 1645-1656.

[23] Kongpeth, J., Jampasa, S., Chaumpluk, P., Chailapakul, O., and Vilaivan, T. Immobilization-free electrochemical DNA detection with anthraquinone-labeled pyrrolidinyl peptide nucleic acid probe. Talanta 146 (2016): 318-325.

[24] Jirakittiwut, N., Panyain, N., Nuanyai, T., Vilaivan, T., and Praneenararat, T. Pyrrolidinyl peptide nucleic acids immobilised on cellulose paper as a DNA sensor. RSC Advances 5(31) (2015): 24110-24114.

[25] Teengam, P., Siangproh, W., Tuantranont, A., Henry, C.S., Vilaivan, T., and Chailapakul, O. Electrochemical paper-based peptide nucleic acid biosensor for detecting human papillomavirus. Analytica Chimica Acta 952 (2017): 32-40.

[26] Teengam, P., Siangproh, W., Tuantranont, A., Vilaivan, T., Chailapakul, O., and Henry, C.S. Multiplex paper-based colorimetric DNA sensor using pyrrolidinyl peptide nucleic acid-induced AgNPs aggregation for detecting MERS-CoV, MTB, and HPV oligonucleotides. Analytical Chemistry 89(10) (2017): 5428-5435.

[27] Cate, D.M., Adkins, J.A., Mettakoonpitak, J., and Henry, C.S. Recent developments in paper-based microfluidic devices. Analytical Chemistry 87(1) (2015): 19-41.

[28] Mettakoonpitak, J., et al. Electrochemistry on paper-based analytical devices: a review. Electroanalysis 28(7) (2016): 1420-1436.

[29] Nery, E.W. and Kubota, L.T. Sensing approaches on paper-based devices: a review. Analytical and Bioanalytical Chemistry 405(24) (2013): 7573-7595.

[30] Liana, D.D., Raguse, B., Gooding, J.J., and Chow, E. Recent advances in paper-based sensors. Sensors 12(9) (2012): 11505.

[31] Apilux, A., Dungchai, W., Siangproh, W., Praphairaksit, N., Henry, C.S., and Chailapakul, O. Lab-on-paper with dual electrochemical/colorimetric detection for simultaneous determination of gold and iron. Analytical Chemistry 82(5) (2010): 1727-1732.

[32] Chaiyo, S., Siangproh, W., Apilux, A., and Chailapakul, O. Highly selective and sensitive paper-based colorimetric sensor using thiosulfate catalytic etching of silver nanoplates for trace determination of copper ions. Analytica Chimica Acta 866 (2015): 75-83.

[33] Rattanarat, P., Dungchai, W., Cate, D., Volckens, J., Chailapakul, O., and Henry, C.S. Multilayer paper-based device for colorimetric and electrochemical quantification of metals. Analytical Chemistry 86(7) (2014): 3555-3562.

[34] Cate, D.M., Nanthasurasak, P., Riwkulkajorn, P., L'Orange, C., Henry, C.S., and Volckens, J. Rapid detection of transition metals in welding fumes using paper-based analytical devices. Annals of Occupational Hygiene 58(4) (2014): 413-423.

[35] Grieshaber, D., MacKenzie, R., Vörös, J., and Reimhult, E. Electrochemical biosensors - sensor principles and architectures. Sensors (Basel, Switzerland) 8(3) (2008): 1400-1458.

[36] Gs, S., Cv, A., and Mathew, B.B. Biosensors: A modern day achievement. Journal of Instrumentation Technology 2(1) (2014): 26-39.

[37] Mungroo, N. and Neethirajan, S. Biosensors for the detection of antibiotics in poultry Industry—a review. Biosensors 4(4) (2014): 472.

[38] Damborský, P., Švitel, J., and Katrlík, J. Optical biosensors. Essays in Biochemistry 60(1) (2016): 91-100.

[39] Rajasekaran, P., et al. Peptide nucleic acids inhibit growth of Brucella suis in pure culture and in infected murine macrophages. International Journal of Antimicrobial Agents 41(4): 358-362.

[40] Abdel-Aziz, M., Yamasaki, T., and Otsuka, M. Synthesis and hybridization property of novel 2′,5′-isoDNA mimic chiral peptide nucleic acids. Bioorganic & Medicinal Chemistry Letters 13(6) (2003): 1041-1043.

[41] Vysabhattar, R. and Ganesh, K.N. In situ, on-resin synthesis of 8-Br/NH2 adeninyl peptide nucleic acid (PNA) oligomers and complementation studies with DNA. Tetrahedron Letters 51(50) (2010): 6560-6564.

[42] Wang, G. and Xu, X.S. Peptide nucleic acid (PNA) binding-mediated gene regulation. Cell Res 14(2) (2004): 111-116.

[43] Martinez, A.W., Phillips, S.T., Butte, M.J., and Whitesides, G.M. Patterned paper as a platform for inexpensive, low-Volume, portable bioassays. Angewandte Chemie International Edition 46(8) (2007): 1318-1320.

[44] Pelton, R. Bioactive paper provides a low-cost platform for diagnostics. TrAC Trends in Analytical Chemistry 28(8) (2009): 925-942.

[45] Yang, Y., Noviana, E., Nguyen, M.P., Geiss, B.J., Dandy, D.S., and Henry, C.S. Paper-based microfluidic devices: emerging themes and applications. Analytical Chemistry 89(1) (2017): 71-91.

[46] Schultz, S., Smith, D.R., Mock, J.J., and Schultz, D.A. Single-target molecule detection with nonbleaching multicolor optical immunolabels. Proceedings of the National Academy of Sciences of the United States of America 97(3) (2000): 996-1001.

[47] Martinez, A.W., Phillips, S.T., Butte, M.J., and Whitesides, G.M. Patterned paper as a platform for inexpensive, low volume, portable bioassays. Angewandte Chemie (International ed. in English) 46(8) (2007): 1318-1320.

[48] Bruzewicz, D.A., Reches, M., and Whitesides, G.M. Low-cost printing of poly(dimethylsiloxane) barriers to define microchannels in paper. Analytical Chemistry 80(9) (2008): 3387-3392.

[49] Li, X., Tian, J., Nguyen, T., and Shen, W. Paper-based microfluidic devices by plasma treatment. Analytical Chemistry 80(23) (2008): 9131-9134.

[50] Abe, K., Suzuki, K., and Citterio, D. Inkjet-printed microfluidic multianalyte chemical sensing paper. Analytical Chemistry 80(18) (2008): 6928-6934.

[51] Fenton, E.M., Mascarenas, M.R., López, G.P., and Sibbett, S.S. Multiplex lateral-flow test strips fabricated by two-dimensional shaping. Acs Applied Materials & Interfaces 1(1) (2009): 124-129.

[52] Whitesides, G.M. The origins and the future of microfluidics. Nature 442(7101) (2006): 368-373.

[53] Carrilho, E., Martinez, A.W., and Whitesides, G.M. Understanding wax printing: a simple micropatterning process for paper-based microfluidics. Analytical Chemistry 81(16) (2009): 7091-7095.

[54] Dungchai, W., Chailapakul, O., and Henry, C.S. Electrochemical detection for paper-based microfluidics. Analytical Chemistry 81(14) (2009): 5821-5826.

[55] Chang, J., Li, H., Hou, T., and Li, F. Paper-based fluorescent sensor for rapid naked-eye detection of acetylcholinesterase activity and organophosphorus pesticides with high sensitivity and selectivity. Biosensors and Bioelectronics 86 (2016): 971-977.

[56] Xu, S., et al. Paper-based upconversion fluorescence resonance energy transfer biosensor for sensitive detection of multiple cancer biomarkers. Scientific Reports 6 (2016): 23406.

[57] Liu, Y.-M. and Perry, R.H. Paper-based electrochemical cell coupled to mass spectrometry. Journal of The American Society for Mass Spectrometry 26(10) (2015): 1702-1712.

[58] Chen, S., Wan, Q., and Badu-Tawiah, A.K. Mass spectrometry for paper-based immunoassays: toward on-demand diagnosis. Journal of the American Chemical Society 138(20) (2016): 6356-6359.

[59] Bakker, E. and Qin, Y. Electrochemical sensors. Analytical Chemistry 78(12) (2006): 3965-3984.

[60] Wang, J. Analytical electrochemistry.

[61] Martinez, A.W., Phillips, S.T., Carrilho, E., Thomas, S.W., Sindi, H., and Whitesides, G.M. Simple telemedicine for developing regions: camera phones and paper-based microfluidic devices for real-time, off-site diagnosis. Analytical Chemistry 80(10) (2008): 3699-3707.

[62] Cunningham, J.C., Brenes, N.J., and Crooks, R.M. Paper electrochemical device for detection of DNA and thrombin by target-induced conformational switching. Analytical Chemistry 86(12) (2014): 6166-6170.

[63] Songjaroen, T., Dungchai, W., Chailapakul, O., and Laiwattanapaisal, W. Novel, simple and low-cost alternative method for fabrication of paper-based microfluidics by wax dipping. Talanta 85(5) (2011): 2587-2593.

[64] Oh, J.-M. and Chow, K.-F. Recent developments in electrochemical paper-based analytical devices. Analytical Methods 7(19) (2015): 7951-7960.

[65] Nie, Z., et al. Electrochemical sensing in paper-based microfluidic devices. Lab on a Chip 10(4) (2010): 477-483.

[66] Adkins, J., Boehle, K., and Henry, C. Electrochemical paper-based microfluidic devices. ELECTROPHORESIS 36(16) (2015): 1811-1824.

[67] Zhang, J., Song, S., Wang, L., Pan, D., and Fan, C. A gold nanoparticle-based chronocoulometric DNA sensor for amplified detection of DNA. Nat Protoc 2(11) (2007): 2888-95.

[68] Lao, R., et al. Electrochemical interrogation of DNA monolayers on gold surfaces. Anal Chem 77(19) (2005): 6475-80.

[69] García, T., Revenga-Parra, M., Añorga, L., S.Arana, Pariente, F., and Lorenzo, E. Disposable DNA biosensor based on thin-film gold electrodes for selective Salmonella detection. Sensors and Actuators B: Chemical 161(1) (2012): 1030-1037.

[70] Ozkan, D., et al. DNA and PNA sensing on mercury and carbon electrodes by using methylene blue as an electrochemical label. Bioelectrochemistry 58(1) (2002): 119-26.

[71] Palaska, P., Aritzoglou, E., and Girousi, S. Sensitive detection of cyclophosphamide using DNA-modified carbon paste, pencil graphite and hanging mercury drop electrodes. Talanta 72(3) (2007): 1199-206.

[72] Du, D., Guo, S., Tang, L., Ning, Y., Yao, Q., and Zhang, G.-J. Graphene-modified electrode for DNA detection via PNA–DNA hybridization. Sensors and Actuators B: Chemical 186 (2013): 563-570.

[73] Santiago-Rodríguez, L., Sánchez-Pomales, G., and Cabrera, C.R. Electrochemical DNA sensing at single-walled carbon nanotubes chemically assembled on gold surfaces. Electroanalysis 22(23) (2010): 2817-2824.

[74] Wang, Z., et al. Label-free, electrochemical detection of methicillin-resistant staphylococcus aureus DNA with reduced graphene oxide-modified electrodes. Biosensors and Bioelectronics 26(9) (2011): 3881-3886.

[75] Zhou, M., Zhai, Y., and Dong, S. Electrochemical sensing and biosensing platform based on chemically reduced graphene oxide. Anal Chem 81(14) (2009): 5603-13.

[76] Novoselov, K.S., Falko, V.I., Colombo, L., Gellert, P.R., Schwab, M.G., and Kim, K. A roadmap for graphene. Nature 490(7419) (2012): 192-200.

[77] Choi, W., Lahiri, I., Seelaboyina, R., and Kang, Y.S. Synthesis of Graphene and Its Applications: A Review. Critical Reviews in Solid State and Materials Sciences 35(1) (2010): 52-71.

[78] Allen, M.J., Tung, V.C., and Kaner, R.B. Honeycomb carbon: a review of graphene. Chemical Reviews 110(1) (2010): 132-145.

[79] Potts, J.R., Dreyer, D.R., Bielawski, C.W., and Ruoff, R.S. Graphene-based polymer nanocomposites. Polymer 52(1) (2011): 5-25.

[80] Geim, A.K. and Novoselov, K.S. The rise of graphene. Nat Mater 6(3) (2007): 183-191.

[81] Feng, X.-M., et al. One-step electrochemical synthesis of graphene/polyaniline composite film and its applications. Advanced Functional Materials 21(15) (2011): 2989-2996.

[82] Manivel, P., Dhakshnamoorthy, M., Balamurugan, A., Ponpandian, N., Mangalaraj, D., and Viswanathan, C. Conducting polyaniline-graphene oxide fibrous nanocomposites: preparation, characterization and simultaneous electrochemical detection of ascorbic acid, dopamine and uric acid. RSC Advances 3(34) (2013): 14428-14437.

[83] Ruecha, N., Rangkupan, R., Rodthongkum, N., and Chailapakul, O. Novel paper-based cholesterol biosensor using graphene/polyvinylpyrrolidone/polyaniline nanocomposite. Biosensors and Bioelectronics 52 (2014): 13-19.

[84] Qiu, J.-D., Shi, L., Liang, R.-P., Wang, G.-C., and Xia, X.-H. Controllable deposition of a platinum nanoparticle ensemble on a polyaniline/graphene hybrid as a novel electrode material for electrochemical sensing. Chemistry – A European Journal 18(25) (2012): 7950-7959.

[85] Bo, Y., Yang, H., Hu, Y., Yao, T., and Huang, S. A novel electrochemical DNA biosensor based on graphene and polyaniline nanowires. Electrochimica Acta 56(6) (2011): 2676-2681.

[86] Chang, H., Yuan, Y., Shi, N., and Guan, Y. Electrochemical DNA biosensor based on conducting polyaniline nanotube array. Analytical Chemistry 79(13) (2007): 5111-5115.

[87] Luo, X., Lee, T.M.-H., and Hsing, I.M. Immobilization-free sequence-specific electrochemical detection of DNA using ferrocene-labeled peptide nucleic acid. Analytical Chemistry 80(19) (2008): 7341-7346.

[88] Nielsen, P.E., Egholm, M., Berg, R.H., and Buchardt, O. Sequence-selective recognition of DNA by strand displacement with a thymine-substituted polyamide. Science 254(5037) (1991): 1497-500.

[89] Ozkan, D., et al. Electrochemical detection of hybridization using peptide nucleic acids and methylene blue on self-assembled alkanethiol monolayer modified gold electrodes. Electrochemistry Communications 4(10) (2002): 796-802.

[90] Steichen, M., Decrem, Y., Godfroid, E., and Buess-Herman, C. Electrochemical DNA hybridization detection using peptide nucleic acids and [Ru(NH3)6]3+ on gold electrodes. Biosensors and Bioelectronics 22(9–10) (2007): 2237-2243.

[91] Wang, J., et al. Peptide nucleic acid probes for sequence-specific DNA biosensors. Journal of the American Chemical Society 118(33) (1996): 7667-7670.

[92] Jampasa, S., et al. Electrochemical detection of human papillomavirus DNA type 16 using a pyrrolidinyl peptide nucleic acid probe immobilized on screen-printed carbon electrodes. Biosensors and Bioelectronics 54(0) (2014): 428-434.

[93] Global Burden of Disease Cancer, C. The global burden of cancer 2013. JAMA oncology 1(4) (2015): 505-527.

[94] Karuwan, C., Sriprachuabwong, C., Wisitsoraat, A., Phokharatkul, D., Sritongkham, P., and Tuantranont, A. Inkjet-printed graphene-poly(3,4-ethylenedioxythiophene):poly(styrene-sulfonate) modified on screen printed carbon electrode for electrochemical sensing of salbutamol. Sensors and Actuators B: Chemical 161(1) (2012): 549-555.

[95] Mentele, M.M., Cunningham, J., Koehler, K., Volckens, J., and Henry, C.S. Microfluidic paper-based analytical device for particulate metals. Analytical Chemistry 84(10) (2012): 4474-4480.

[96] Lu, Y., Shi, W., Qin, J., and Lin, B. Fabrication and characterization of paper-based microfluidics prepared in nitrocellulose membrane by wax printing. Analytical Chemistry 82(1) (2010): 329-335.

[97] Bardpho, C., Rattanarat, P., Siangproh, W., and Chailapakul, O. Ultra-high performance liquid chromatographic determination of antioxidants in teas using inkjet-printed graphene–polyaniline electrode. Talanta 148 (2016): 673-679.

[98] Abi, A. and Ferapontova, E.E. Unmediated by DNA electron transfer in redox-labeled DNA duplexes end-tethered to gold electrodes. Journal of the American Chemical Society 134(35) (2012): 14499-14507.

[99] Farjami, E., Clima, L., Gothelf, K., and Ferapontova, E.E. "Off-on" electrochemical hairpin-DNA-based genosensor for cancer diagnostics. Anal Chem 83(5) (2011): 1594-602.

[100] Campos-Ferreira, D.S., et al. Electrochemical DNA biosensor for human papillomavirus 16 detection in real samples. Analytica Chimica Acta 804 (2013): 258-263.

[101] Pournaghi-Azar, M.H., Hejazi, M.S., and Alipour, E. Developing an electrochemical deoxyribonucleic acid (DNA) biosensor on the basis of human interleukine-2 gene using an electroactive label. Analytica Chimica Acta 570(2) (2006): 144-150.

[102] Tran, L.D., Nguyen, D.T., Nguyen, B.H., Do, Q.P., and Le Nguyen, H. Development of interdigitated arrays coated with functional polyaniline/MWCNT for electrochemical biodetection: Application for human papilloma virus. Talanta 85(3) (2011): 1560-1565.

[103] Zhu, L., Luo, L., and Wang, Z. DNA electrochemical biosensor based on thionine-graphene nanocomposite. Biosensors and Bioelectronics 35(1) (2012): 507-511.

[104] Huang, H., Bai, W., Dong, C., Guo, R., and Liu, Z. An ultrasensitive electrochemical DNA biosensor based on graphene/Au nanorod/polythionine for human papillomavirus DNA detection. Biosensors and Bioelectronics 68 (2015): 442-446.

[105] Davies, P.D.O. and Pai, M. The diagnosis and misdiagnosis of tuberculosis [State of the art series. Tuberculosis. Edited by I. D. Rusen. Number 1 in the series]. The International Journal of Tuberculosis and Lung Disease 12(11) (2008): 1226-1234.

[106] Steingart, K.R., et al. Sputum processing methods to improve the sensitivity of smear microscopy for tuberculosis: a systematic review. The Lancet Infectious Diseases 6(10) (2006): 664-674.

[107] Lee, J.J., Suo, J., Lin, C.B., Wang, J.D., Lin, T.Y., and Tsai, Y.C. Comparative evaluation of the BACTEC MGIT 960 system with solid medium for isolation of mycobacteria. The International Journal of Tuberculosis and Lung Disease 7(6) (2003): 569-574.

[108] Al-Zamel, F.A. Detection and diagnosis of Mycobacterium tuberculosis. Expert Review of Anti-infective Therapy 7(9) (2009): 1099-1108.

[109] Noordhoek, G.T., et al. Sensitivity and specificity of PCR for detection of mycobacterium tuberculosis: a blind comparison study among seven laboratories. Journal of Clinical Microbiology 32(2) (1994): 277-284.

[110] Yang, Y.-C., Lu, P.-L., Huang, S.C., Jenh, Y.-S., Jou, R., and Chang, T.C. Evaluation of the cobas taqMan MTB test for direct detection of mycobacterium tuberculosis Complex in Respiratory Specimens. Journal of Clinical Microbiology 49(3) (2011): 797-801.

[111] Zhao, X., Tapec-Dytioco, R., and Tan, W. Ultrasensitive DNA detection using highly fluorescent bioconjugated nanoparticles. Journal of the American Chemical Society 125(38) (2003): 11474-11475.

[112] Miao, W. and Bard, A.J. Electrogenerated chemiluminescence. 77. DNA hybridization detection at high amplification with [Ru(bpy)3]2+-containing microspheres. Analytical Chemistry 76(18) (2004): 5379-5386.

[113] Castro, A., Dalvit, D.A.R., and Paz-Matos, L. Ultrasensitive detection of DNA sequences in solution by specific enzymatic labeling. Analytical Chemistry 76(14) (2004): 4169-4174.

[114] Guedon, P., et al. Characterization and optimization of a real-time, parallel, label-free, polypyrrole-based DNA sensor by surface plasmon resonance imaging. Analytical Chemistry 72(24) (2000): 6003-6009.

[115] Erdem, A., Kerman, K., Meric, B., Akarca, U.S., and Ozsoz, M. Novel hybridization indicator methylene blue for the electrochemical detection of short DNA sequences related to the hepatitis B virus. Analytica Chimica Acta 422(2) (2000): 139-149.

[116] Hashimoto, K., Ito, K., and Ishimori, Y. Sequence-specific gene detection with a gold electrode modified with DNA probes and an electrochemically active dye. Analytical Chemistry 66(21) (1994): 3830-3833.

[117] Wong, E.L.S. and Gooding, J.J. Charge transfer through DNA: a selective electrochemical DNA biosensor. Analytical Chemistry 78(7) (2006): 2138-2144.

[118] Maruyama, K., Motonaka, J., Mishima, Y., Matsuzaki, Y., Nakabayashi, I., and Nakabayashi, Y. Detection of target DNA by electrochemical method. Sensors and Actuators B: Chemical 76(1–3) (2001): 215-219.

[119] Steel, A.B., Herne, T.M., and Tarlov, M.J. Electrochemical quantitation of DNA immobilized on gold. Analytical Chemistry 70(22) (1998): 4670-4677.

[120] Wang, J., Cai, X., Rivas, G., Shiraishi, H., Farias, P.A.M., and Dontha, N. DNA electrochemical biosensor for the detection of short DNA sequences related to the human immunodeficiency virus. Analytical Chemistry 68(15) (1996): 2629-2634.

[121] Ting, B.P., Zhang, J., Gao, Z., and Ying, J.Y. A DNA biosensor based on the detection of doxorubicin-conjugated Ag nanoparticle labels using solid-state voltammetry. Biosensors and Bioelectronics 25(2) (2009): 282-287.

[122] Sankoh, S., et al. A comparative study of a label-free DNA capacitive sensor using a pyrrolidinyl peptide nucleic acid probe immobilized through polyphenylenediamine and polytyramine non-conducting polymers. Sensors and Actuators B: Chemical 177 (2013): 543-554.

[123] Thipmanee, O., et al. Label-free capacitive DNA sensor using immobilized pyrrolidinyl PNA probe: Effect of the length and terminating head group of the blocking thiols. Biosensors and Bioelectronics 38(1) (2012): 430-435.

[124] Paleček, E., Kizek, R., Havran, L., Billova, S., and Fojta, M. Electrochemical enzyme-linked immunoassay in a DNA hybridization sensor. Analytica Chimica Acta 469(1) (2002): 73-83.

[125] Wang, J., Kawde, A.-N., and Musameh, M. Carbon-nanotube-modified glassy carbon electrodes for amplified label-free electrochemical detection of DNA hybridization. Analyst 128(7) (2003): 912-916.

[126] Thorp, H.H. Cutting out the middleman: DNA biosensors based on electrochemical oxidation. Trends in Biotechnology 16(3): 117-121.

[127] Yang, I.V. and Thorp, H.H. Modification of indium tin oxide electrodes with repeat polynucleotides: electrochemical detection of trinucleotide repeat expansion. Analytical Chemistry 73(21) (2001): 5316-5322.

[128] Boontha, B., Nakkuntod, J., Hirankarn, N., Chaumpluk, P., and Vilaivan, T. Multiplex mass spectrometric genotyping of single nucleotide polymorphisms employing pyrrolidinyl peptide nucleic acid in combination with ion-exchange capture. Anal Chem 80(21) (2008): 8178-86.

[129] Rattanarat, P., et al. A microfluidic paper-based analytical device for rapid quantification of particulate chromium. Analytica Chimica Acta 800 (2013): 50-55.

[130] Liu, H. and Crooks, R.M. Three-dimensional paper microfluidic devices assembled using the principles of origami. Journal of the American Chemical Society 133(44) (2011): 17564-17566.

[131] Zhang, M., et al. Three-dimensional paper-based electrochemiluminescence device for simultaneous detection of Pb2+ and Hg2+ based on potential-control technique. Biosensors and Bioelectronics 41 (2013): 544-550.

[132] Su, S., Nutiu, R., Filipe, C.D.M., Li, Y., and Pelton, R. Adsorption and covalent coupling of ATP-binding DNA aptamers onto cellulose. Langmuir 23(3) (2007): 1300-1302.

[133] Sirvio, J., Hyvakko, U., Liimatainen, H., Niinimaki, J., and Hormi, O. Periodate oxidation of cellulose at elevated temperatures using metal salts as cellulose activators. Carbohydrate Polymers 83(3) (2011): 1293-1297.

[134] Eisenach, K.D., Cave, M.D., Bates, J.H., and Crawford, J.T. Polymerase chain reaction amplification of a repetitive DNA sequence specific for mycobacterium tuberculosis. The Journal of Infectious Diseases 161(5) (1990): 977-981.

[135] Wang, J., Rivas, G., Fernandes, J.R., Lopez Paz, J.L., Jiang, M., and Waymire, R. Indicator-free electrochemical DNA hybridization biosensor. Analytica Chimica Acta 375(3) (1998): 197-203.

[136] Oliveira-Brett, A.M., Diculescu, V., and Piedade, J.A.P. Electrochemical oxidation mechanism of guanine and adenine using a glassy carbon microelectrode. Bioelectrochemistry 55(1–2) (2002): 61-62.

[137] Li, Q., Batchelor-McAuley, C., and Compton, R.G. Electrochemical oxidation of guanine: electrode reaction mechanism and tailoring carbon electrode surfaces to switch between adsorptive and diffusional responses. The Journal of Physical Chemistry B 114(21) (2010): 7423-7428.

[138] Wei, F., Lillehoj, P.B., and Ho, C.-M. DNA diagnostics: nanotechnology-enhanced electrochemical detection of nucleic acids. Pediatr Res 67(5) (2010): 458-468.

[139] Smith, I. Mycobacterium tuberculosis pathogenesis and molecular determinants of virulence. Clinical Microbiology Reviews 16(3) (2003): 463-496.

[140] Burd, E.M. Human papillomavirus and cervical cancer. Clinical Microbiology Reviews 16(1) (2003): 1-17.

[141] de Wit, E., et al. Middle east respiratory syndrome coronavirus (MERS-CoV) causes transient lower respiratory tract infection in rhesus macaques. Proceedings of the National Academy of Sciences of the United States of America 110(41) (2013): 16598-16603.

[142] Bhadra, S., Jiang, Y.S., Kumar, M.R., Johnson, R.F., Hensley, L.E., and Ellington, A.D. Real-time sequence-validated loop-mediated isothermal amplification

assays for detection of middle east respiratory syndrome coronavirus (MERS-CoV). PLoS ONE 10(4) (2015): e0123126.

[143] Lörincz, A. and Anthony, J. Advances in HPV detection by Hybrid Capture®. Papillomavirus Report 12(6) (2001): 145-154.

[144] Gravitt, P.E. and Jamshidi, R. Diagnosis and management of oncogenic cervical human papillomavirus infection. Infectious Disease Clinics of North America 19(2) (2005): 439-458.

[145] Yetisen, A.K., Akram, M.S., and Lowe, C.R. Paper-based microfluidic point-of-care diagnostic devices. Lab on a Chip 13(12) (2013): 2210-2251.

[146] Adkins, J., Boehle, K., and Henry, C. Electrochemical paper-based microfluidic devices. ELECTROPHORESIS 36(16) (2015): 1811-1824.

[147] Apilux, A., Siangproh, W., Praphairaksit, N., and Chailapakul, O. Simple and rapid colorimetric detection of Hg(II) by a paper-based device using silver nanoplates. Talanta 97 (2012): 388-394.

[148] Shim, S.-Y., Lim, D.-K., and Nam, J.-M. Ultrasensitive optical biodiagnostic methods using metallic nanoparticles. Nanomedicine 3(2) (2008): 215-232.

[149] Baptista, P., et al. Gold nanoparticles for the development of clinical diagnosis methods. Analytical and Bioanalytical Chemistry 391(3) (2008): 943-950.

[150] Zhao, W., Brook, M.A., and Li, Y. Design of gold nanoparticle-based colorimetric biosensing assays. ChemBioChem 9(15) (2008): 2363-2371.

[151] Thaxton, C.S., Georganopoulou, D.G., and Mirkin, C.A. Gold nanoparticle probes for the detection of nucleic acid targets. Clinica Chimica Acta 363(1–2) (2006): 120-126.

[152] Li, H., Cui, Z., and Han, C. Glutathione-stabilized silver nanoparticles as colorimetric sensor for Ni2+ ion. Sensors and Actuators B: Chemical 143(1) (2009): 87-92.

[153] Vilela, D., González, M.C., and Escarpa, A. Sensing colorimetric approaches based on gold and silver nanoparticles aggregation: Chemical creativity behind the assay. A review. Analytica Chimica Acta 751 (2012): 24-43.

[154] Wei, H., Chen, C., Han, B., and Wang, E. Enzyme colorimetric assay using unmodified silver nanoparticles. Analytical Chemistry 80(18) (2008): 7051-7055.

[155] Lee, J.-S., Lytton-Jean, A.K.R., Hurst, S.J., and Mirkin, C.A. Silver nanoparticle–oligonucleotide conjugates based on DNA with triple cyclic disulfide moieties. Nano Letters 7(7) (2007): 2112-2115.

[156] Thompson, D.G., Enright, A., Faulds, K., Smith, W.E., and Graham, D. Ultrasensitive DNA detection using oligonucleotide–silver nanoparticle conjugates. Analytical Chemistry 80(8) (2008): 2805-2810.

[157] Yeo, S.Y., Lee, H.J., and Jeong, S.H. Preparation of nanocomposite fibers for permanent antibacterial effect. Journal of Materials Science 38(10) (2003): 2143-2147.

[158] Chimentao, R.J., et al. Different morphologies of silver nanoparticles as catalysts for the selective oxidation of styrene in the gas phase. Chemical Communications (7) (2004): 846-847.

[159] He, B., Tan, J.J., Liew, K.Y., and Liu, H. Synthesis of size controlled Ag nanoparticles. Journal of Molecular Catalysis A: Chemical 221(1-2) (2004): 121-126.

[160] Abou El-Nour, K.M.M., Eftaiha, A.a., Al-Warthan, A., and Ammar, R.A.A. Synthesis and applications of silver nanoparticles. Arabian Journal of Chemistry 3(3) (2010): 135-140.

[161] Iravani, S., Korbekandi, H., Mirmohammadi, S.V., and Zolfaghari, B. Synthesis of silver nanoparticles: chemical, physical and biological methods. Research in Pharmaceutical Sciences 9(6) (2014): 385-406.

[162] Egholm, M., et al. PNA hybridizes to complementary oligonucleotides obeying the Watson—Crick hydrogen-bonding rules. Nature 365(6446) (1993): 566-568.

[163] Su, X. and Kanjanawarut, R. Control of metal nanoparticles aggregation and dispersion by PNA and PNA–DNA complexes, and its application for colorimetric DNA detection. ACS Nano 3(9) (2009): 2751-2759.

[164] Kanjanawarut, R. and Su, X. Colorimetric detection of DNA using unmodified metallic nanoparticles and peptide nucleic acid probes. Analytical Chemistry 81(15) (2009): 6122-6129.

[165] Laliwala, S.K., Mehta, V.N., Rohit, J.V., and Kailasa, S.K. Citrate-modified silver nanoparticles as a colorimetric probe for simultaneous detection of four triptan-family drugs. Sensors and Actuators B: Chemical 197 (2014): 254-263.

[166] Liu, H., Xiang, Y., Lu, Y., and Crooks, R.M. Aptamer-based origami paper analytical device for electrochemical detection of adenosine. Angewandte Chemie 124(28) (2012): 7031-7034.

[167] Huynh, K.A. and Chen, K.L. Aggregation kinetics of citrate and polyvinylpyrrolidone coated silver nanoparticles in monovalent and divalent electrolyte solutions. Environmental Science & Technology 45(13) (2011): 5564-5571.

[168] Li, X., Lenhart, J.J., and Walker, H.W. Dissolution-accompanied aggregation kinetics of silver nanoparticles. Langmuir 26(22) (2010): 16690-16698.

[169] Shirato, K., et al. Detection of Middle East respiratory syndrome coronavirus using reverse transcription loop-mediated isothermal amplification (RT-LAMP). Virology Journal 11 (2014): 139-139.

[170] Azhar, E.I., et al. Detection of the Middle East respiratory syndrome coronavirus genome in an air sample originating from a camel barn owned by an infected patient. mBio 5(4) (2014): e01450-14.

[171] Abreu, A.L.P., Souza, R.P., Gimenes, F., and Consolaro, M.E.L. A review of methods for detect human Papillomavirus infection. Virology Journal 9 (2012): 262-262.

[172] Villa, L.L. and Denny, L. CHAPTER 7 Methods for detection of HPV infection and its clinical utility. International Journal of Gynecology & Obstetrics 94 (2006): S71-S80.

VITA

Miss Prinjaporn Teengam was born in November 4, 1985. She received her B.Sc. in Chemistry from Srinakharinwirot University and M.Sc. in Petrochemistry and Polymer Science from Chulalongkorn University. During her Ph.D., she received scholarship from Thailand Graduate Institute of Science and Technology (TGIST). She was a visiting scholar at Henry's research group, Department of Chemistry, Colorado State University. She was also received an opportunity from Professor Dr. Toshihiko Imato (Department of Applied Chemistry, Graduate School of Engineering, Kyushu University, Japan) to join his group as an internship. Her research area focuses on the detection of DNA virus using paper-based devices coupled with polyamide nucleic acid. The development around this area was inspired by the need for low cost diagnostic tools in developing countries.

PUBLICATIONS

1. Rattanarat, P., Teengam, P., Siangproh, W., Ishimatsu, R., Nakano, K., Chailapakul, O., and Imato, T. An Electrochemical Compact Disk-type Microfluidics Platform for Use as an Enzymatic Biosensor. Electroanalysis 27(3) (2015): 703-712.

2. Mettakoonpitak, J., Boehle, K., Nantaphol, S., Teengam, P., Adkins, J. A., Srisa-Art, M., and Henry, C. S.Electrochemistry on Paper-based Analytical Devices: A Review. Electroanalysis 28(7) (2016): 1420-1436.

3. Teengam, P., Siangproh, W., Tuantranont, A., Henry, C.S., Vilaivan, T., and Chailapakul, O. Electrochemical paper-based peptide nucleic acid biosensor for detecting human papillomavirus. Analytica Chimica Acta 952 (2017): 32-40.

4. Teengam, P., Siangproh, W., Tuantranont, A., Vilaivan, T., Chailapakul, O., and Henry, C.S. Multiplex Paper-Based Colorimetric DNA Sensor Using Pyrrolidinyl Peptide Nucleic Acid-Induced AgNPs Aggregation for Detecting MERS-CoV, MTB, and HPV Oligonucleotides. Analytical Chemistry 89(10) (2017): 5428-5435.